The Abdus Salam
International Centre for Theoretical Physics

United Nations
Educational, Scientific
and Cultural Organization

International Atomic
Energy Agency

H4.SMR/1747-6

"Workshop on the Conduct of Seismic Hazard Analyses
for Critical Facilities"

15 - 19 May 2006

New Strong Motion Data from Japan and Empirical Relations

Yoshi FUKUSHIMA

Shimizu Corporation, Tokyo, Japan

New strong motion data from Japan and empirical relations

Yoshi. FUKUSHIMA

Contents

Introduction

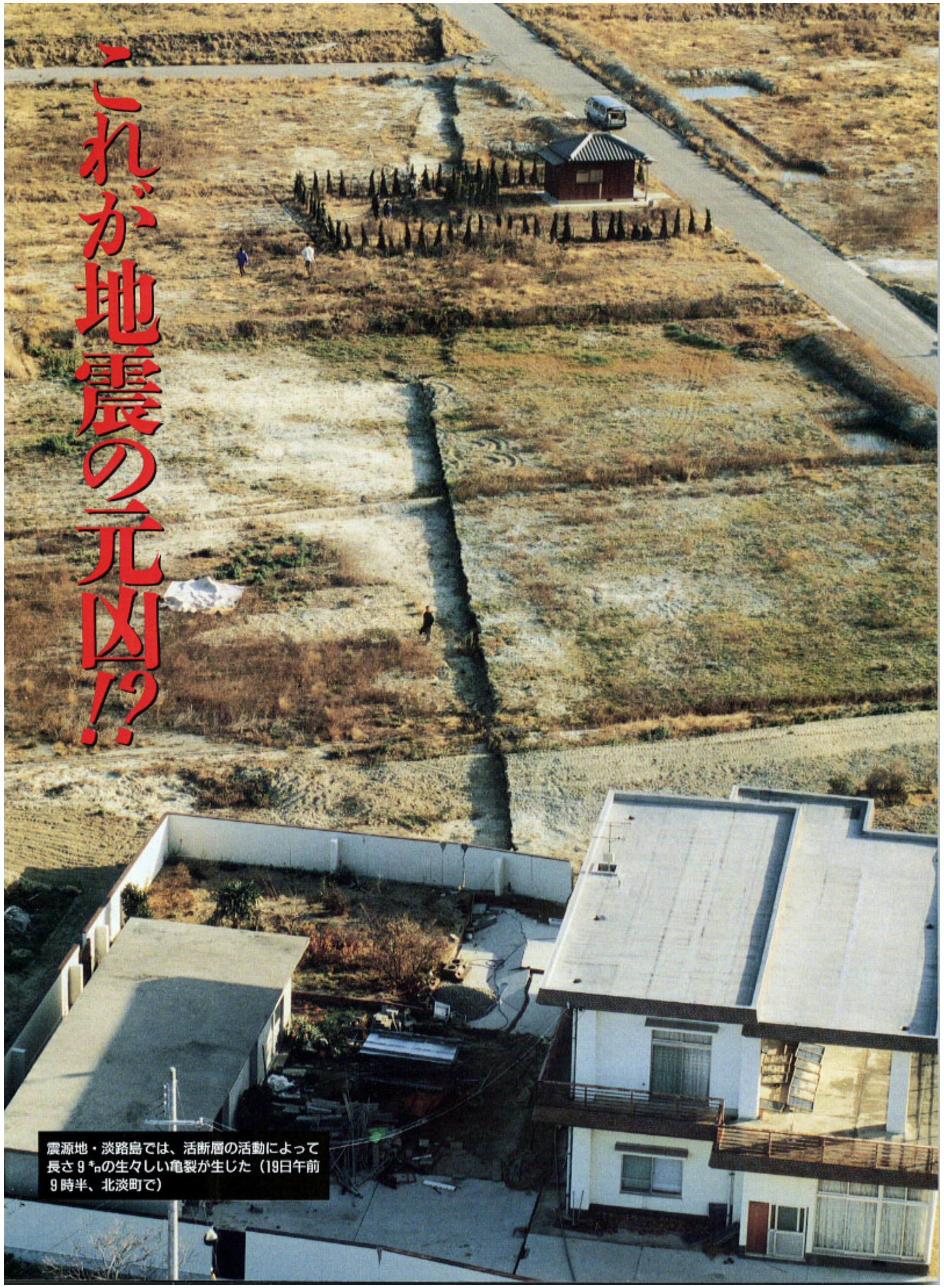

Fault trace of the 1995 Hyogo-ken Nanbu earthquake

サンデー毎日臨時増刊2/4, 1995

Broken wall by the fault displacement

stripes on the fault plane

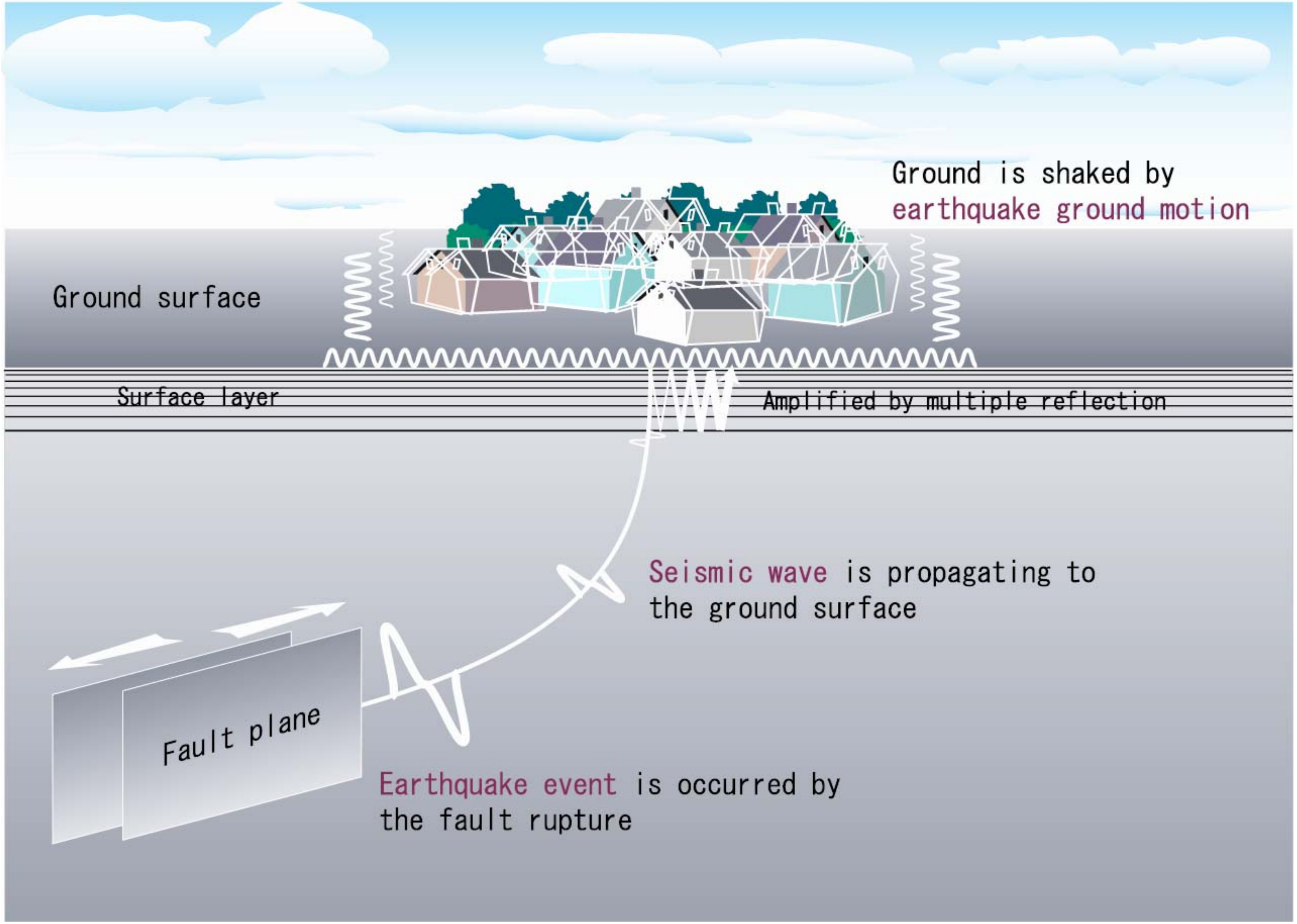
Ground is shaked by
earthquake ground motion
Ground surface
Surface layer
Amplified by multiple reflection
Seismic wave is propagating to
the ground surface
Fault plane
Earthquake event is occurred by
the fault rupture

Estimation of strong ground motion

Theoretical

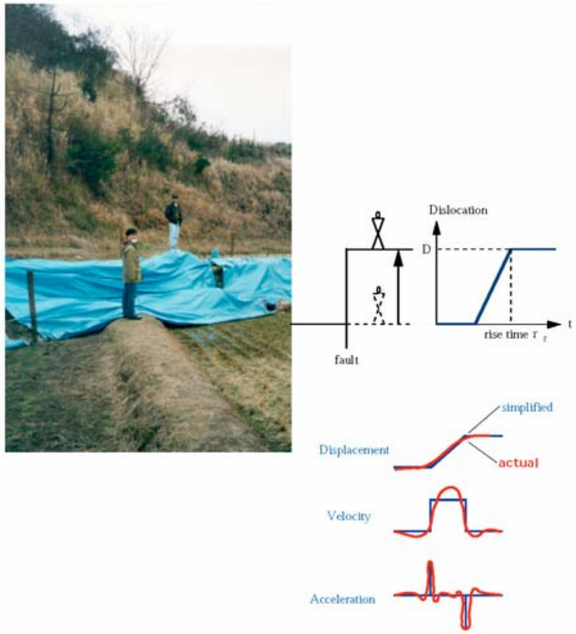

Dislocation in elastic medium simulating by kinematics

Semi-empirical

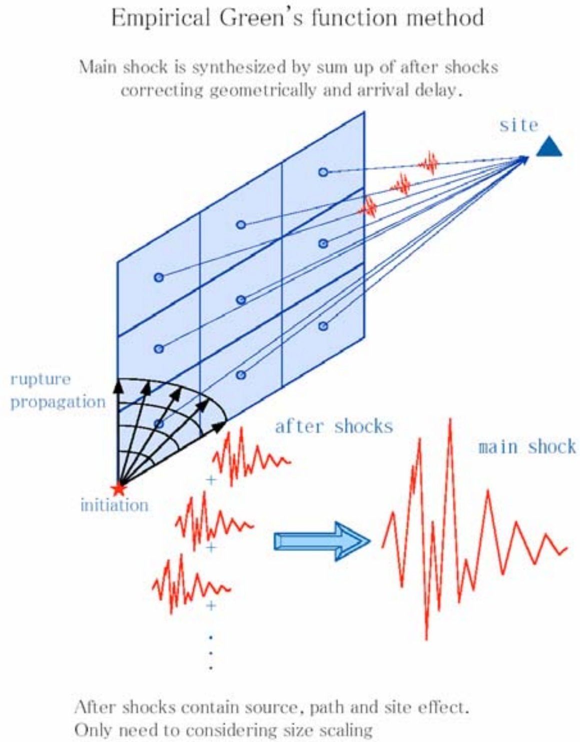

Large motion is synthesized using small records.

Empirical

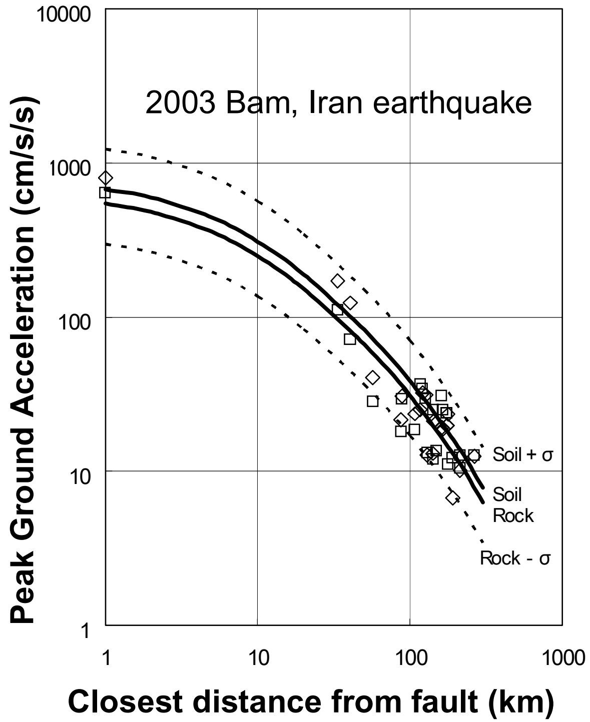

Attenuation relation is determined by regression analysis of SMDB.

Empirical Green’s function method

Main shock is synthesized by sum up of after shocks
correcting geometrically and arrival delay.

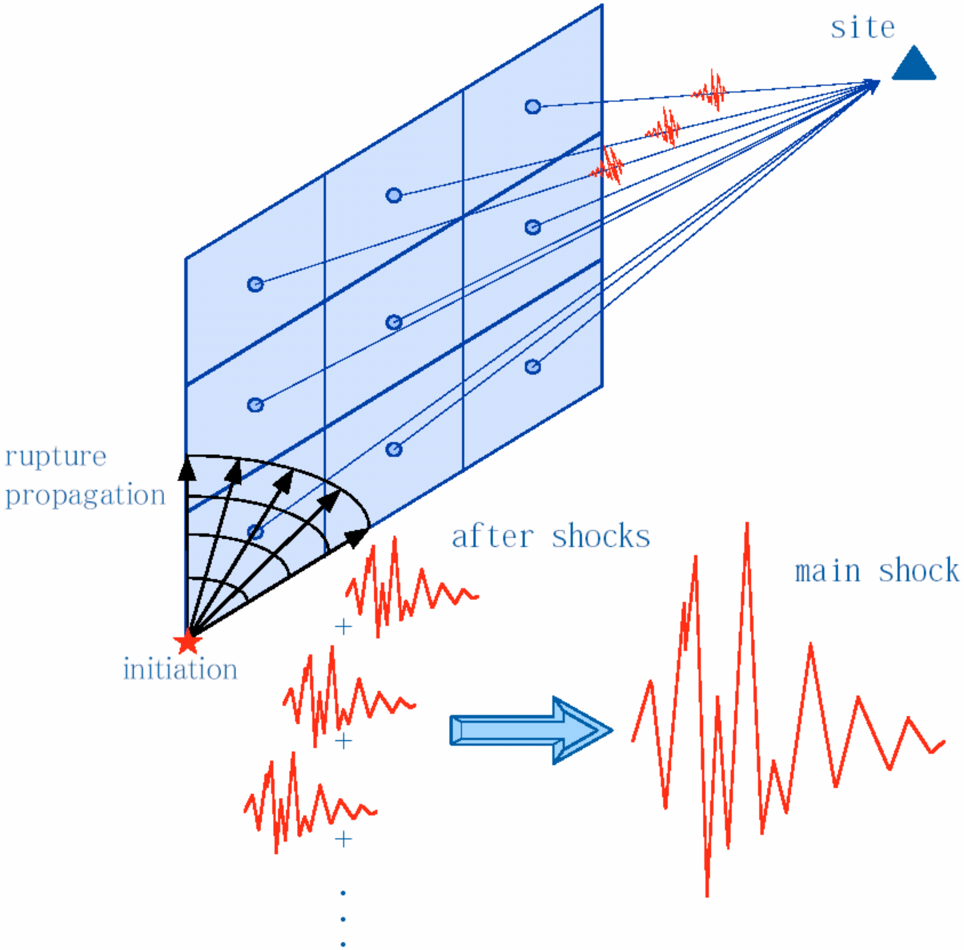

After shocks contain source, path and site effect.
Only need to considering size scaling

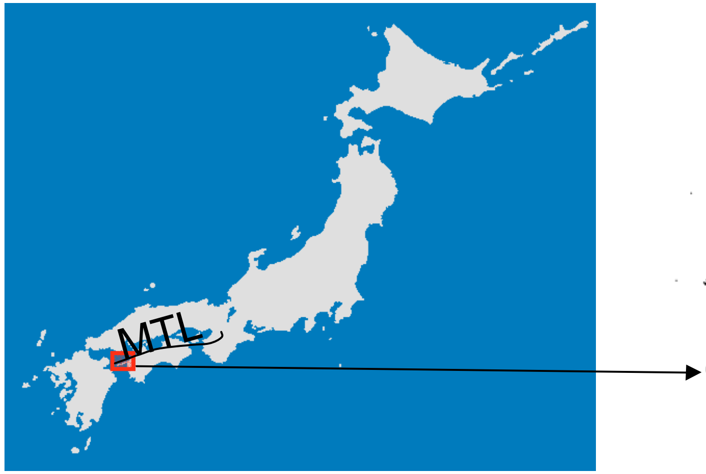

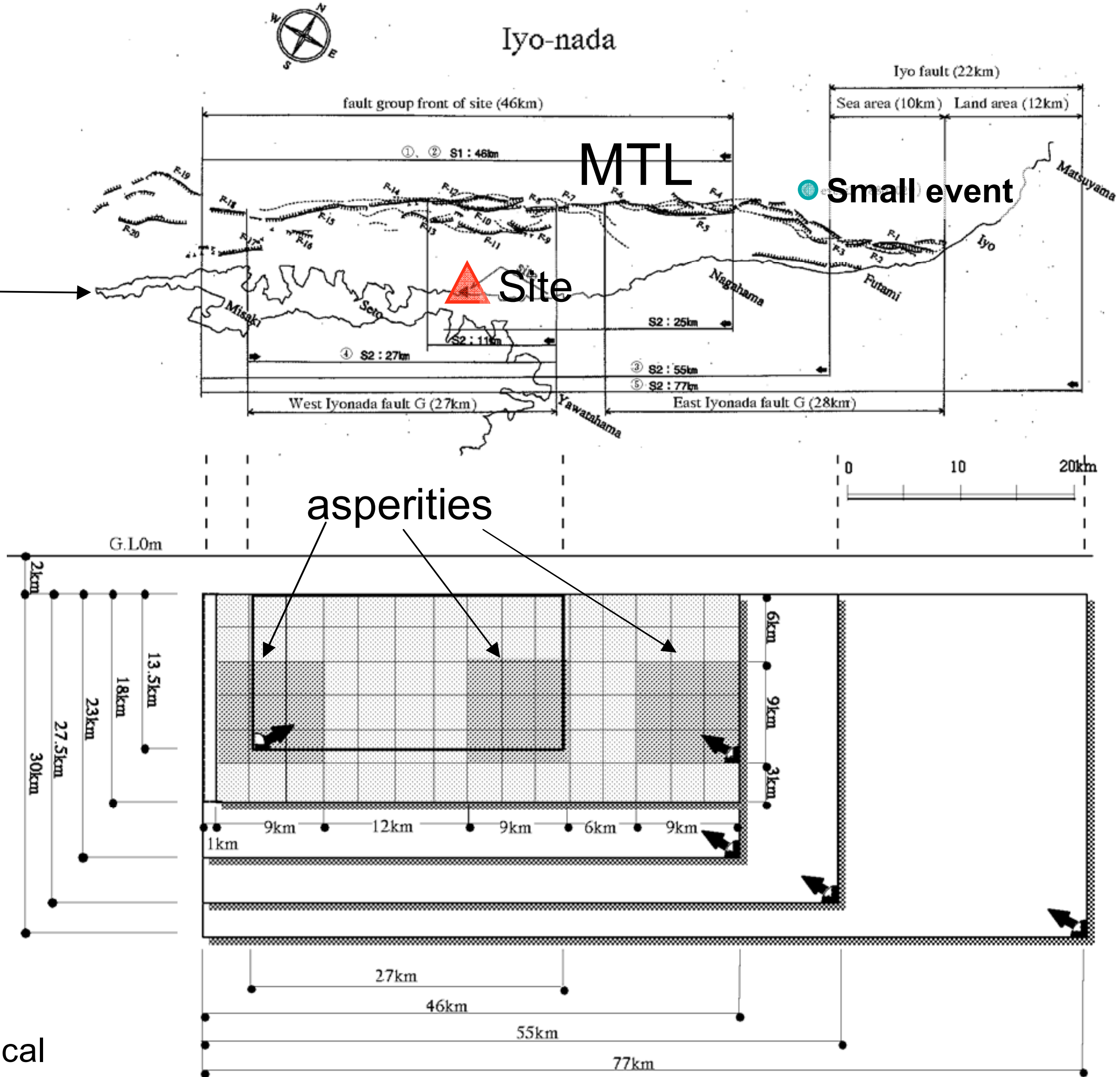

Fukushima et al. (2001). Semi-empirical estimation of ground motion using observed records at a site in Shikoku, Japan, *J. Seismology*, 5, pp.63-72.

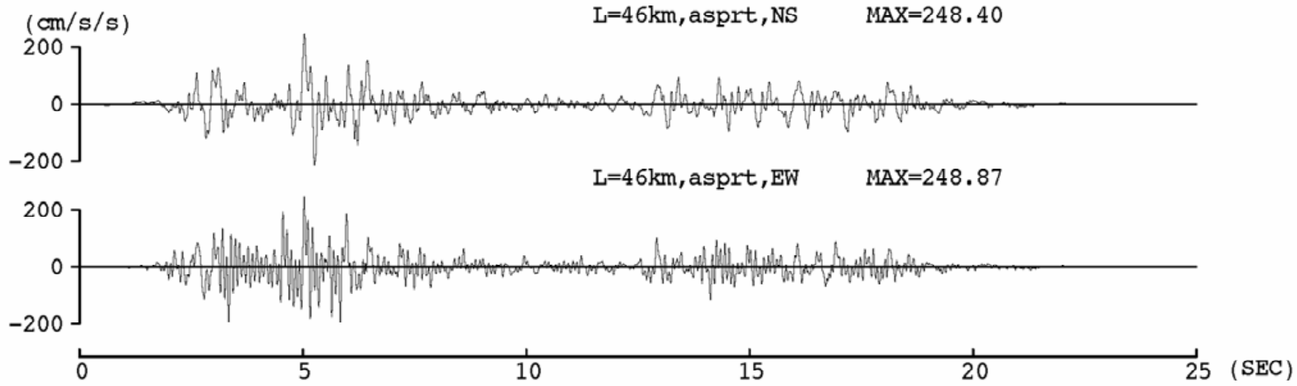

Synthesized wave

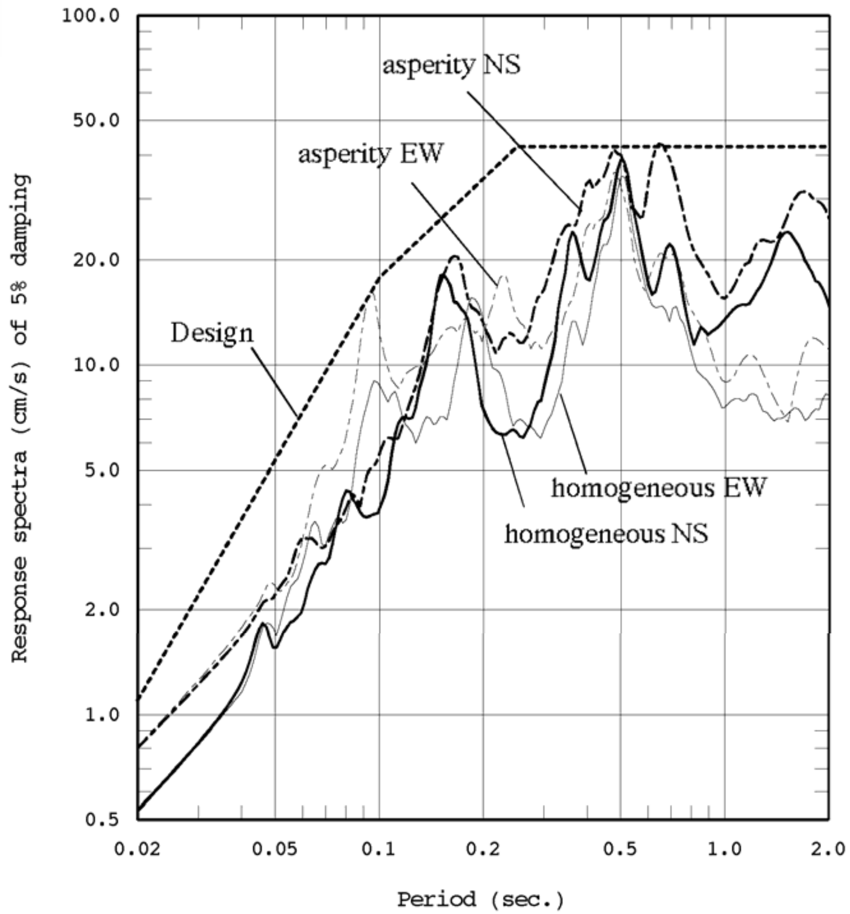

Spectral comparison between design and synthesized waves for homogeneous and heterogeneous fault model

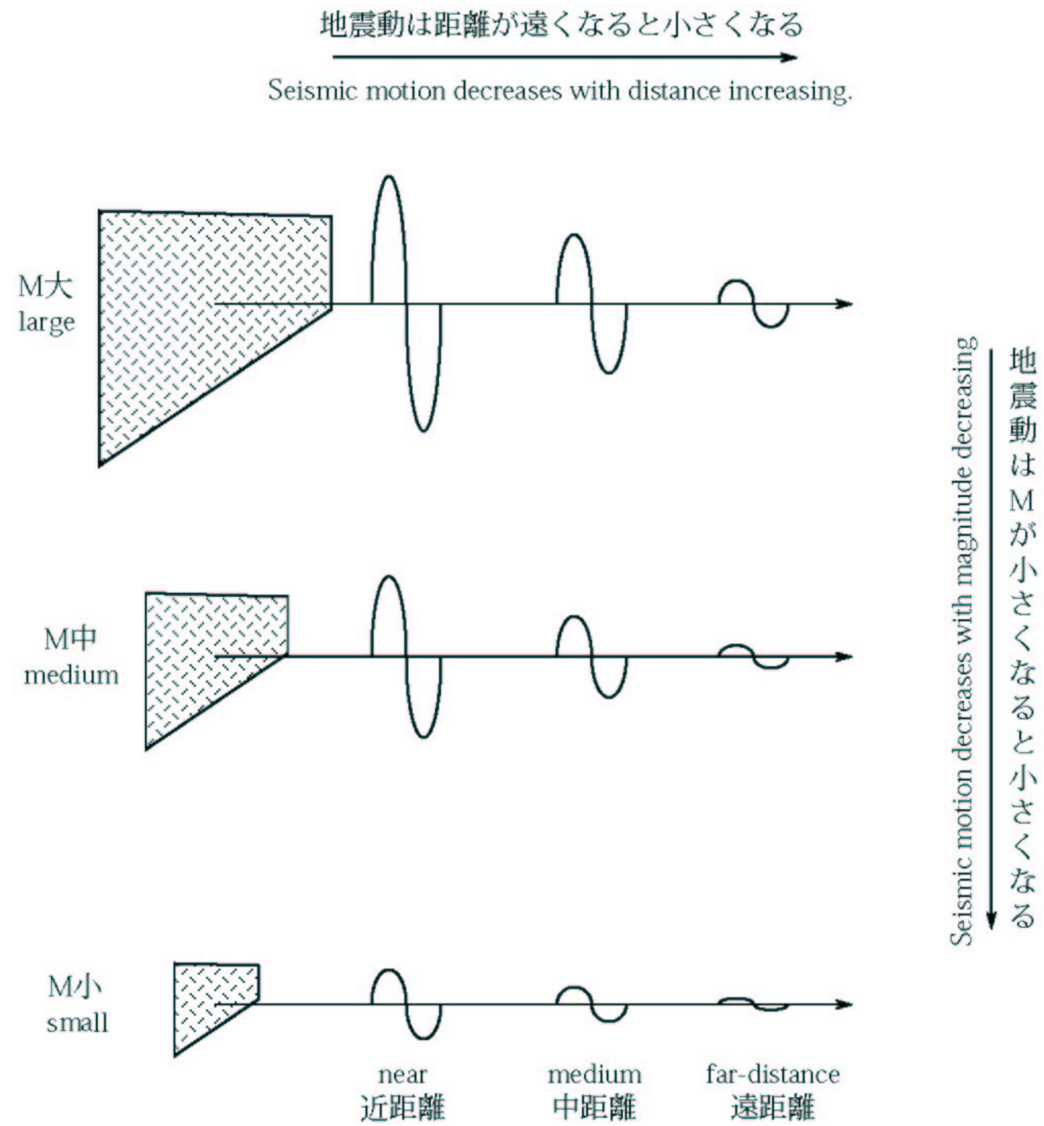
地震動は距離が遠くなると小さくなる
Seismic motion decreases with distance increasing.
M大
large
M中
medium
M小
small
near
近距離
medium
中距離
far-distance
遠距離
地震動はMが小さくなると小さくなる
Seismic motion decreases with magnitude decreasing

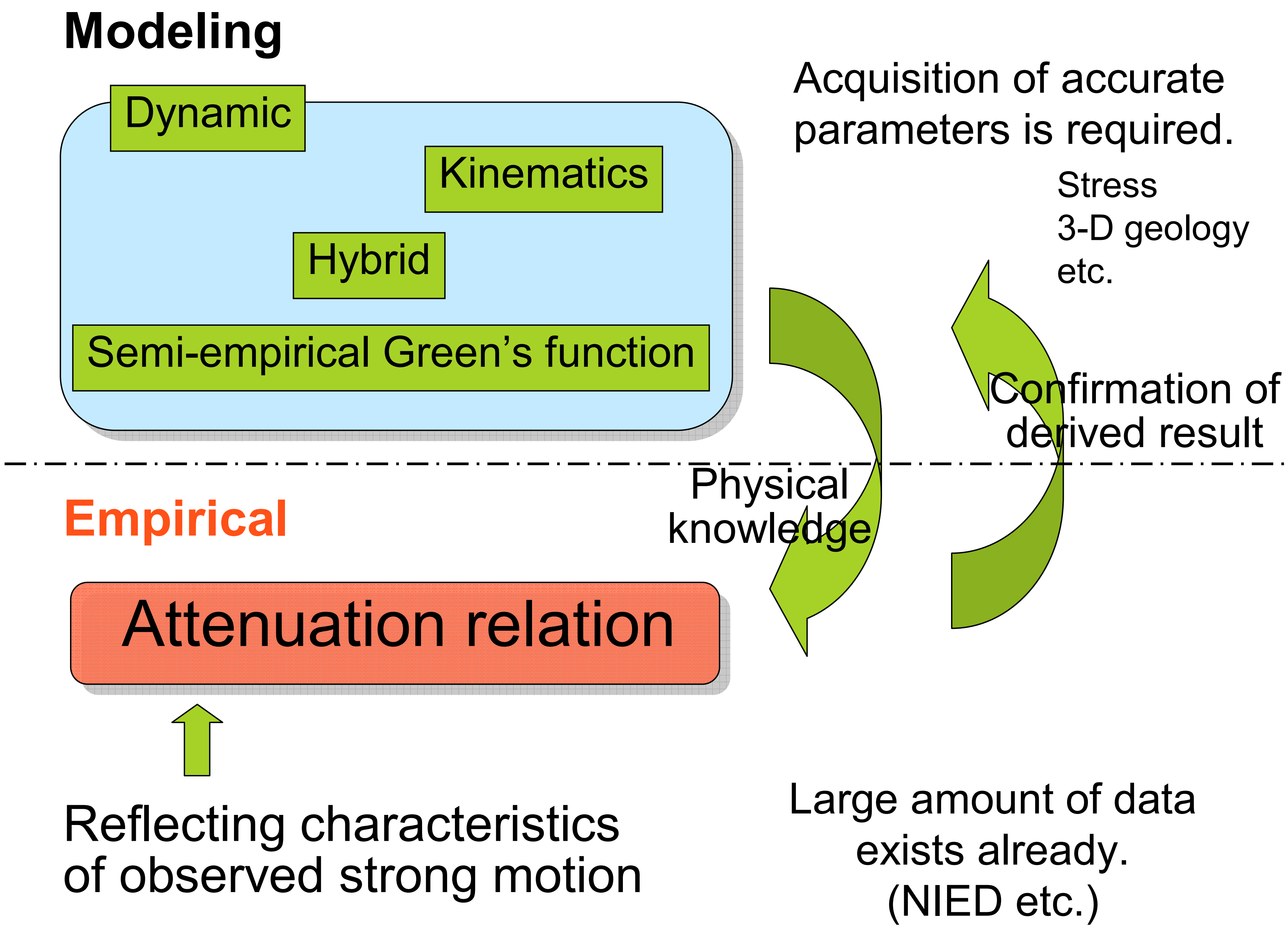
Modeling
Dynamic
Kinematics
Hybrid
Semi-empirical Green's function
Acquisition of accurate parameters is required.
Stress
3-D geology
etc.
Confirmation of derived result
Physical knowledge
Empirical
Attenuation relation
Reflecting characteristics of observed strong motion
Large amount of data exists already.
(NIED etc.)

PGA

PGA, S_a : Decrease with distance, increase with M

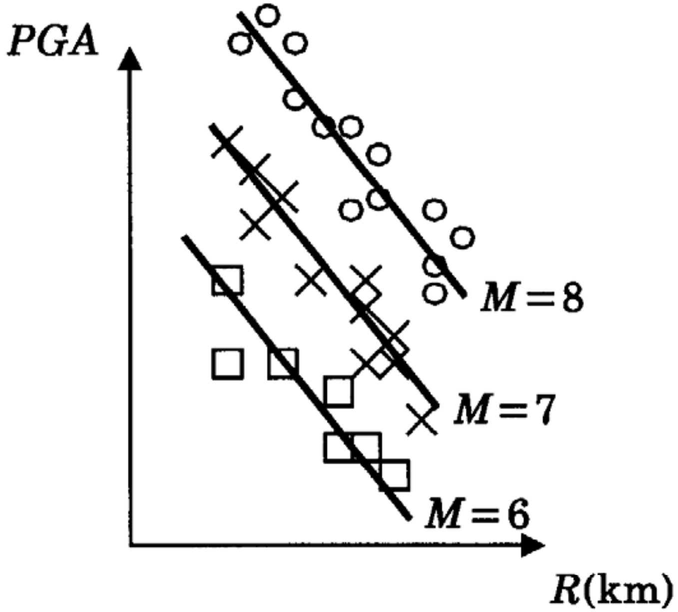

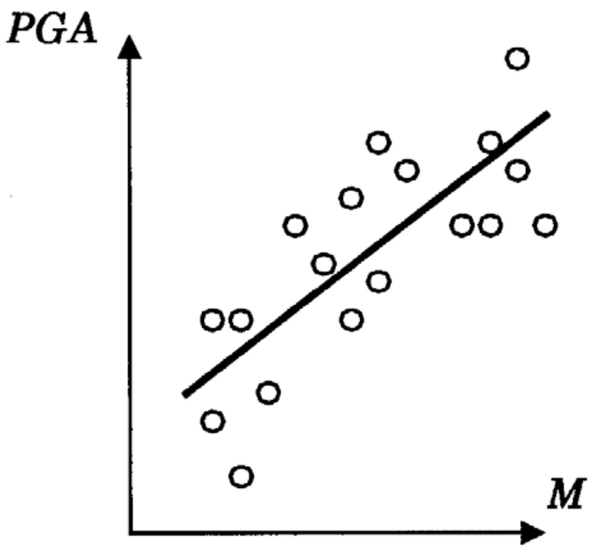

Axis of M is linear

$Y = \log_{10} PGA$, $X = \log_{10} R$, ε_i is a error between predicted and observed data, a,b,c are regression coefficients

$$Y_i = aM_i + bX_i + c + \varepsilon_i$$

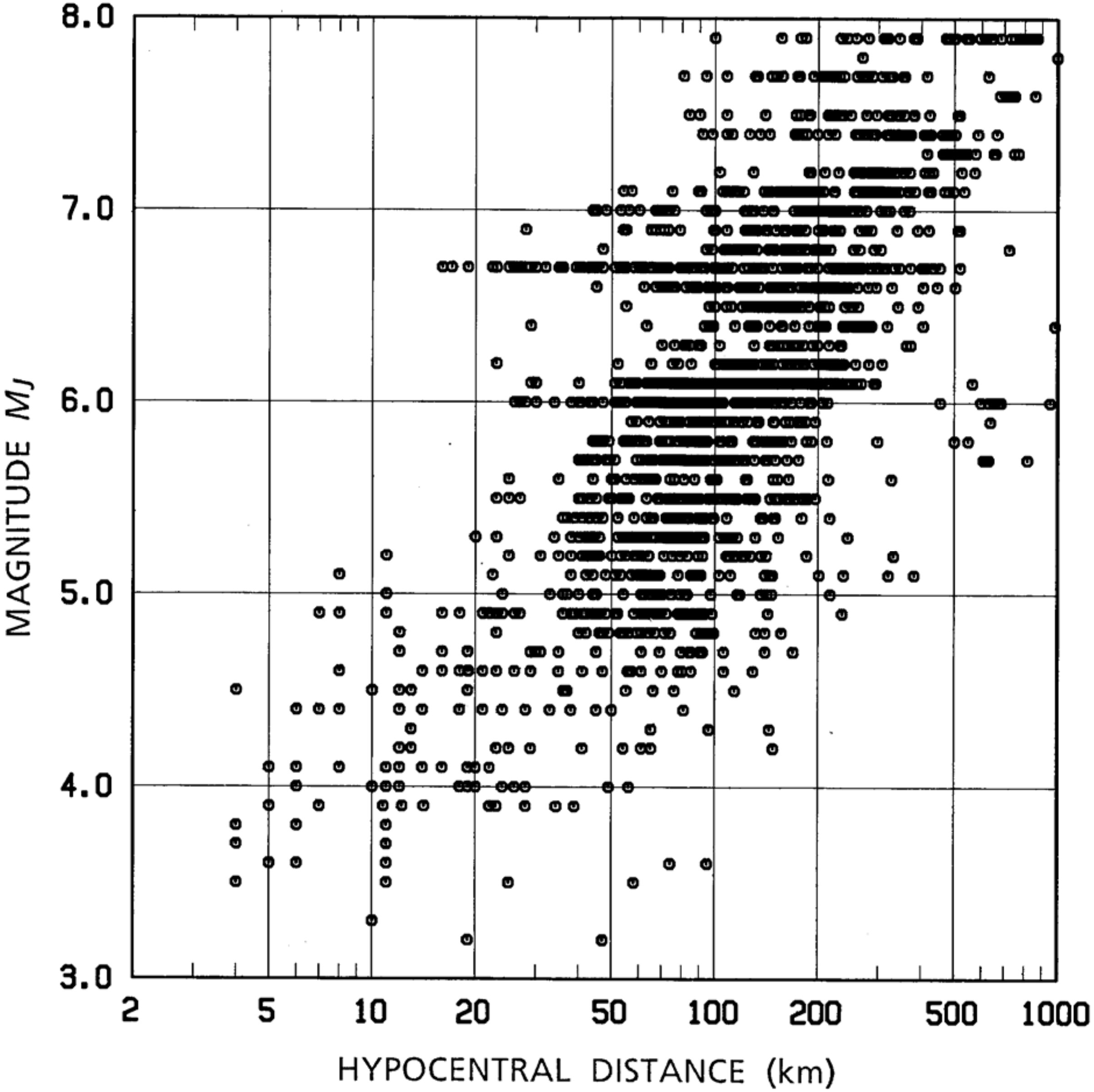

Relation between distance and magnitude of classical database

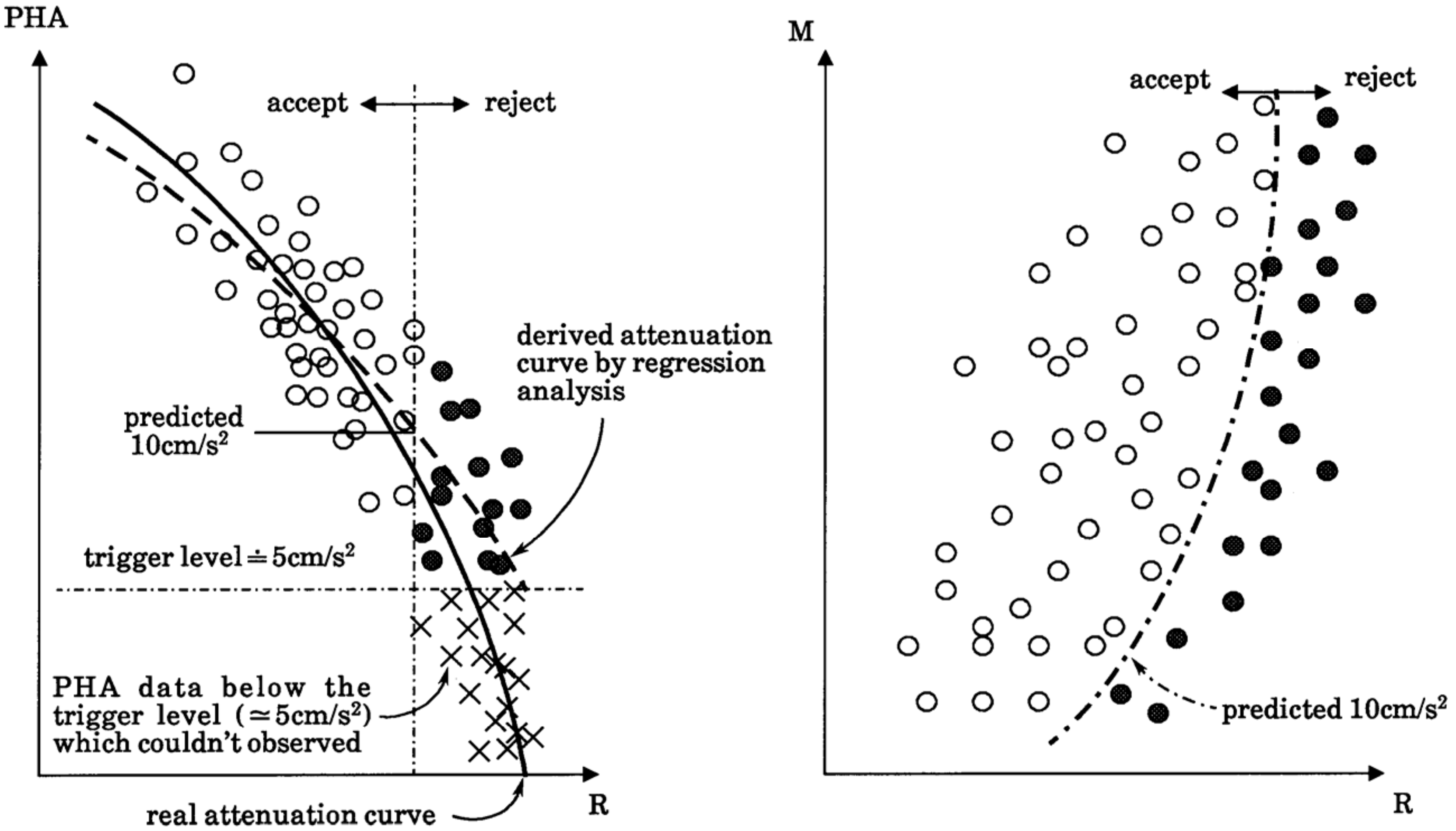

(a) Relation between accepted data to derive real attenuation curve and trigger level

(b) Relation between *M* and distance *R* for rejected data which observed in long distances first step of the 2 step regression analysis

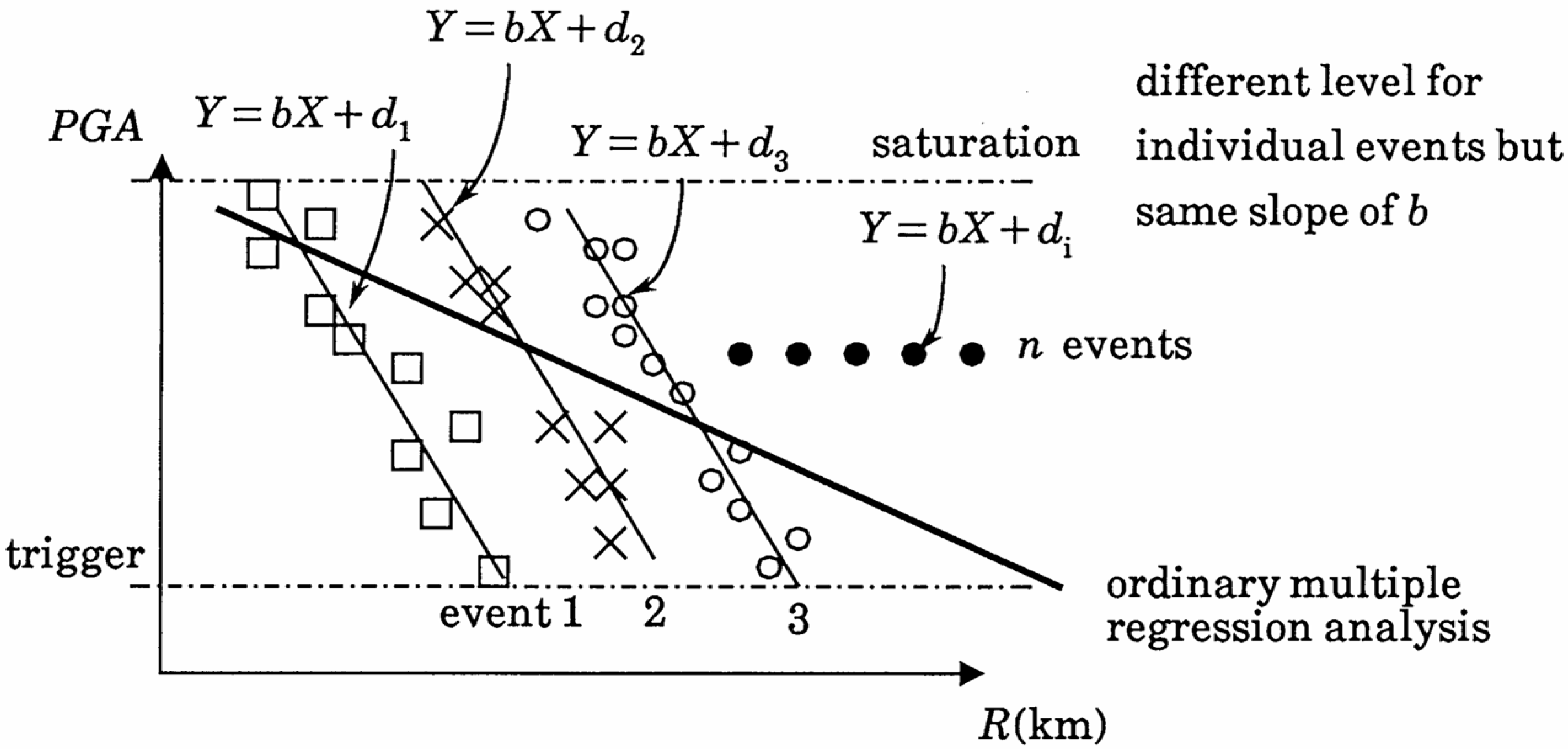

$$Y_i = bX_i + \delta_1 \cdot d_1 + \delta_2 \cdot d_2 + \cdots\cdots\cdots + \delta_n \cdot d_n + \varepsilon_i$$

δ_j is 1 for jth event, otherwise 0.

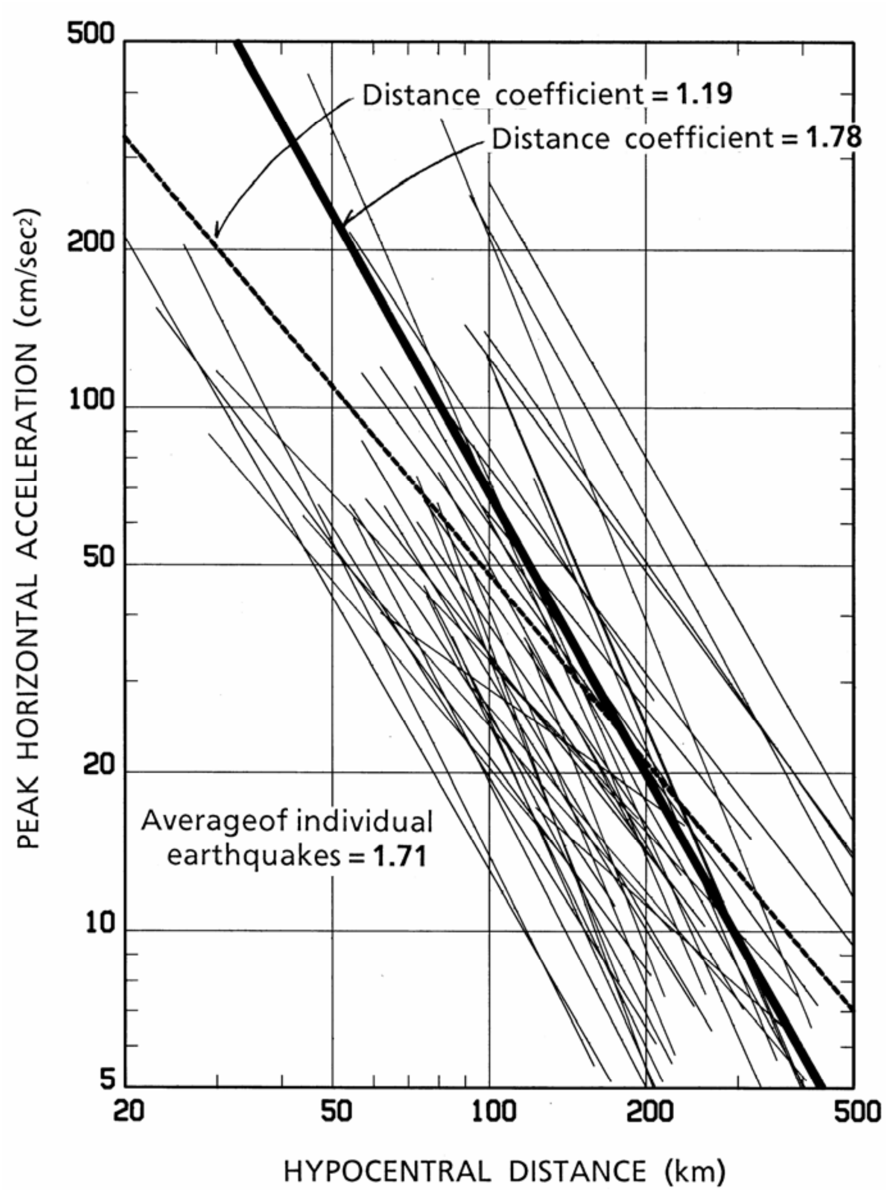

Attenuation relation of PGA for individual events (thin lines), determined by ordinary (chained) and 2 step regression (thick) analysis

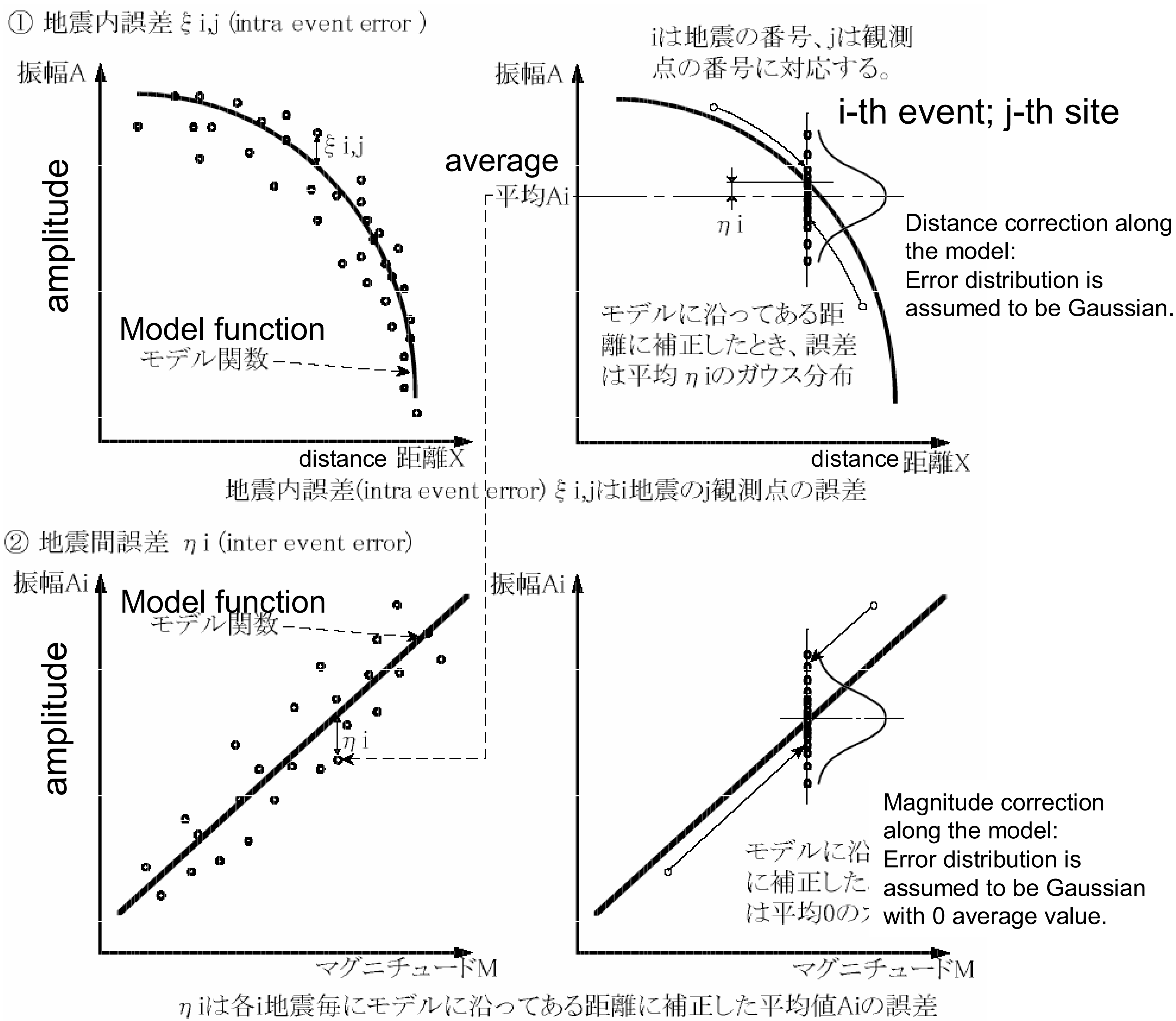
① 地震内誤差 ξ i,j (intra event error)
振幅A
amplitude
ξ i,j
Model function
モデル関数
distance 距離X
iは地震の番号、jは観測点の番号に対応する。
i-th event; j-th site
振幅A
average
平均Ai
η i
Distance correction along the model:
Error distribution is assumed to be Gaussian.
モデルに沿ってある距離に補正したとき、誤差は平均η iのガウス分布
distance 距離X
地震内誤差(intra event error) ξ i,jはi地震のj観測点の誤差
② 地震間誤差 η i (inter event error)
振幅Ai
amplitude
Model function
モデル関数
η i
マグニチュードM
振幅Ai
モデルに沿
に補正した
は平均0の
Magnitude correction along the model:
Error distribution is assumed to be Gaussian with 0 average value.
マグニチュードM
η iは各i地震毎にモデルに沿ってある距離に補正した平均値Aiの誤差

Model of attenuation relation

k is expressed as power of source or *M*

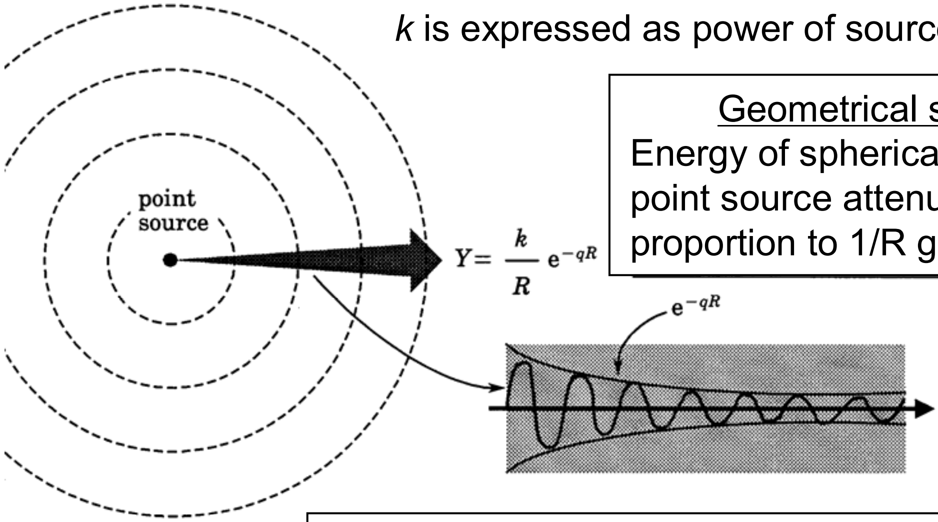

Geometrical spreading
Energy of spherical wave from point source attenuates in proportion to 1/R geometrically.

Intrinsic attenuation
Energy is absorbed in medium constantly for each cycles, if plane wave propagates along a ray.

自然対数をとると　$\ln PGA = -\ln R - qR + \ln k$

常用対数に変換して　$\log PGA = -\log R - qR \cdot \log e + \ln k \cdot \log e = \underline{-\log R - bR + d}$

振動方程式より　$q = \omega / 2cQ$　　$\therefore Q^{-1} = cqT/\pi = bcT/\pi \log e$　　cは位相速度

The regression coefficient *b* can be converted to Q with velocity and predominant period.

cをVsと同等と見なして固有周期Tを決めれば
回帰係数bから$Q(Q=1/2h)$に変換できる。

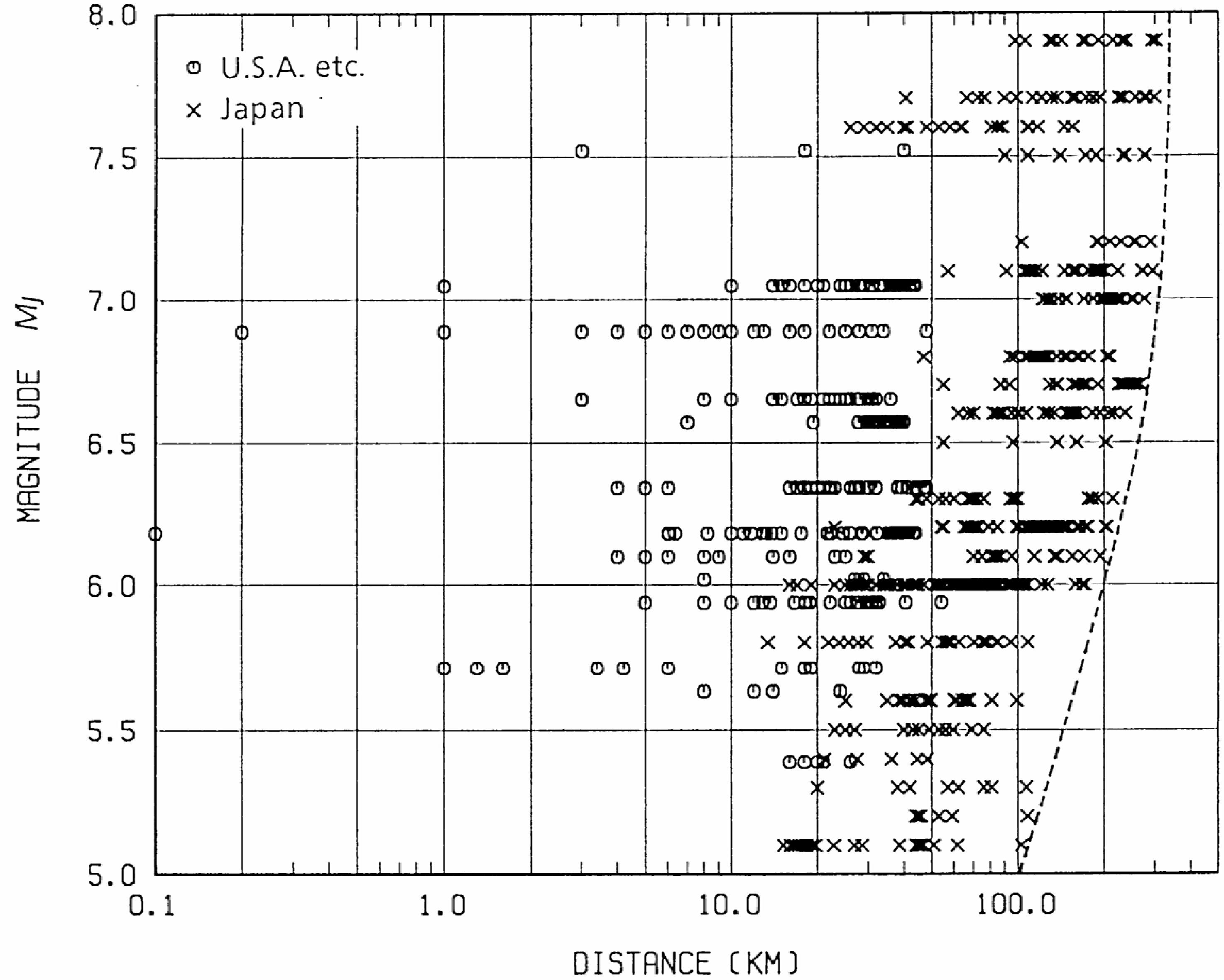

Data distribution used by Fukushima and Tanaka (1990) attenuation relation of PGA

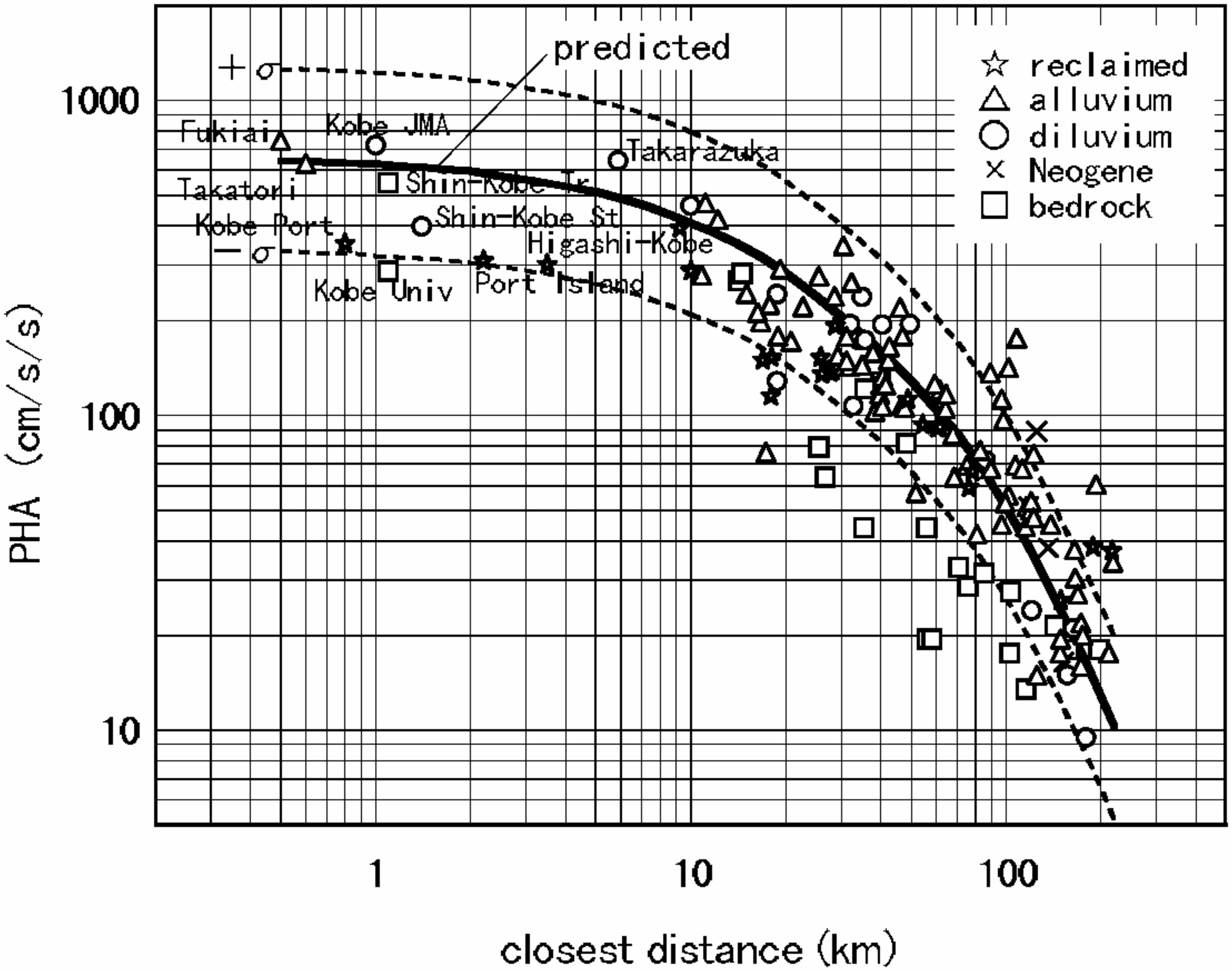

Comparison between predicted PGA by the attenuation relation and data observed during the 1995 Hyogo-ken Nanbu earthquake.

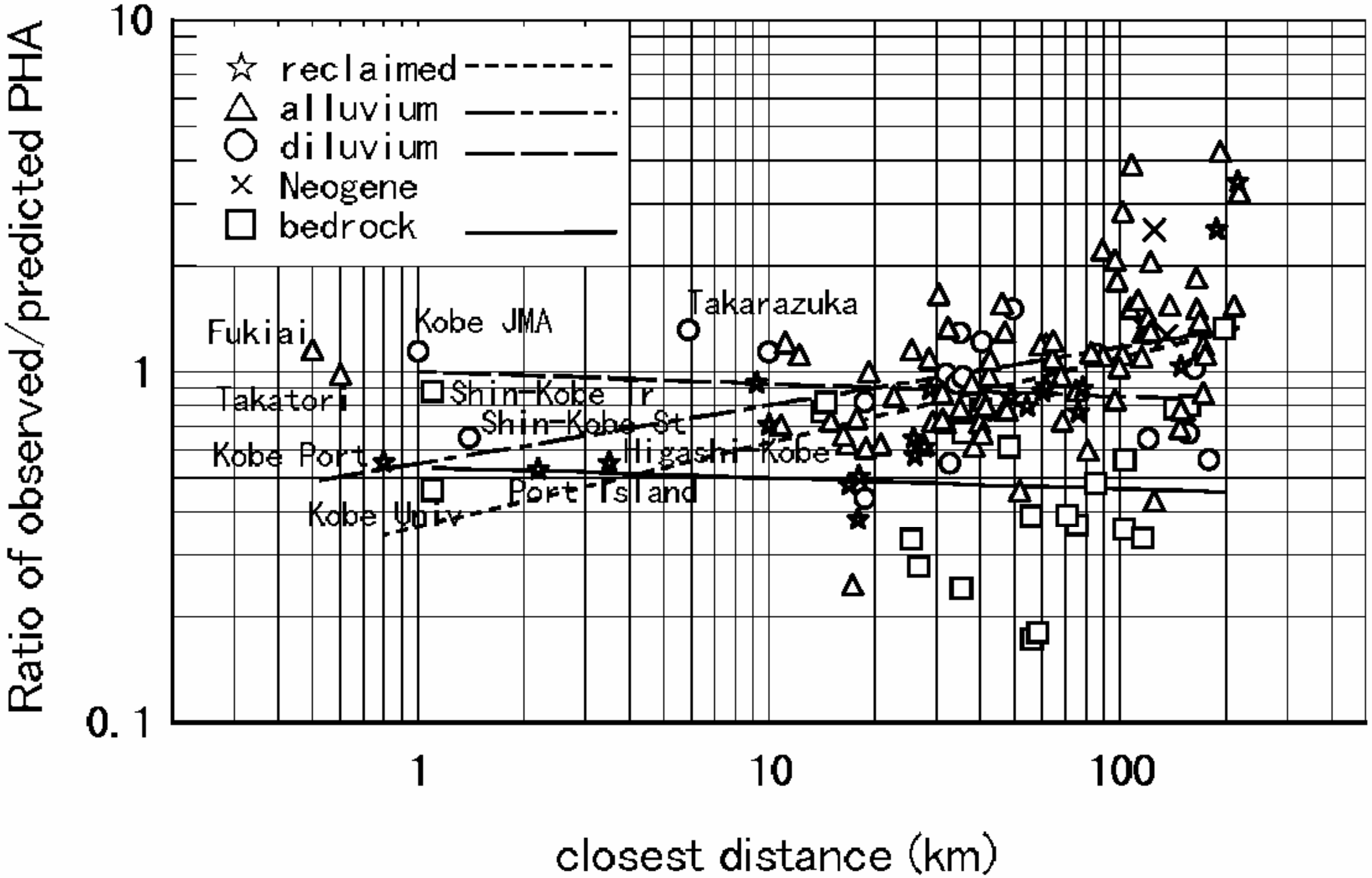

Ratio between observed and predicted PGA by Fukushima & Tanaka (1990)

Damaged pier during the 1995 Hyogo-ken Nanbu earthquake

Vertical array of strong motion observation in Port island Kobe

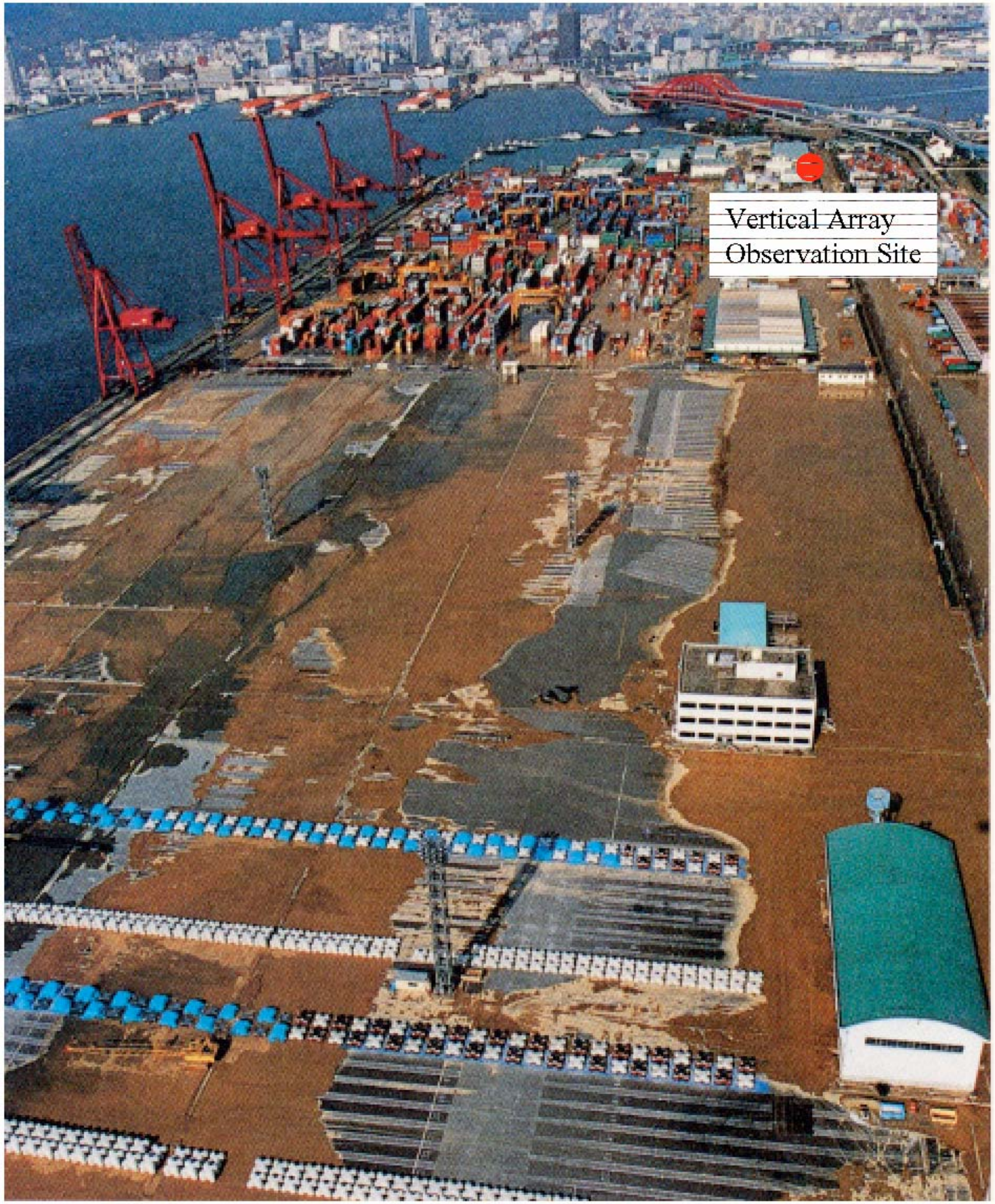

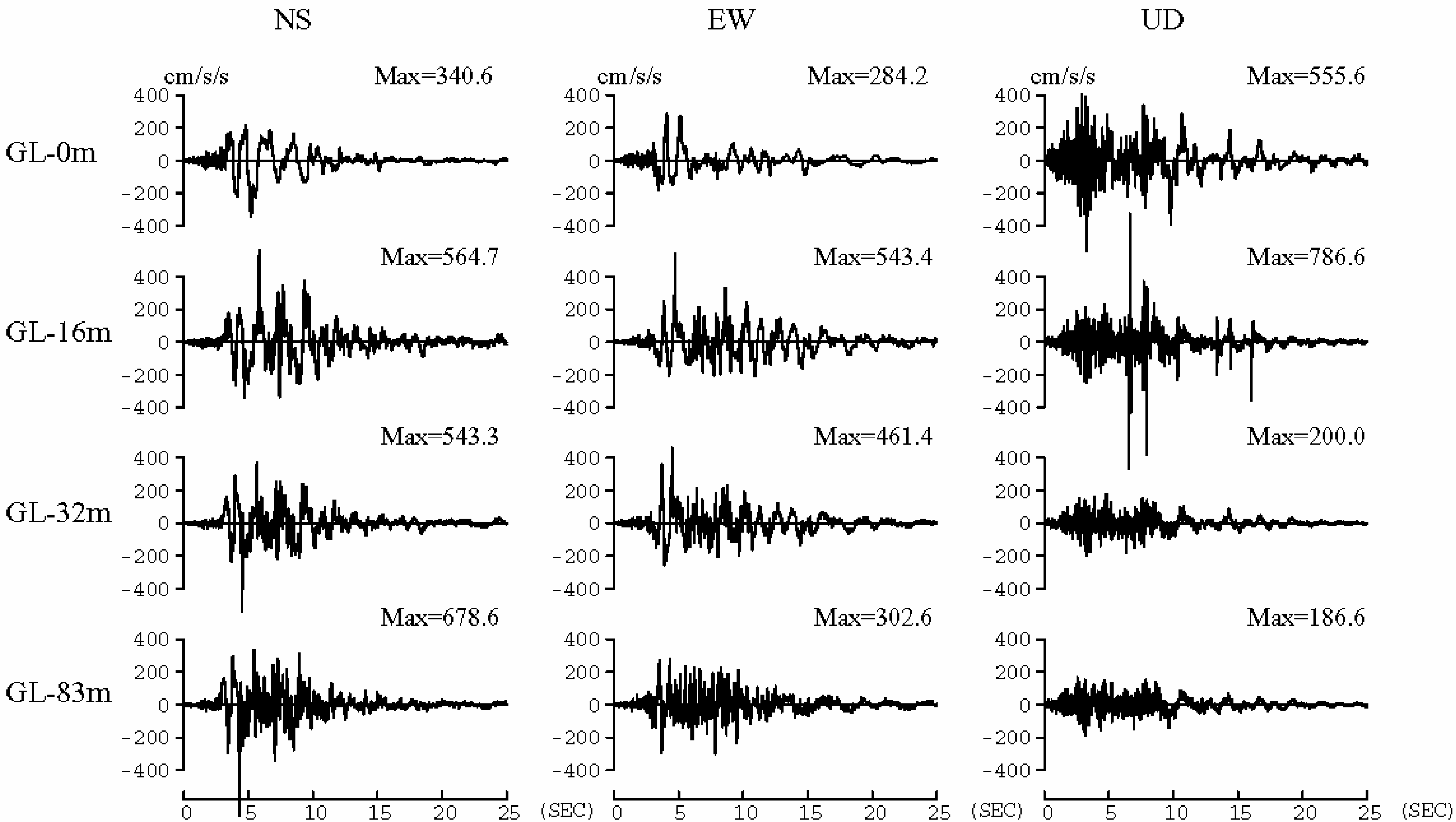

Records of the array

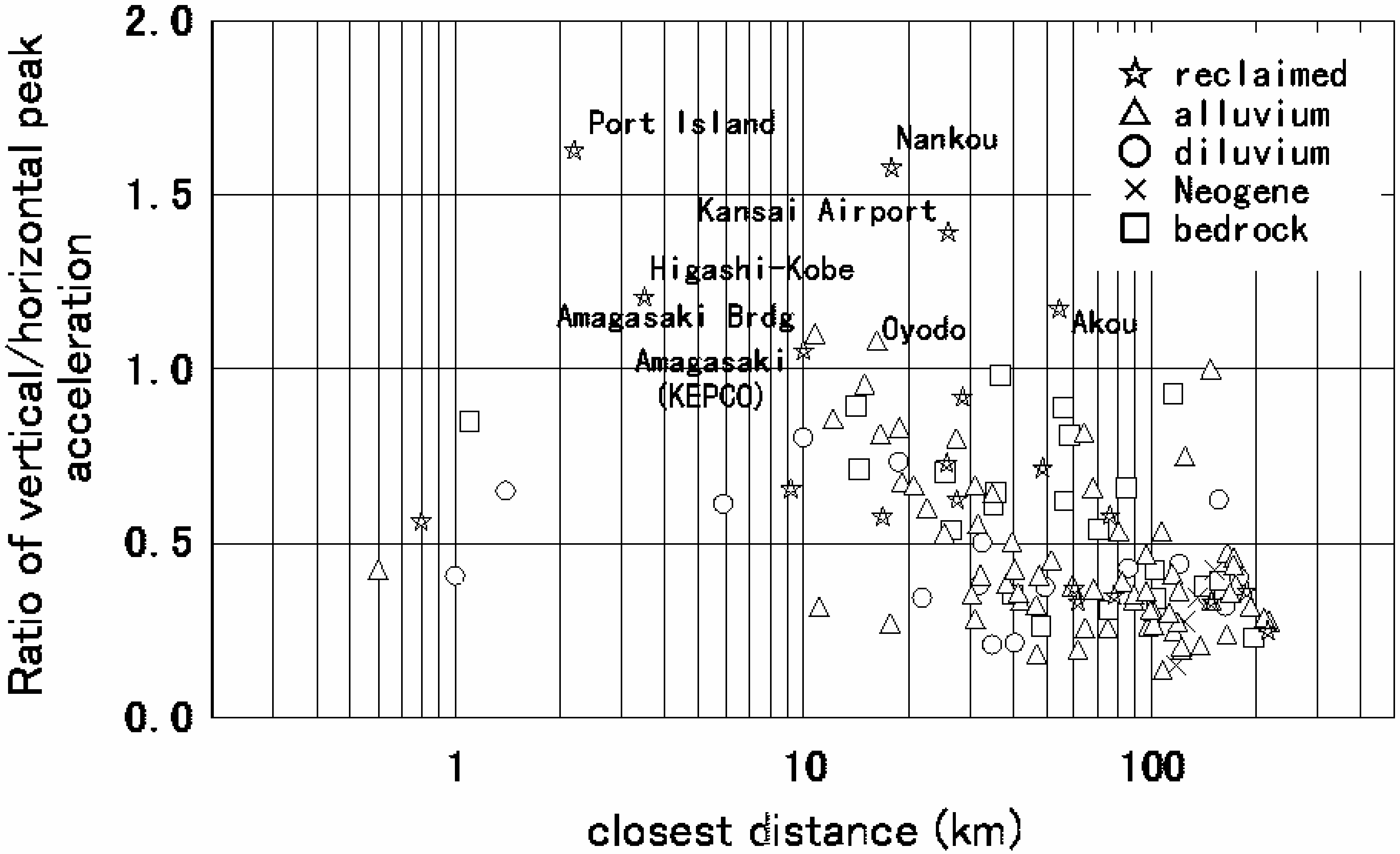

Ratio of vertical/horizontal peak acceleration

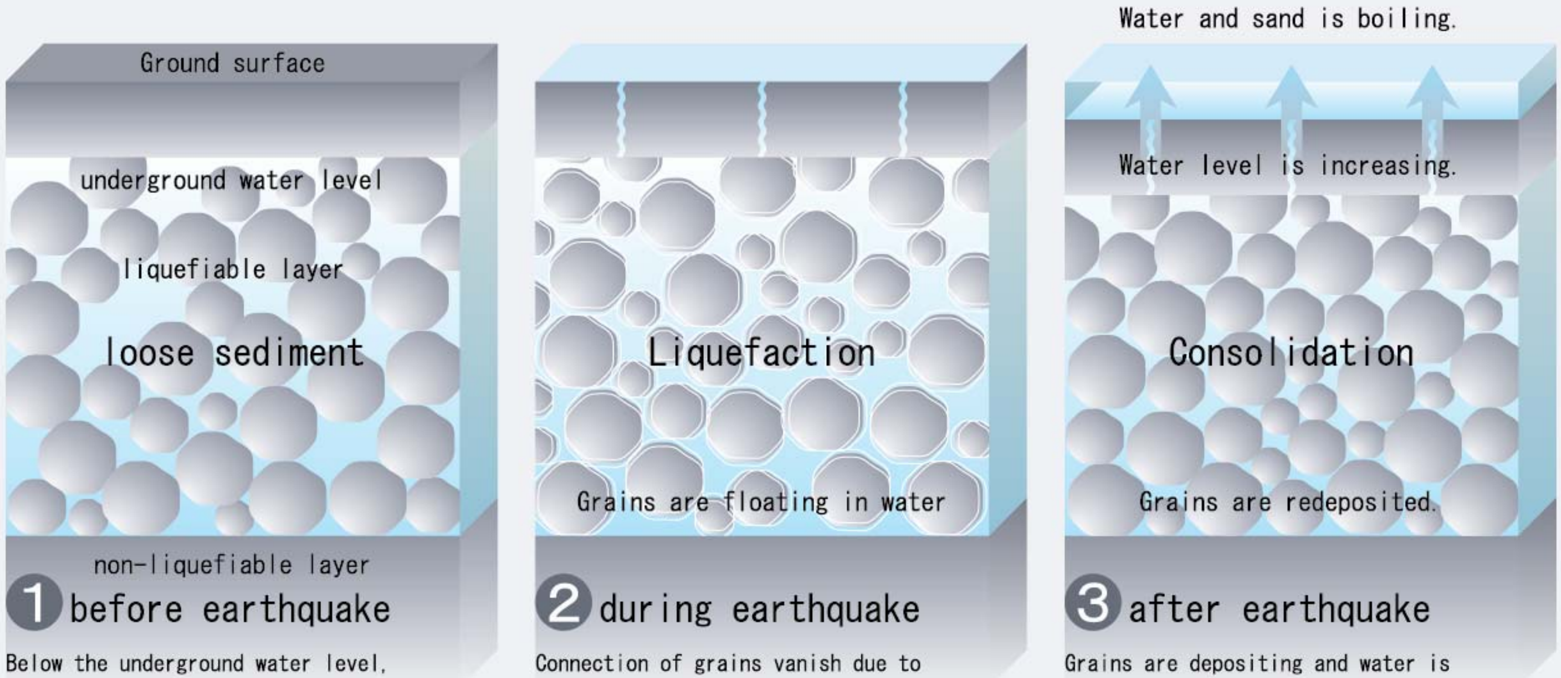

Below the underground water level, grains are stable due to soft contact each other in the loose sand layer.

Connection of grains vanish due to strong ground motion. Namely, grains are floated independently by the water pressure increasing. This unstable situation is continued from several seconds to few ten seconds and buildings are subsided and underground structures are floated.

Grains are depositing and water is drained through cracks of surface layer. Then water pressure gradually decrease. Grains are deposited again in few ten minutes. Finally, grains are consolidated.

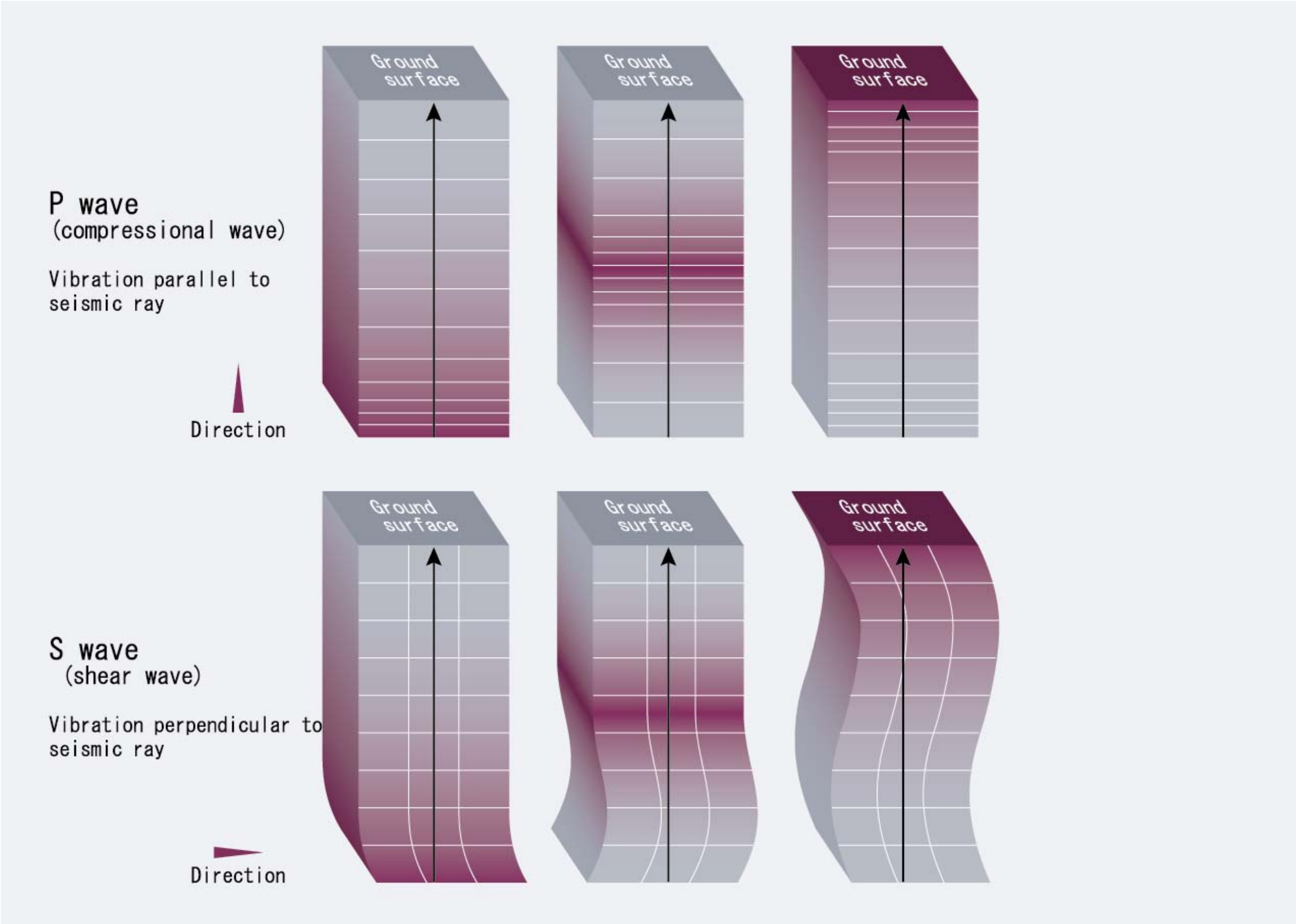
P wave
(compressional wave)
Vibration parallel to seismic ray
Direction
S wave
(shear wave)
Vibration perpendicular to seismic ray
Direction
Ground surface
Ground surface
Ground surface
Ground surface
Ground surface
Ground surface

Relation between predicted PHA and ratio of observed/predicted PHA

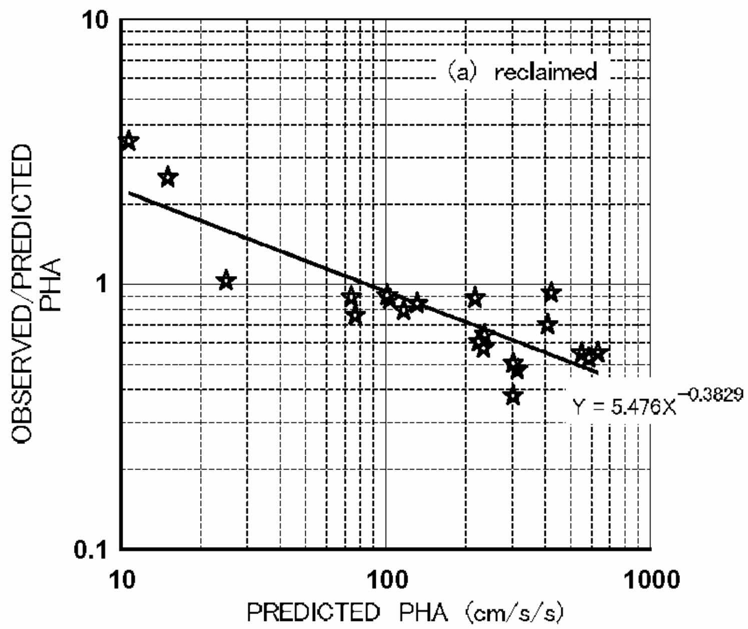

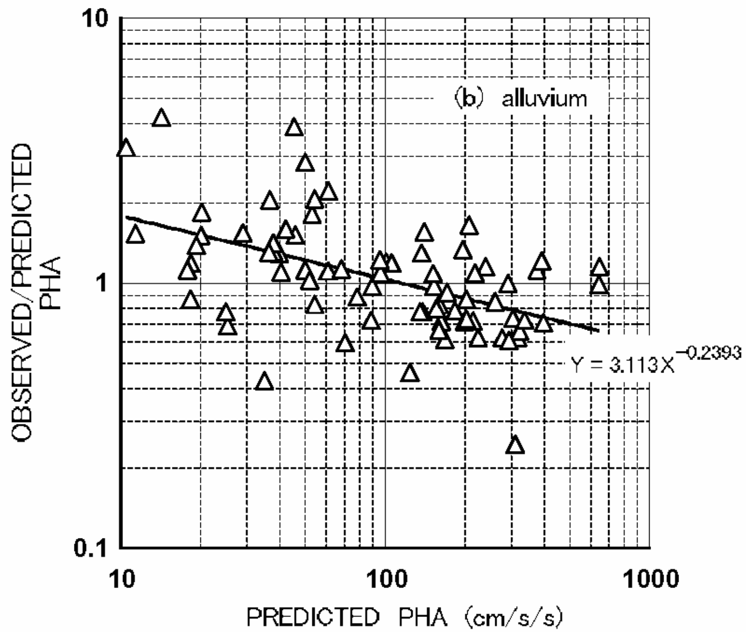

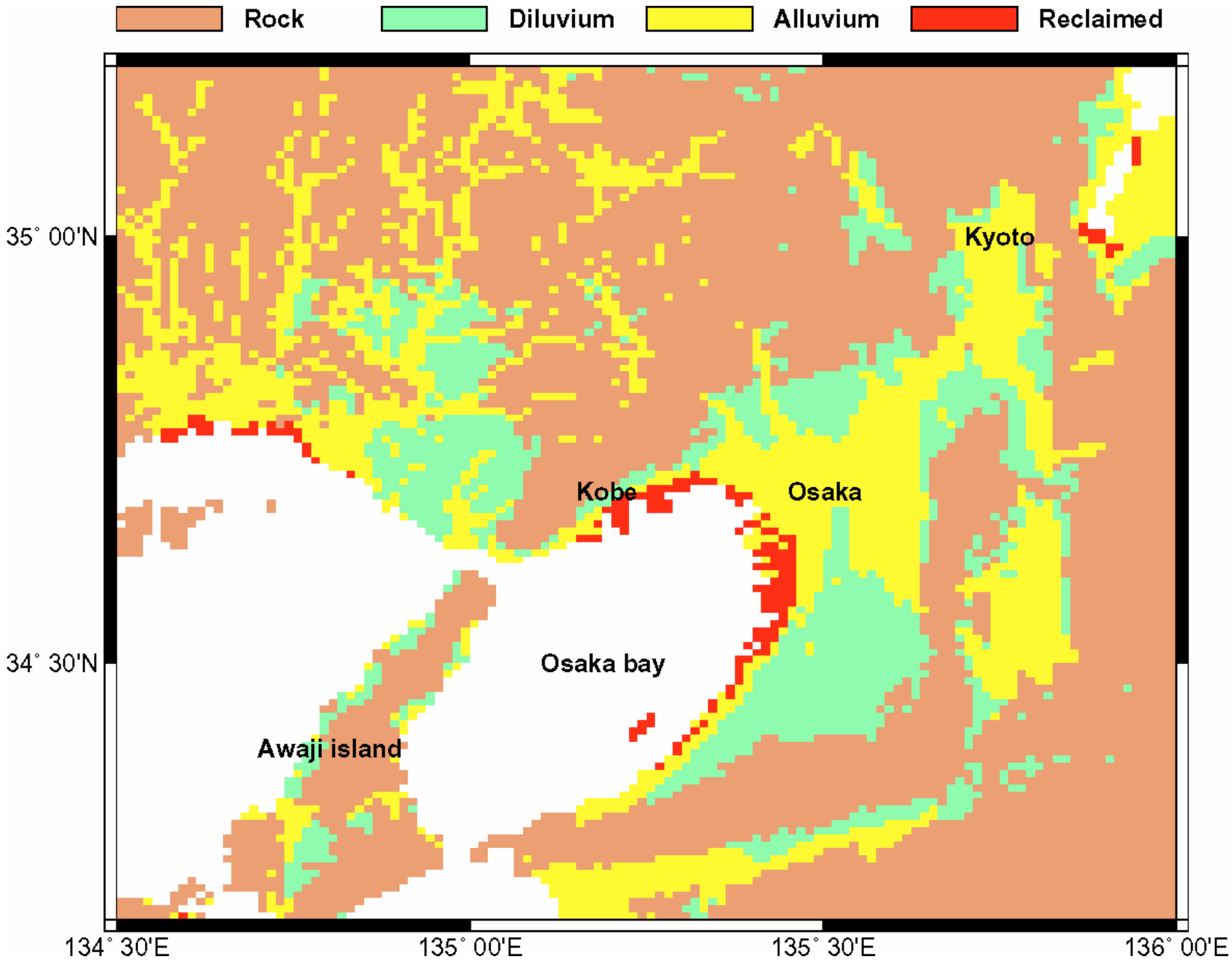

Distribution of rock, diluvium (consolidated), alluvium and reclaimed ground near Kobe

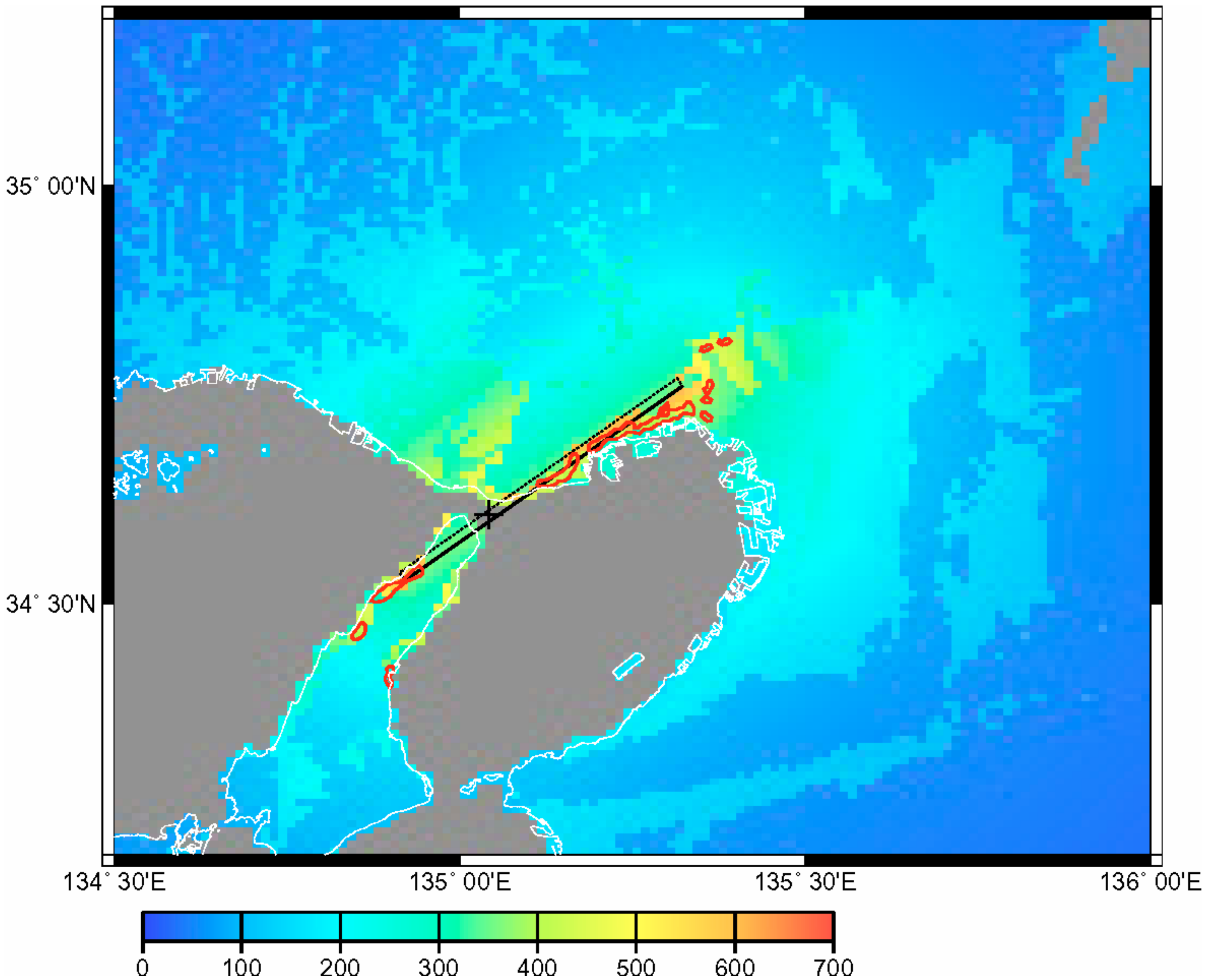

Corrected distribution of predicted PGA by Fukushima & Tanaka (1990)

Incline building due to liquefaction during the Kocaeli earthquake

Sand boiling near the incline building

PGV

Requirement from national project

Advantage

- Corresponding to intensity
- Corresponding to structural damages

Disadvantage

- Less data than PGA
- Confusing frequency component
- Only next attenuation was available

(Si & Midorikawa, 1999 in Japanese local journal)

Data used in Si&Midorikawa(1999)

Table 1. The list of the earthquakes in the database

NO.	Earthquake	Date	M_w	Depth	Number of recordings		Fault Type	Weight	Reference
					Peak acceleration	Peak velocity			
1	Off Tokachi	1968.05.16	8.2	15	10	10	Inter-plate	C	1, 2
2	Off Nemuro Pen.	1973.06.17	7.8	25	6	4	Inter-plate	C	1, 2
3	Near Izu Oshima	1978.01.14	6.6	7	8	12	Crustal	C	1, 3
4	Off Miyagi Pref.	1978.06.12	7.6	37	13	10	Inter-plate	C	1
5	East off Izu Pen.	1980.06.29	6.5	7	19	16	Crustal	B	1, 3
6	Off Urakawa	1982.03.21	6.9	25	19	9	Crustal	C	1, 2
7	Nihonkai-Chubu	1983.05.26	7.8	6	21	17	Inter-plate	C	1
8	Off Hyuganada	1984.08.07	6.9	30	9	8	Intra-plate	C	4,5,6,7
9	Central Iwate Pref.	1987.01.09	6.6	73	10	5	Intra-plate	C	4,8,9
10	Northern Hidaka Mt.	1987.01.14	6.8	120	16	9	Intra-plate	C	4,9,10
11	East off Chiba Pref.	1987.12.17	6.7	30	173	47	Crustal	A	1,3,11
12	Off Kushiro	1993.01.15	7.6	105	51	21	Intra-plate	B	4,11
13	Off Noto Pen.	1993.02.07	6.3	15	21	5	Crustal	C	4,13,14,15,16,17
14	Southwest off Hokkaido	1993.07.12	7.7	10	52	18	Inter-plate	B	4,12,18
15	East off Hokkaido	1994.10.04	8.3	35	41	17	Intra-plate	B	4,18,19,20
16	Far off Sanriku	1994.12.28	7.7	35	83	30	Inter-plate	B	4,22,23,24
17	Hyogo-ken Nanbu	1995.01.17	6.9	10	85	47	Crustal	A	4,25
18	Off Hyuganada	1996.10.19	6.7	25	106	67	Inter-plate	A	4,26
19	Northwestern Kagoshima Pref.	1997.03.26	6.1	6	121	68	Crustal	A	4,27,28
20	Northwestern Kagoshima Pref.	1997.05.13	6.0	7	121	64	Crustal	A	4,27,29
21	Northern Yamaguchi Pref.	1997.06.25	5.8	10	152	59	Crustal	A	4,27,30

Total 394 data

High cut 10Hz ;
Maximum of 2 horizontal components

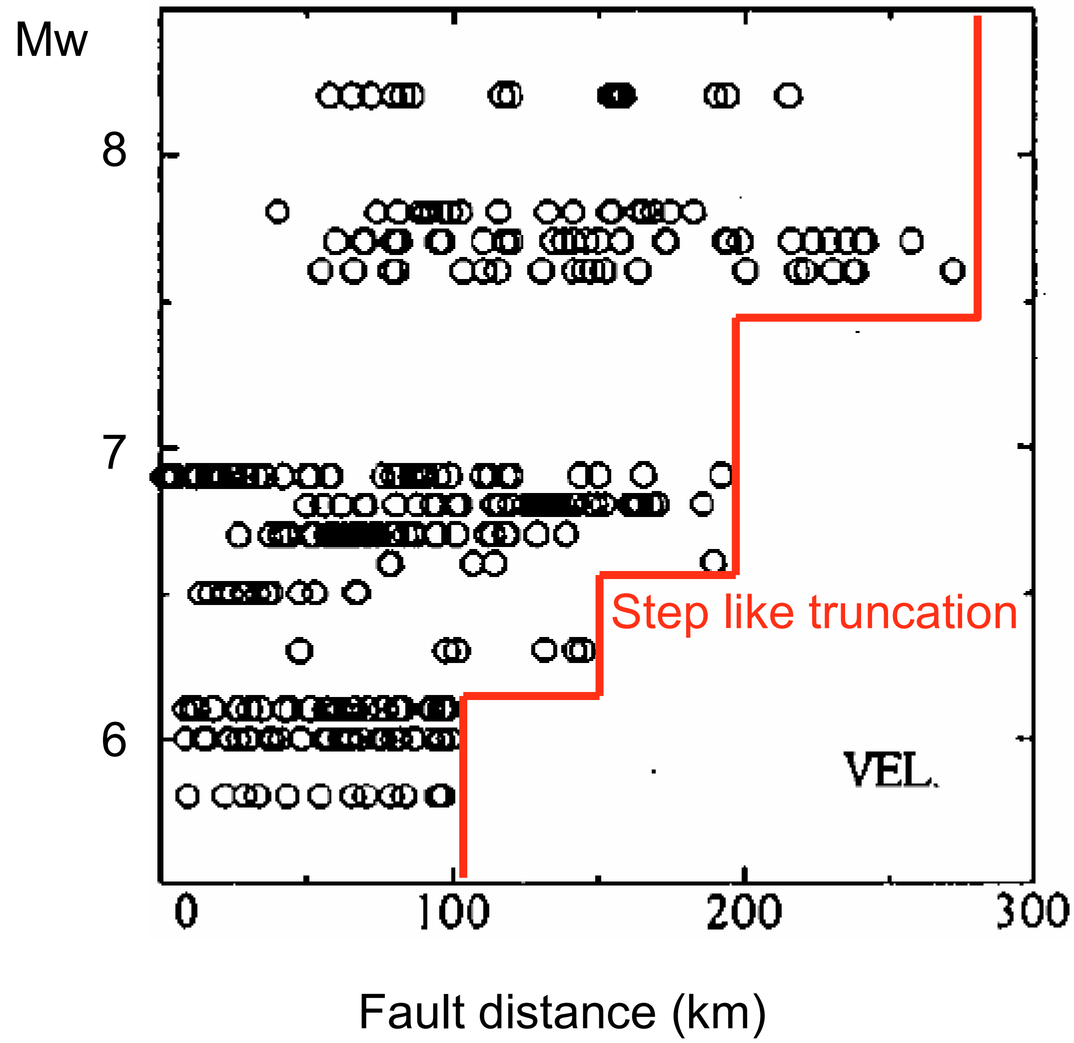

PGVcor=PGVorg/ARV

Matsuoka&Midorikawa (1994)

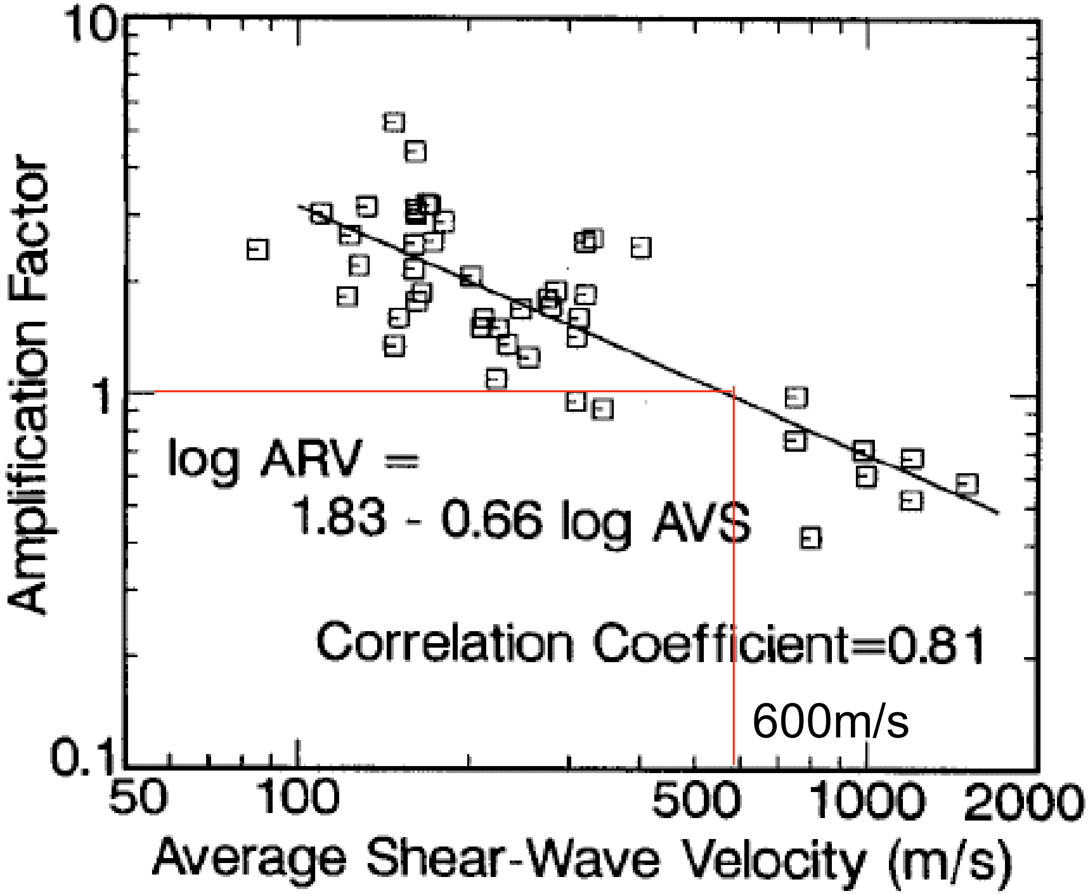

Fig. 6 Correlation of Average Shear Wave Velocity with Amplification Factor for Peak Ground Velocity

Where AVS is average shear wave velocity from surface to depth of 30m, ARV is amplification factor : ratio between ARV of AVS=600 and that of other AVS

Observed PGV is converted to PGV for Vs=600m/s

$$\log A = b - \log(X + c) - kX$$

Where A is peak horizontal velocity, X is closest distance from fault plane to site (if the plane is unknown, hypocentral distance), and b, c and k are coefficients.

Distance coefficient ‘k’ is hypothesized to be 0.002.

$$c = c_1 10^{c_2 M_w}$$

C_2 is hypothesized to be 0.5.

C_1 is determined from 5 events including the 1985 Chile earthquake.

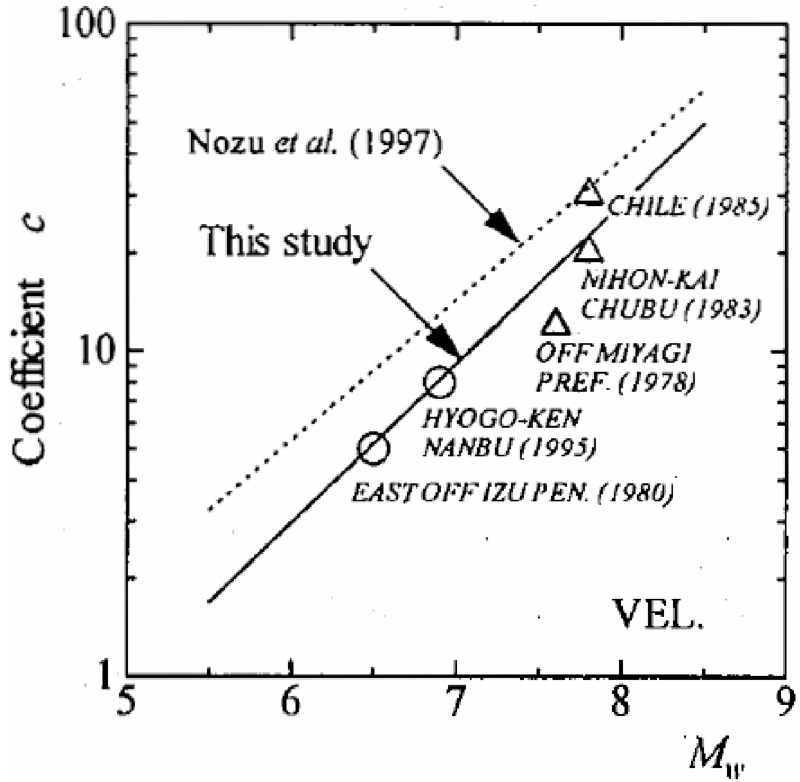

Fig.6. Coefficient c for peak ground velocity

$$\log A = b - \log(X+c) - kX$$

$$b = aMw + hD + \Sigma d_i S_i + e + \varepsilon$$

Where D is focal depth, S is source type, e is a coefficient and is error. a and h are coefficients. di is Kronecher's Delta indicating 3 source types of crustal, inter- and intra-plate events.

'a' is decided just by try&error scheme.

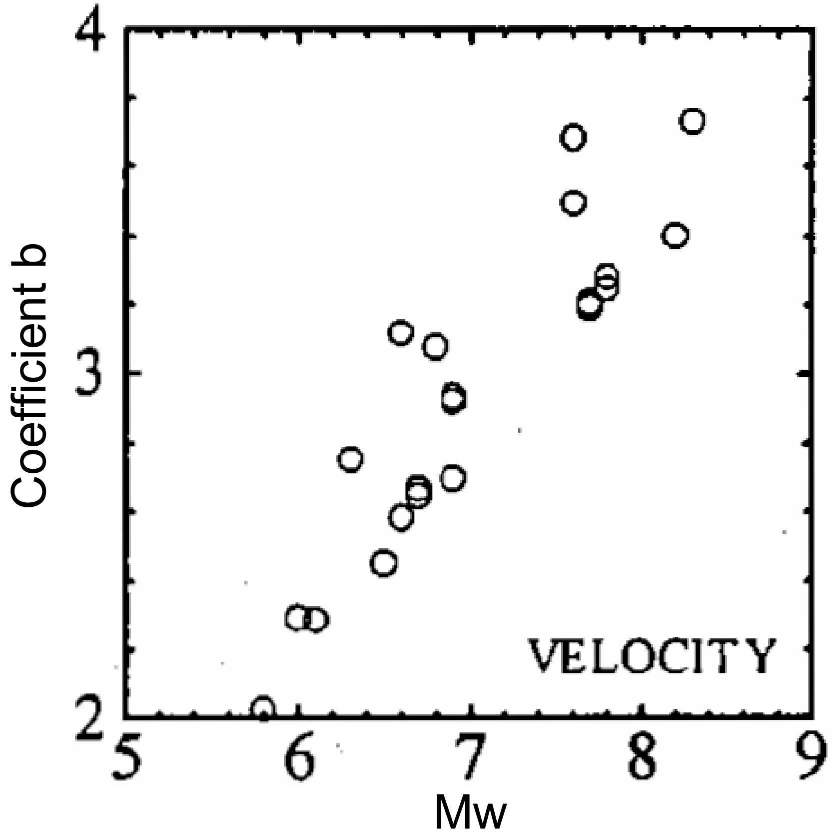

Weighting

X ≤25km: ×8
25<X<50km: ×4
50<x<100km: ×2

Not uniform like Campbell (1981)

A: ×3
B: ×2
C: ×1

Larger weight for larger number of recordings (opposite of Campbell, 1981)

Residual consideration

Without any residual plot for individual parameters, just indicated 0.23 of standard error

Spectral Acceleration

Damaged building in Kobe

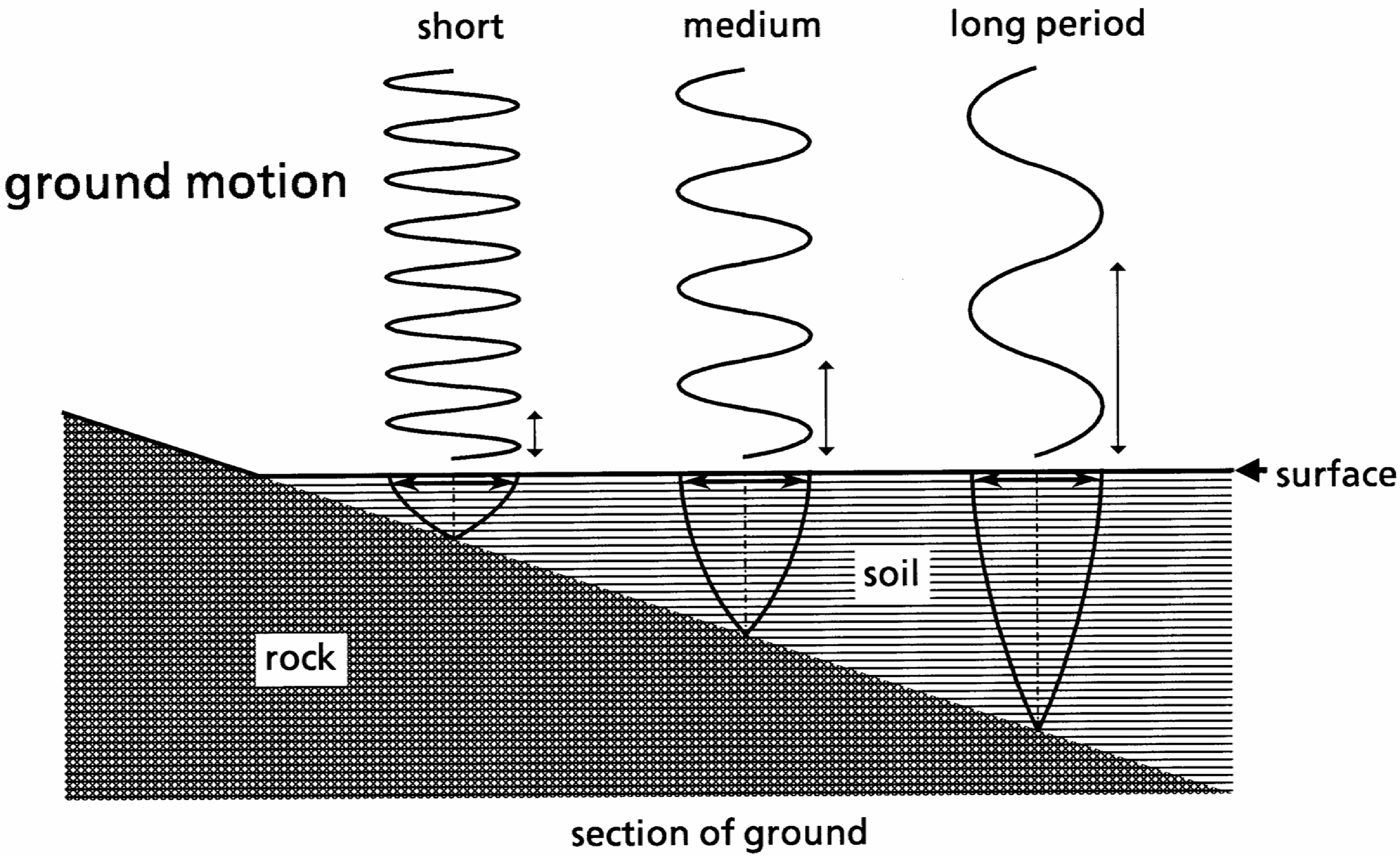
short
medium
long period
ground motion
surface
soil
rock
section of ground

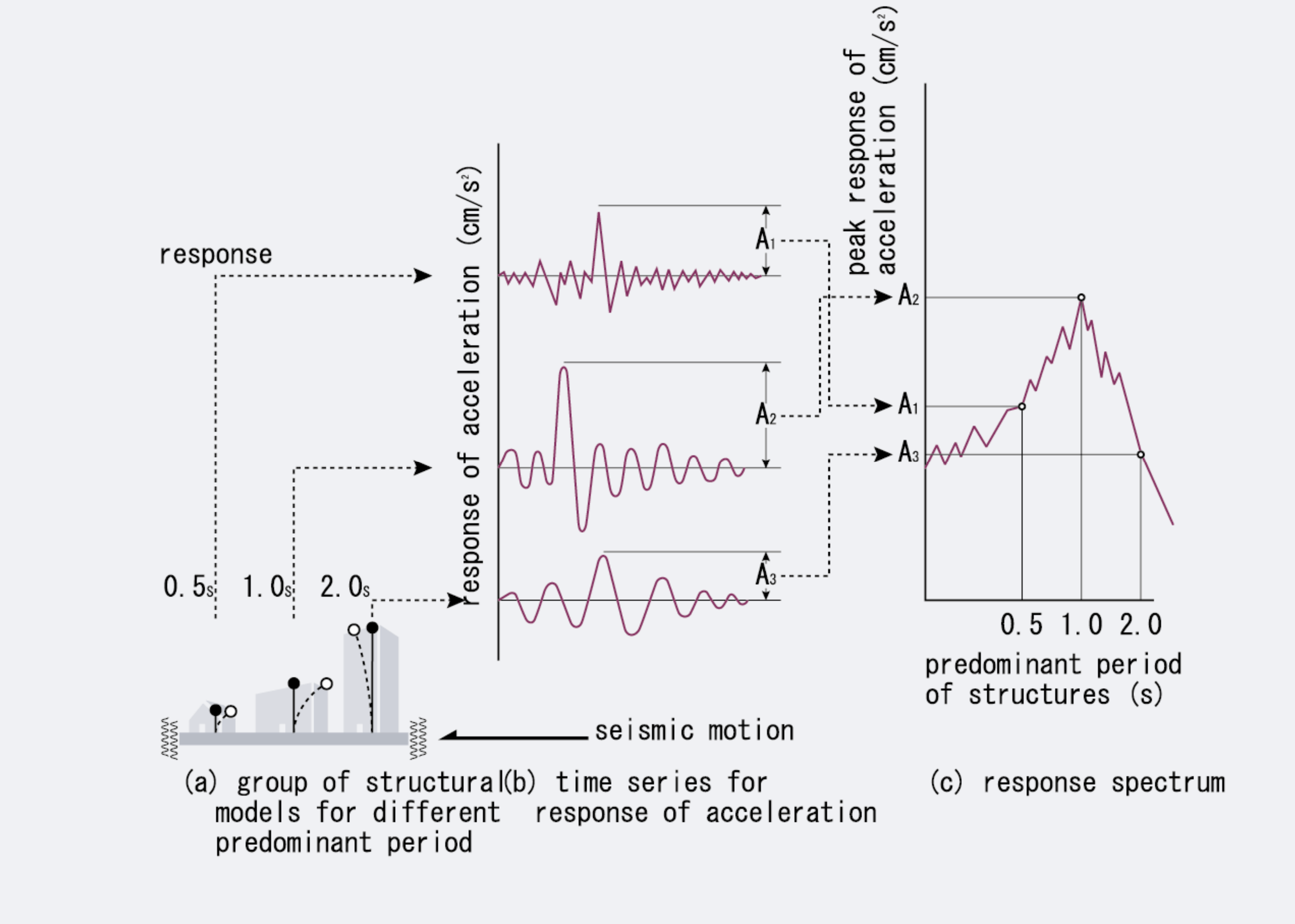
response
0.5s
1.0s
2.0s
response of acceleration (cm/s²)
A1
A2
A3
peak response of acceleration (cm/s²)
A2
A1
A3
0.5 1.0 2.0
predominant period of structures (s)
seismic motion
(a) group of structural models for different predominant period
(b) time series for response of acceleration
(c) response spectrum

Attenuation relation for west Eurasia determined with recent near-fault records from California, Japan and Turkey

Yoshimitsu Fukushima, (Shimizu Corp.) Japan
Catherine Berge-Thierry, (IRSN) France
Philippe Volant, (IRSN) France
Daphné-Anne Griot-Pommera, (*Hémisphères*) France
Fabrice Cotton, (*Université Joseph Fourier*) France

J. Earthq Eng., 7(3), pp.1-26.

Resume

- An attenuation relation for west Eurasia (mainly in Europe)
- Adding an near fault amplitude saturation term in the regression model
- West Eurasian strong-motions recorded plus near fault records of California, USA, the 1995 Hyogo-ken Nanbu (Kobe), Japan and the 1999 Kocaeli (Izmit), Turkey
- An Iterative regression procedure is applied for non-linear model.

Object

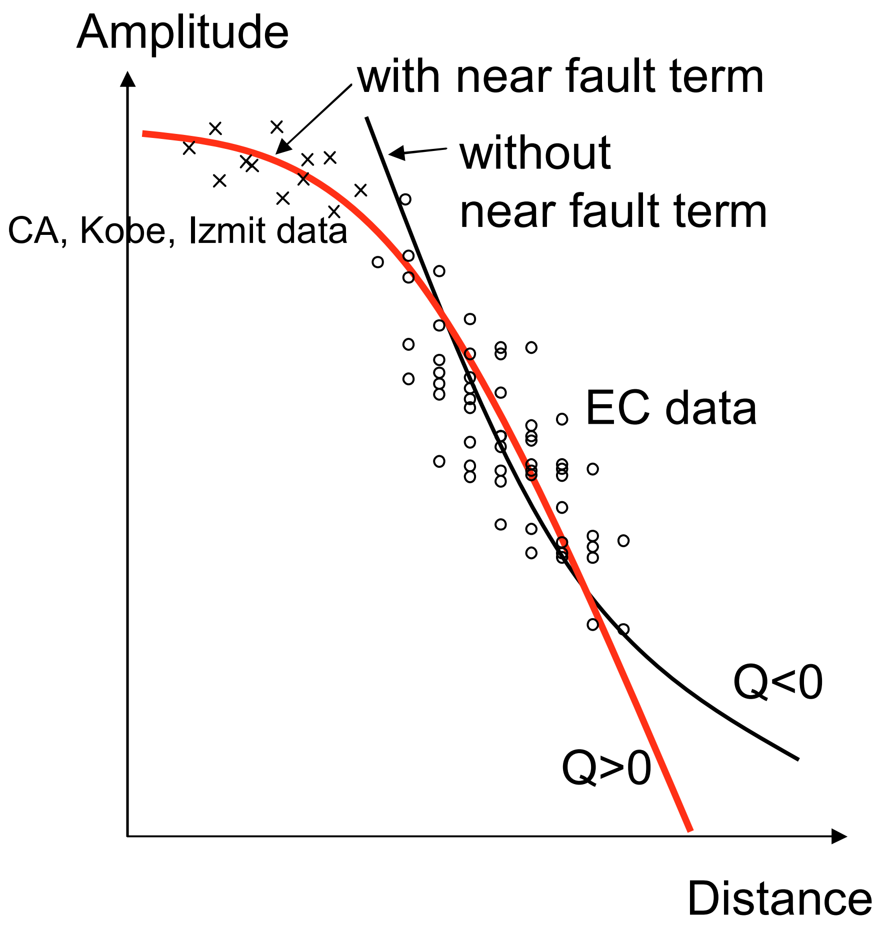

- In France, an empirical attenuation model has been recently developed to support the French Safety Rule for nuclear power plants [Berge-Thierry *et al*., 2003].
- However it was without near fault saturation term
- Therefore, negative Q values were determined.
- Near fault saturation term may constrain Q in positive.

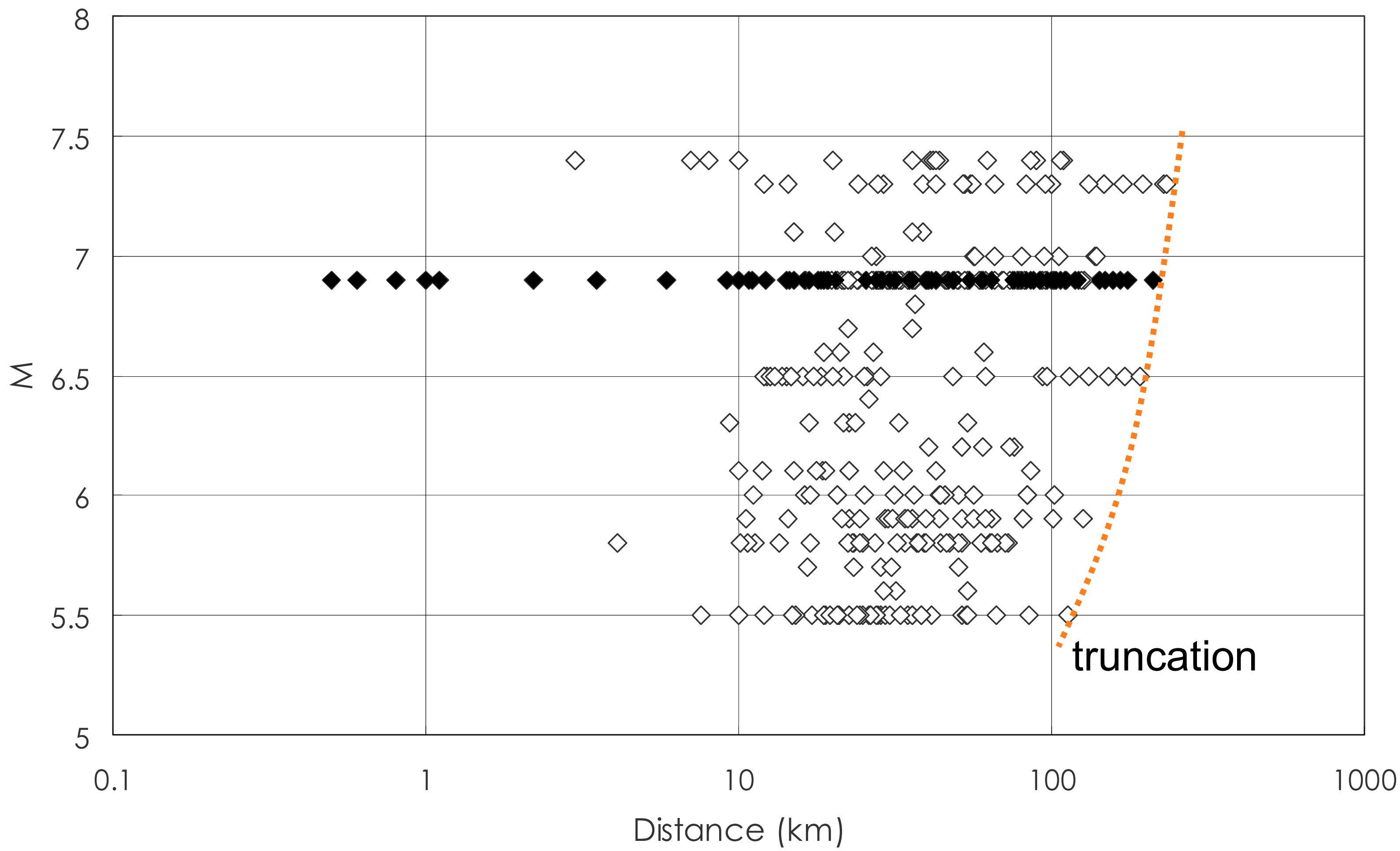

Distribution of magnitude and distance for records used in this study.
Dark points indicate the Hyogo-ken Nanbu earthquake

Regression Model: $\log Sa(f)=a(f)M - \log(R+d(f)*10^{e(f)M})+b(f)R+\Sigma cj(f)\delta j$

where $Sa(f)$ is the spectral acceleration with 5% damping in cm/s^2. Coefficients a, b, cj, d, and e (functions of frequency f (Hz)) are the regression coefficients. The suffix j is 1 for rock sites and 2 for soil sites. Variable δj is a dummy variable related to the quality of the soil; $\delta 1$ is equal to 1 for rock and $\delta 2$ is equal to 1 for soil.

At 0 km distance, this model converges to $\{a(f)+e(f)\}M-\log d(f)+\Sigma cj(f)\delta j$.

At far distance ($R>> d(f)*10^{e(f)M}$), the model converges to $a(f)M-\log R+b(f)R+\Sigma cj(f)\delta j$, the body wave attenuation model.

Two-step regression analysis: Fukushima & Tanaka (1990, BSSA)

The differences between recorded and predicted values are:

$$\varepsilon i = \log Sa(f)i - \{a(f)Mi - \log(Ri + d(f)*10^{e(f)Mi}) - b(f)Ri + \Sigma cj(f)\delta j\}$$

where i indicates individual data points. The total error, which should be minimized, is

$$\varepsilon = \Sigma \varepsilon\, i^2$$

The error becomes a minimum when

$$\partial\varepsilon/\partial d(f) = 0$$

$d(f)$ is derived iteratively using an initial value of $d(f)_1=0$:

$$d(f)_{k+1} = d(f)_k - \{\partial\varepsilon/\partial d(f)_k\}/\{\partial^2\varepsilon/\partial d(f)_k^2\}$$

When the difference between $d(f)_{k+1}$ and $d(f)_k$ falls below 0.1%, iteration is stopped. With this computed value of $d(f)$, two-step regression analysis is repeated until the standard error is minimized.
Because of instability, we ultimately fixed $e(f)$ at 0.42 [Fukushima *et al*., 2002].

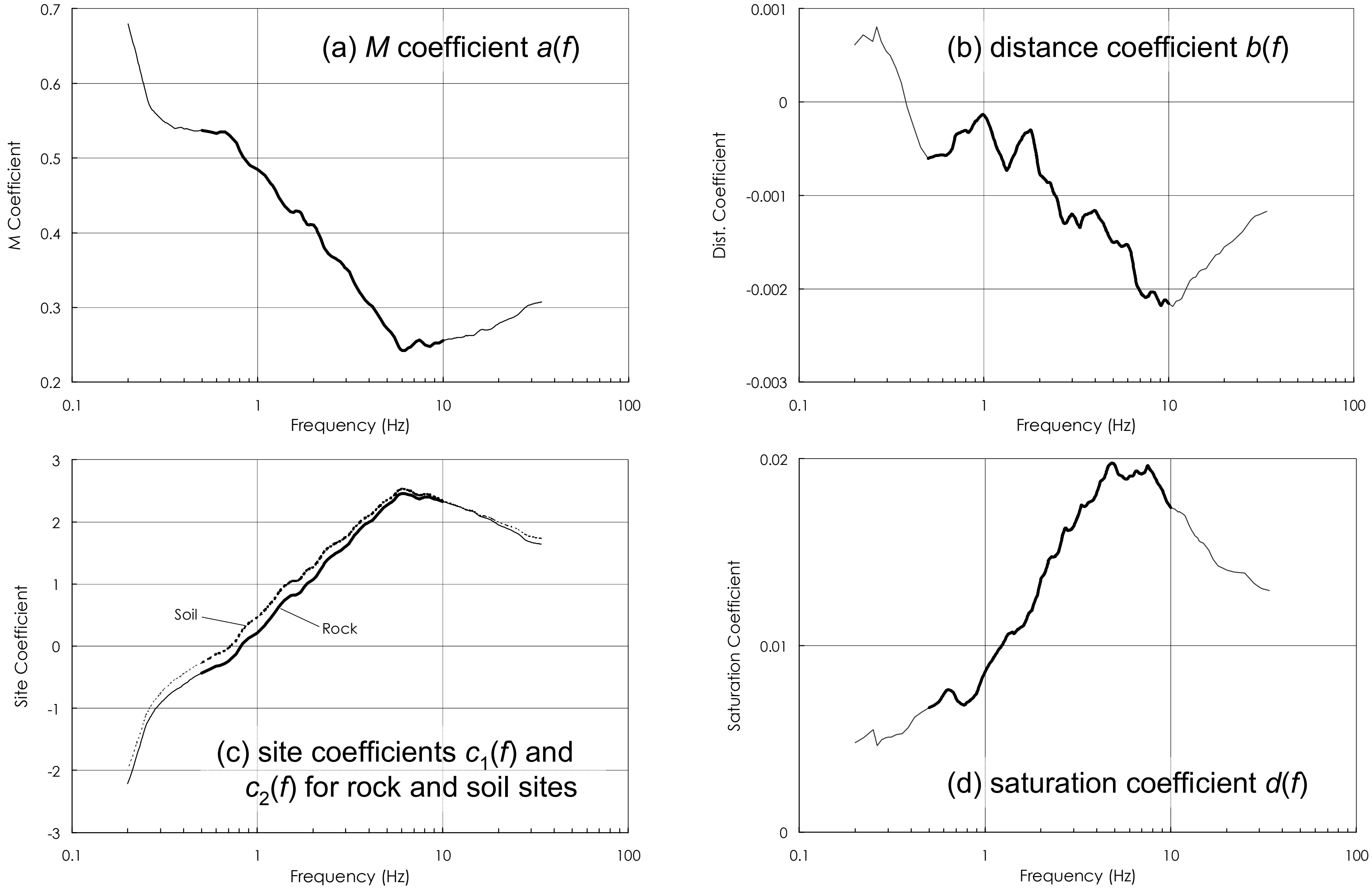

Regression coefficients, Results in reliable range are indicated with thick lines.

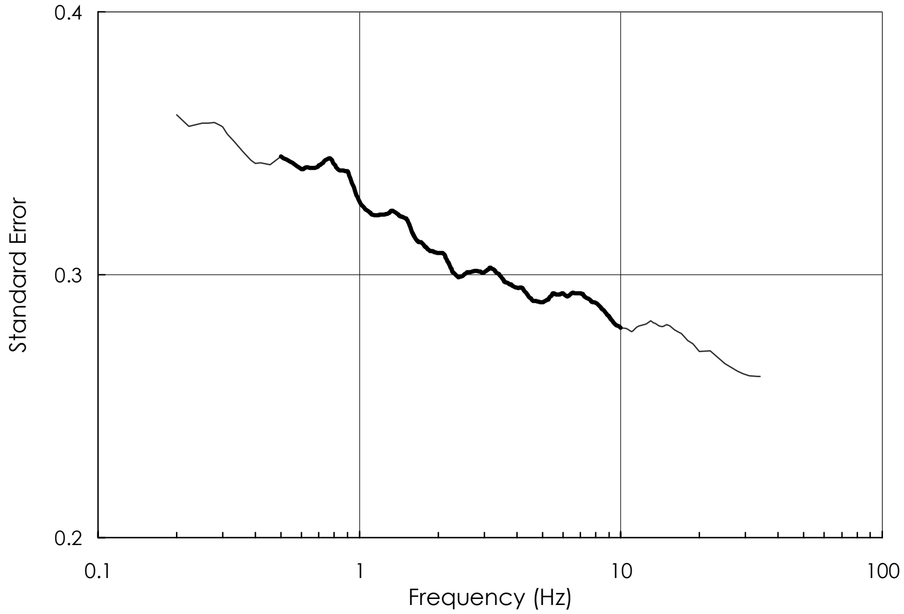

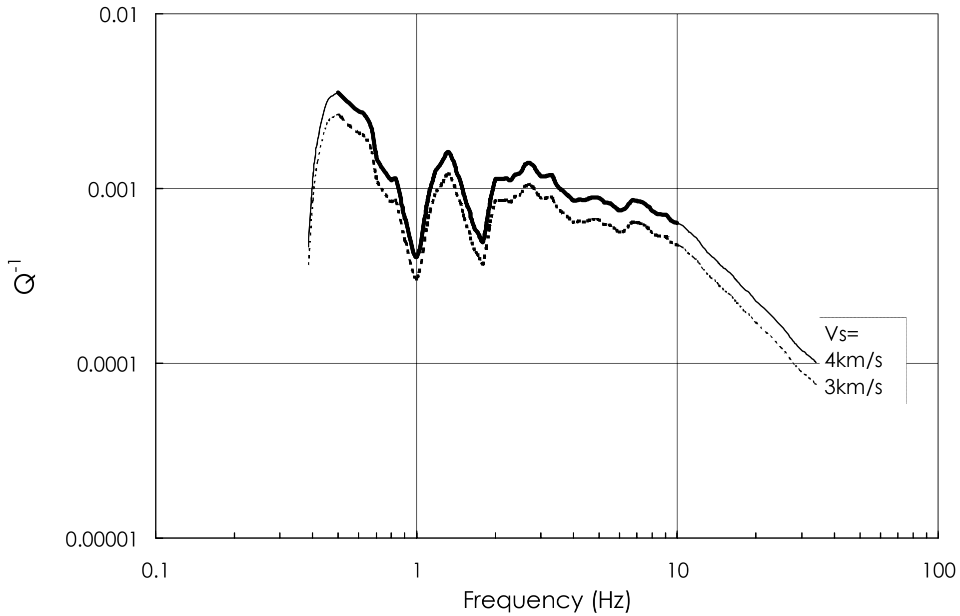

standard errors

converted Q value from *b*(*f*), Solid and broken lines are Q-1 for *Vs* equal to 4.0 and 3.0 km/s

$$Q(f)^{-1} = -b(f)^* Vs/(f^* \pi \log_{10} e) \quad [d(f)^* 10^{e(f)M} \ll R]$$

PGA

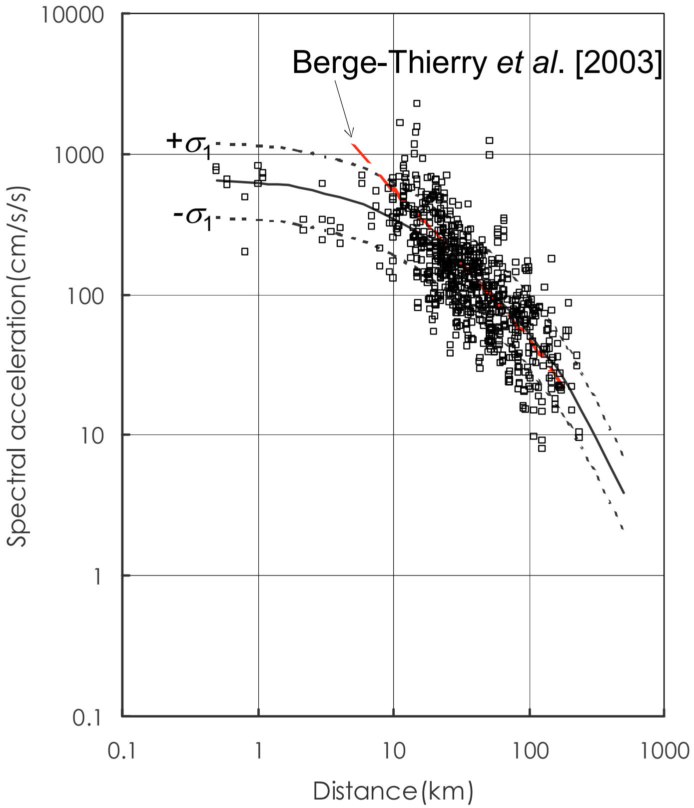

Comparison between predicted spectral acceleration by derived attenuation relation and observed spectral acceleration at *M*7.0.

Observed data points are normalized to *M*7.0 and soil site.

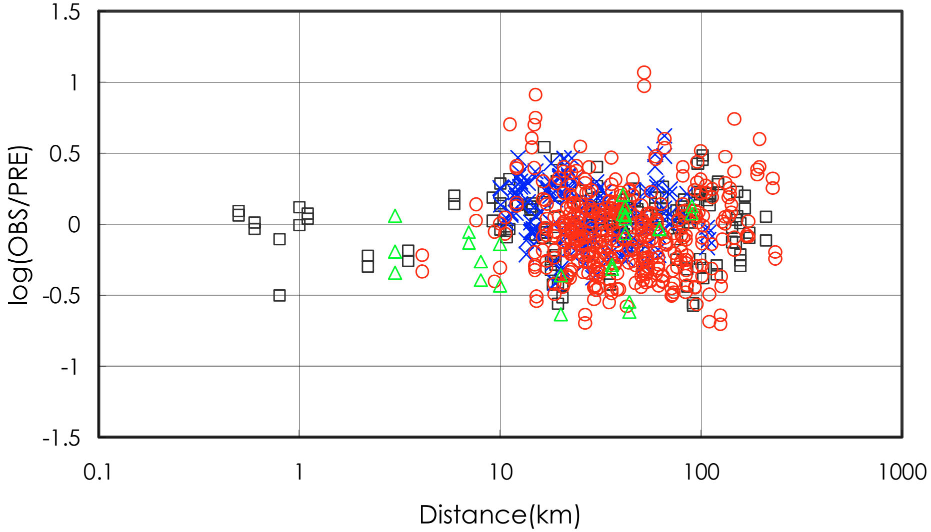

residuals between observed and predicted accelerations as function of distance.

Squares, crosses, circles, and triangles indicate the Hyogo-ken Nanbu, U.S., west Eurasian, and Kocaeli data, respectively

0.5Hz

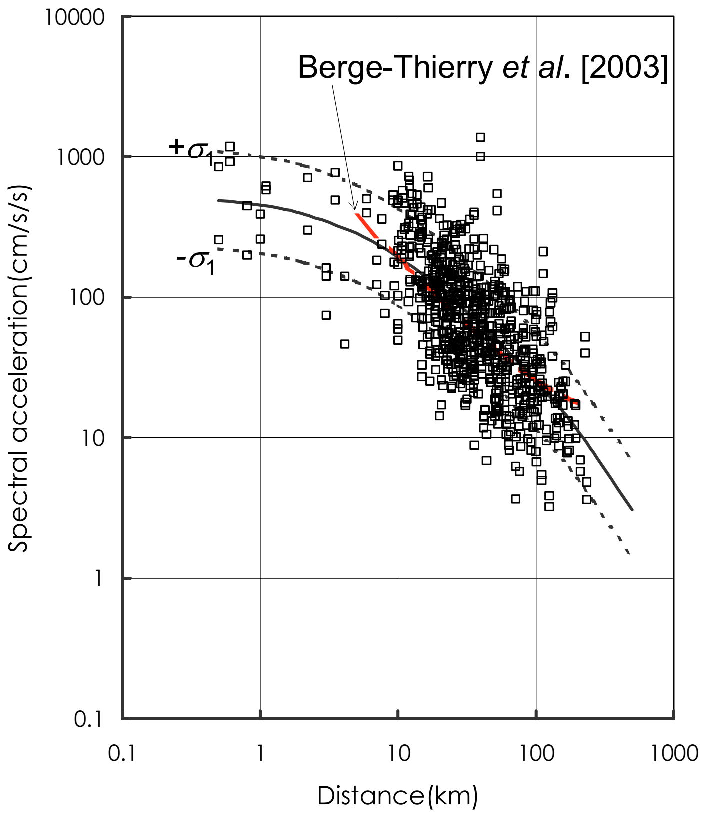

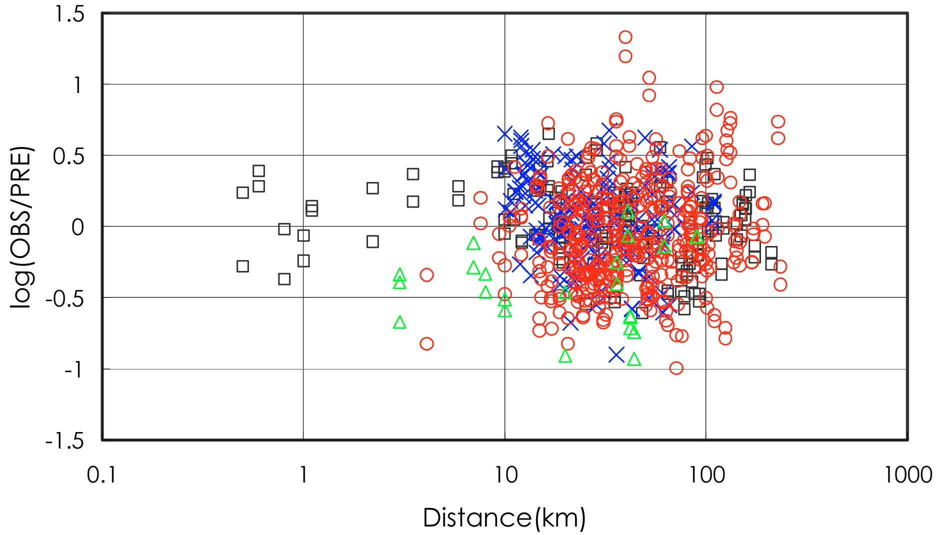

Comparison between predicted spectral acceleration by derived attenuation relation and observed spectral acceleration at *M*7.0.

Observed data points are normalized to *M*7.0 and soil site.

residuals between observed and predicted accelerations as function of distance.

Squares, crosses, circles, and triangles indicate the Hyogo-ken Nanbu, U.S., west Eurasian, and Kocaeli data, respectively

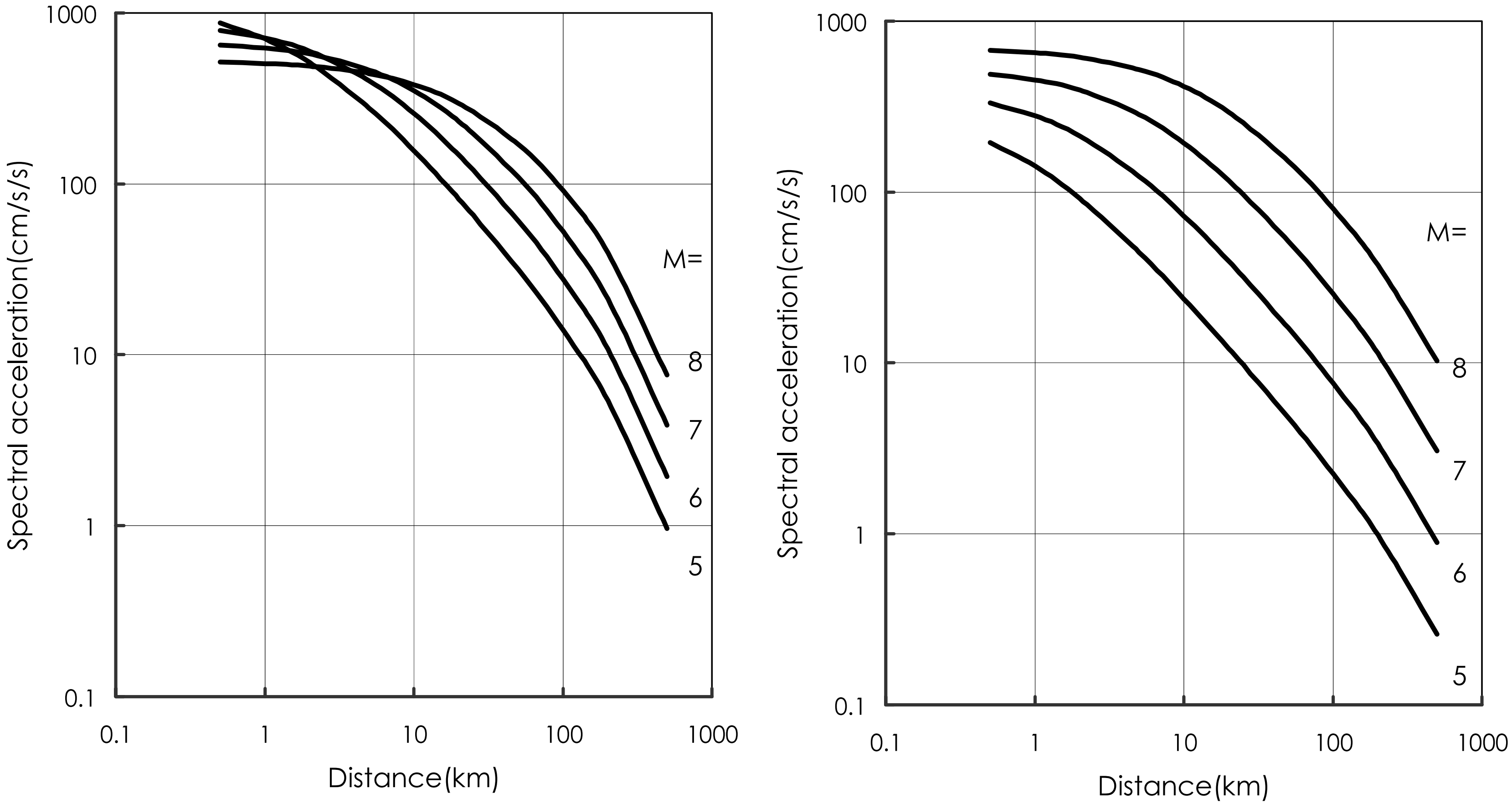

(a) PGA

(b) 0.5Hz

Attenuation curves considering soil site conditions for different earthquake magnitudes: *M* 5 and 8 are outside magnitude range of the dataset

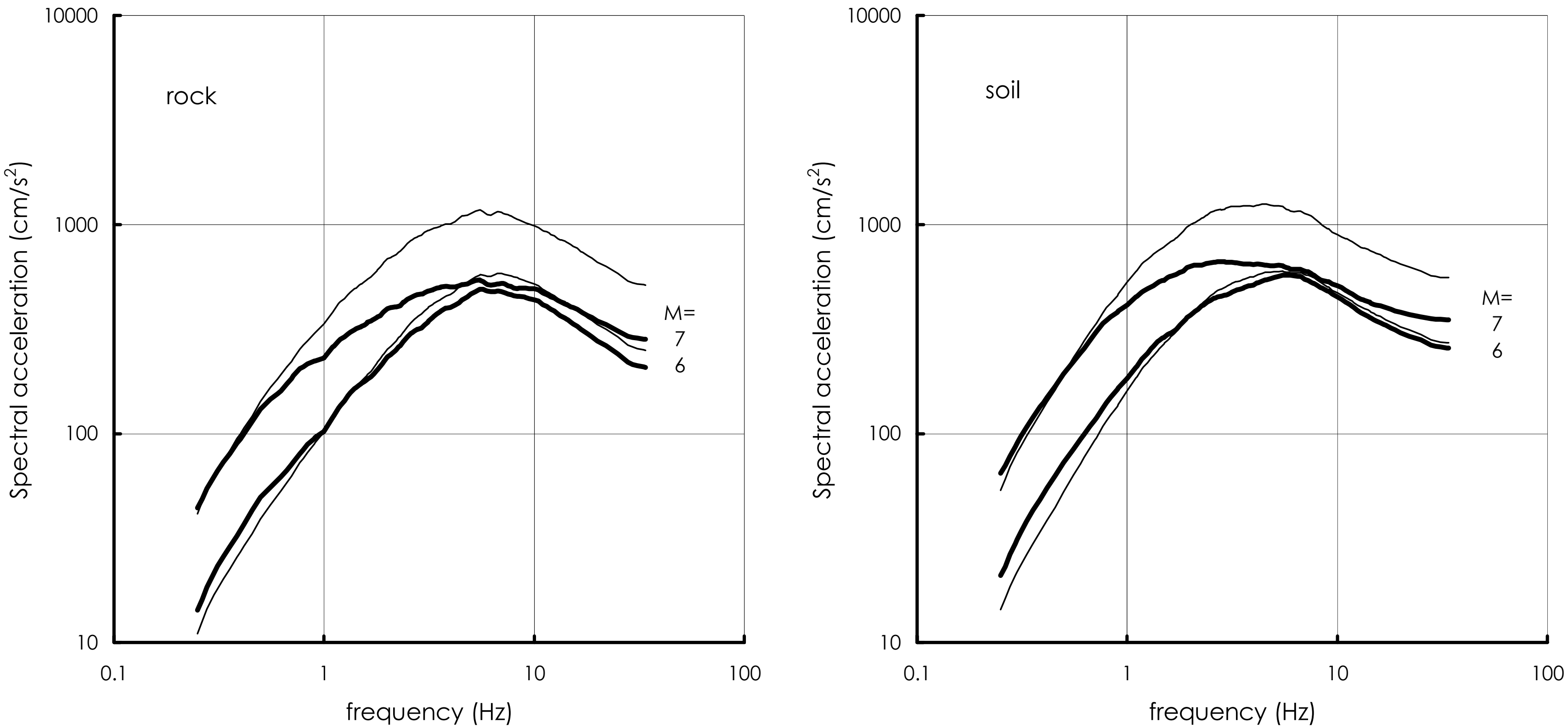

(a) rock sites (b) soil sites

Comparison between predicted spectral accelerations for *M* 6 and *M* 7 at a distance of 10 km using results by Berge-Thierry *et al*. [2003] (thin lines) and this study (thick lines)

The 2003 BAM Iran earthquake

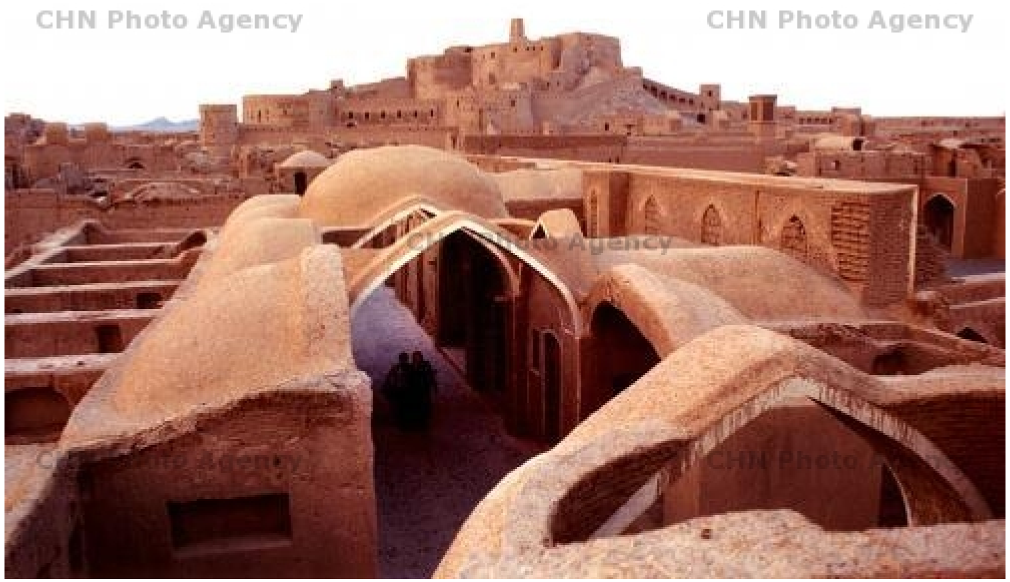

before

after

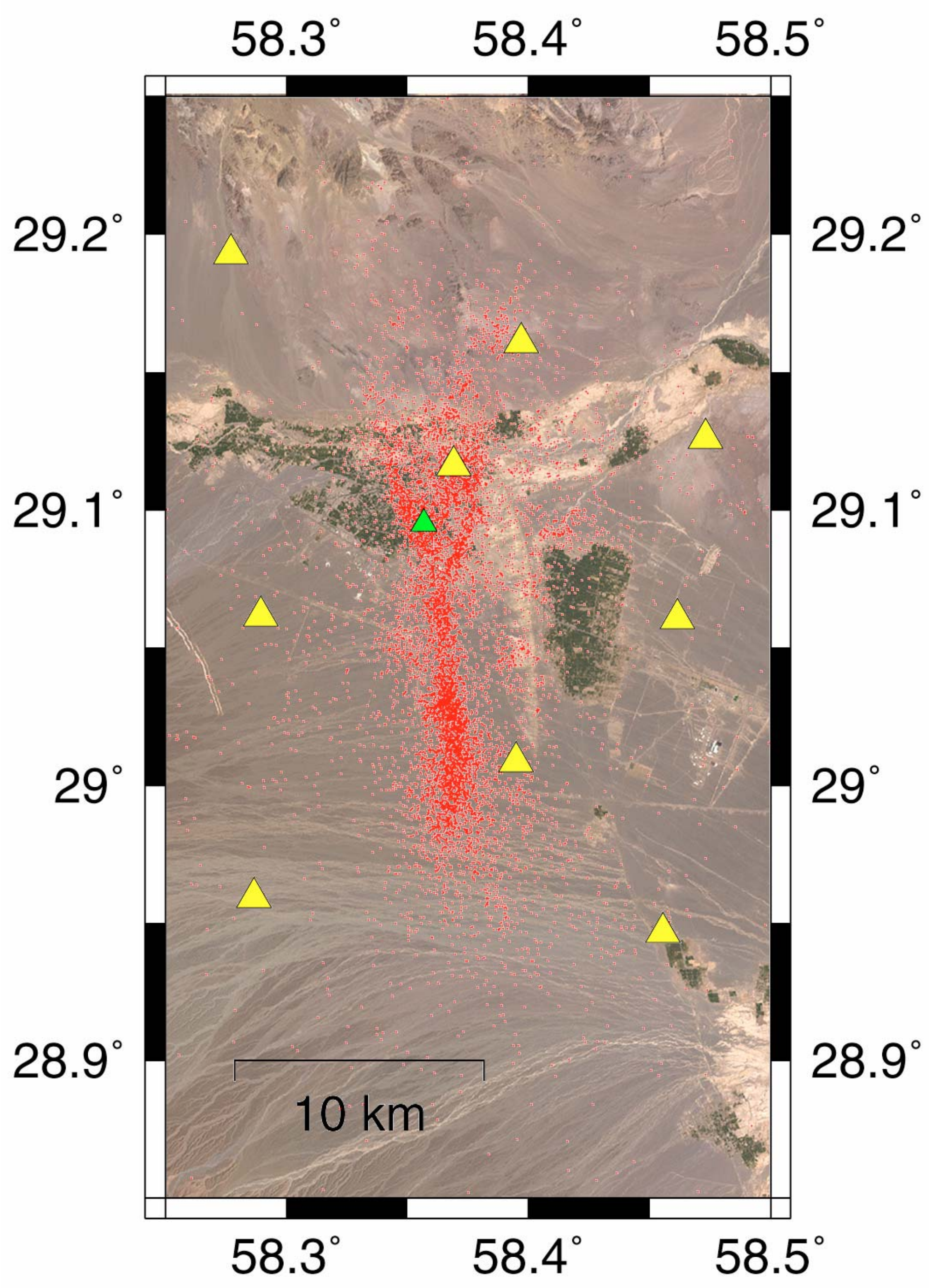

Aftershock distribution

By Temporal High-Sensitive-Seismograph Network

Red points are epicenters of aftershocks, Yellow triangles are the observation stations and Green triangle is the strong motion station of Bam.

Ref.:
Suzuki et al. (2004). Japan Earth Planetary Science Joint Meeting

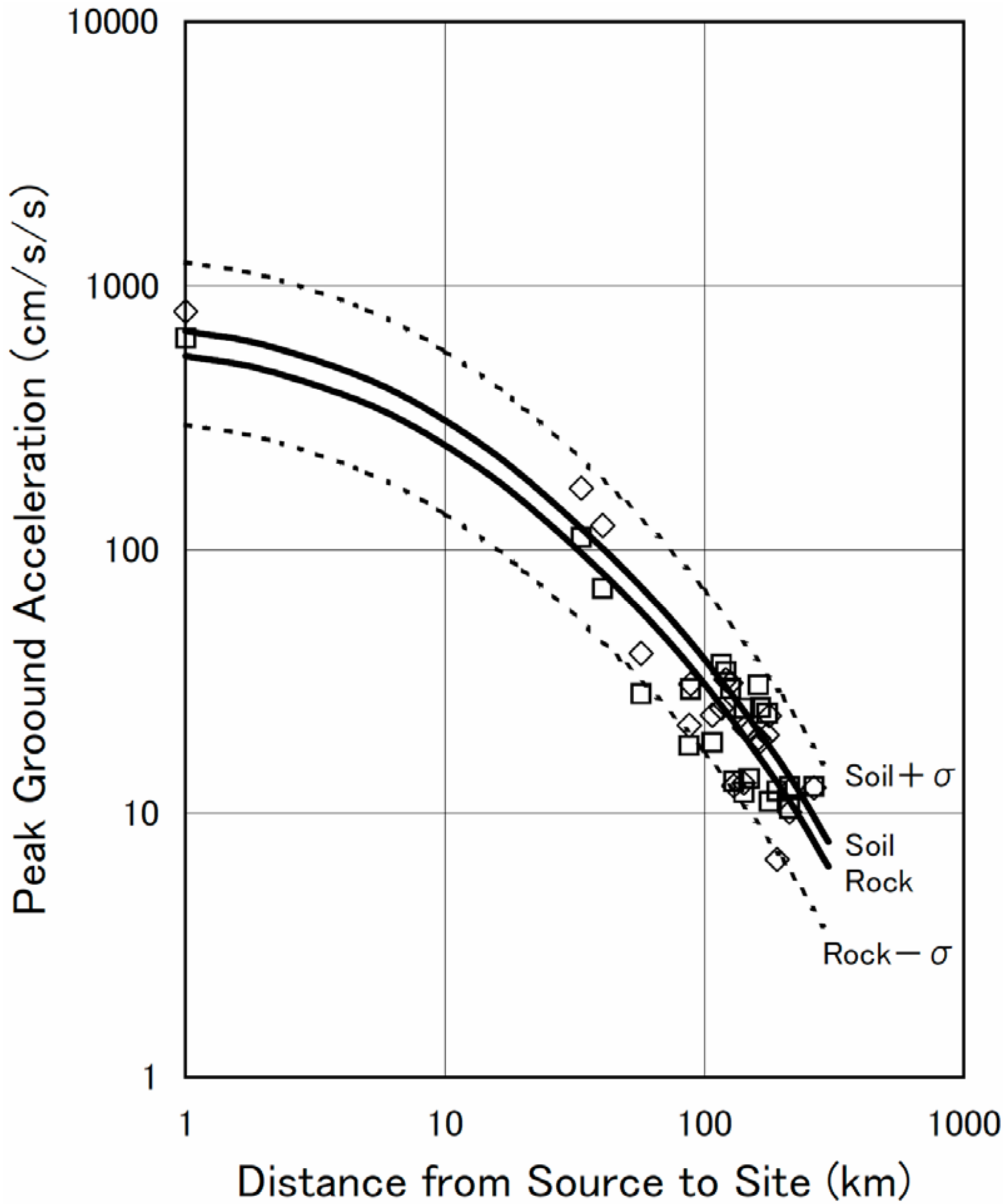

Comparison of PGA predicted by Fukushima et al. (2003) and observed PGA from the 2003 Bam, Iran earthquake. The distance of Bam site (1km) came from personal communication with Dr. Zare, IIEES, Iran, otherwise from Yagi's source model

With same procedure, Kanno et al., 2006 will come soon in BSSA

- 91,731 records from 4,967 events in Japan and 788 records from 12 events in abroad are acquired. About 12,000 records from 200 events are selected.
- Following two models are adopted to shallow and deep events individually.

$$\log pre = a_1 M_w + b_1 X - \log\left(X + d_1 \cdot 10^{e_1 M_w}\right) + c_1 + \sigma_1 \quad (D \leq 30 \text{ km})$$

$$\log pre = a_2 M_w + b_2 X - \log(X) + c_2 + \sigma_2 \quad (D > 30 \text{ km})$$

where *pre* is the predicted PGA (cm/sec2), PGV (cm/sec), or 5 % damped acceleration response spectra (cm/sec2), *D* is the focal depth (km), and *a*1, *b*1, *c*1, *d*1, *a*2, *b*2, and *c*2 are the regression coefficients. *e*1 = 0.5 was selected from another study. σ is error.

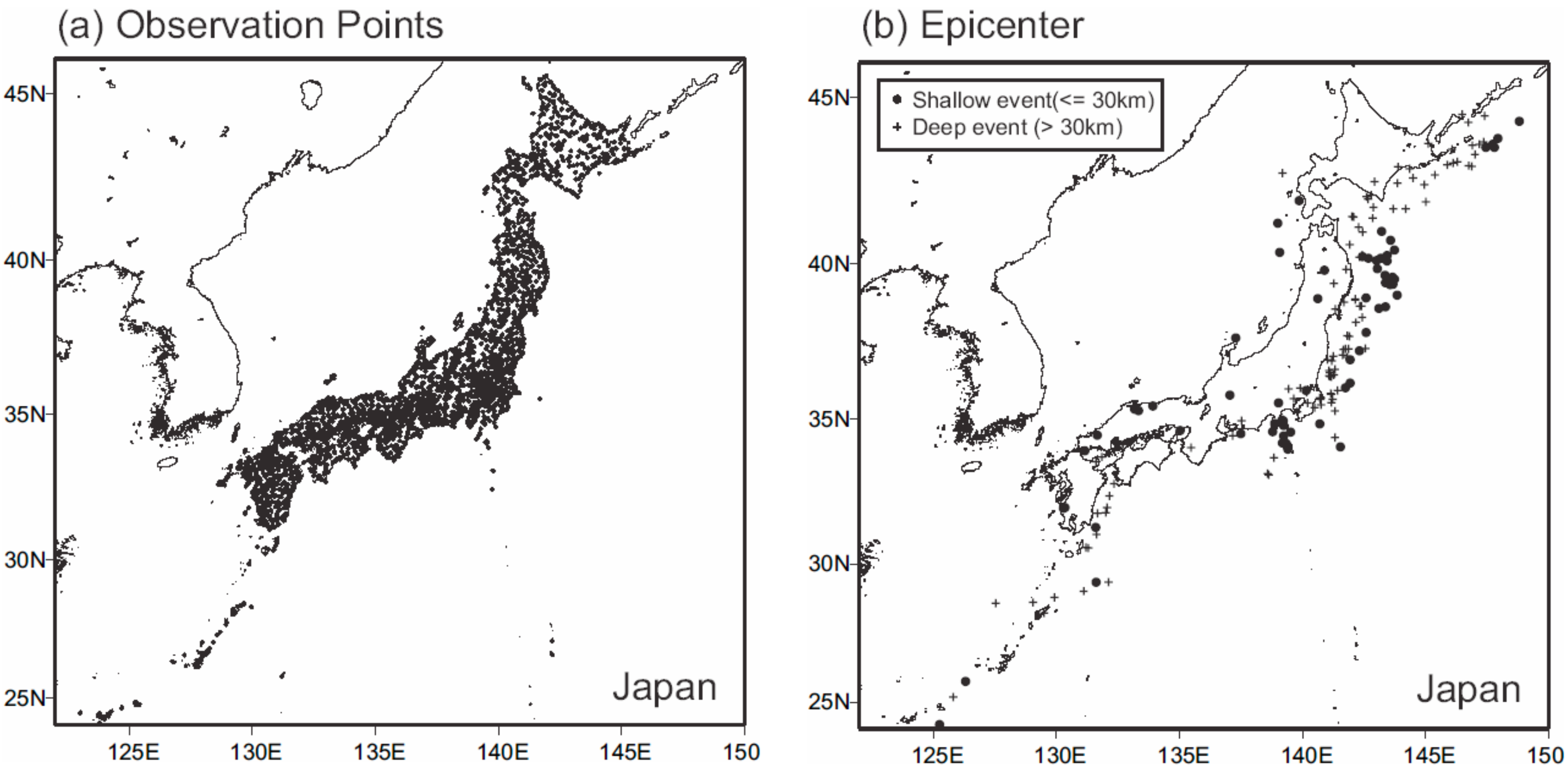
(a) Observation Points
(b) Epicenter
Shallow event(<= 30km)
Deep event (> 30km)
45N
40N
35N
30N
25N
125E
130E
135E
140E
145E
150
Japan

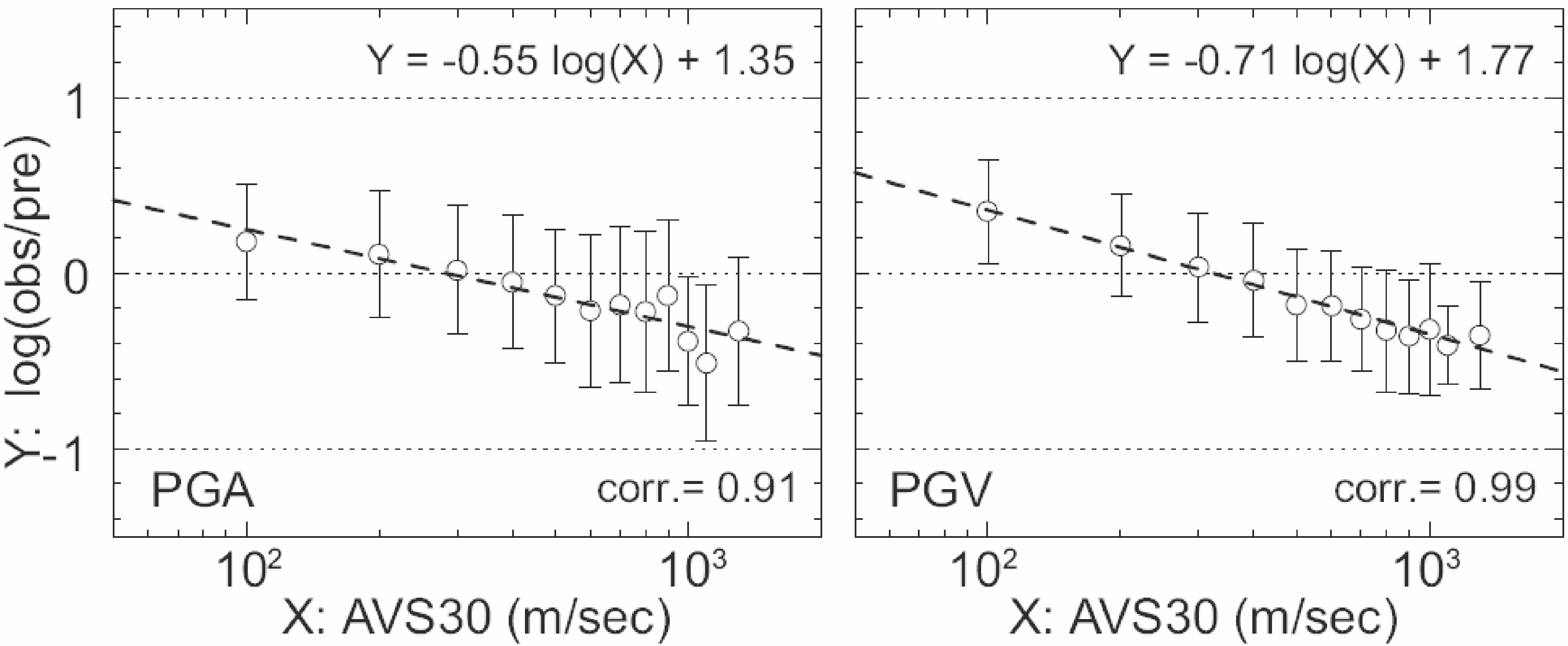

Relation between residual and *AVS30* for PGA and PGV.
Other relations for individual Sa are determined as well.

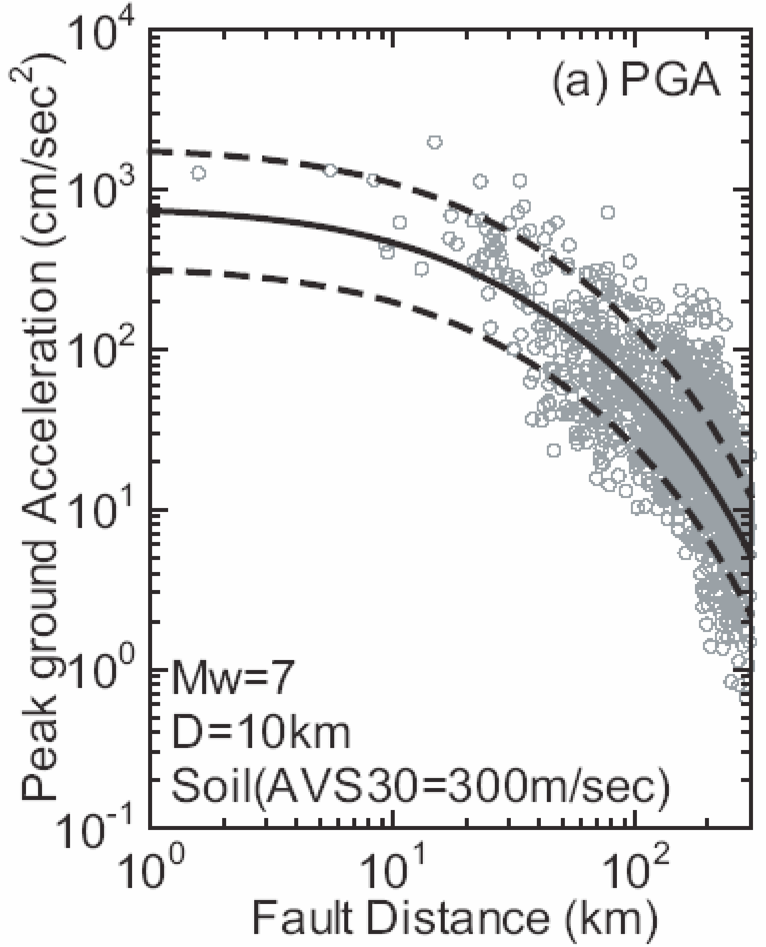

Comparison of attenuation curves with normalized data to *Mw* = 7.0, *D* = 10 km and *AVS30* = 300 m/sec (soil) for shallow events. Solid and broken lines are the new attenuation curves and standard deviations.

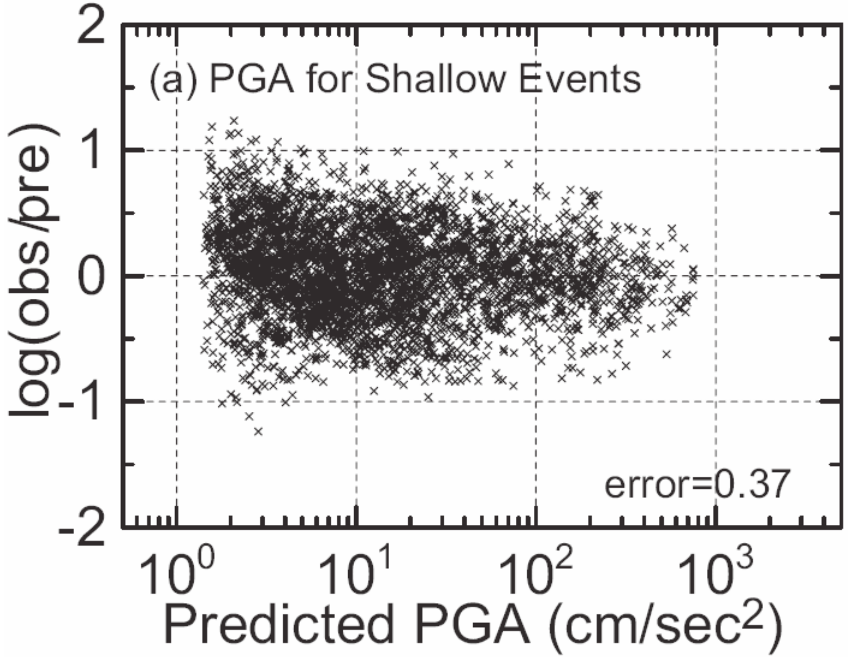

Relations between residuals and predicted amplitude. "Error" in these figures means total error between observed and predicted values.

See detail in future BSSA

We need more precise consideration for uncertainty.

Uncertainty

Assumed to be amplitude dependent: lower dispersion for higher amplitude (really?)

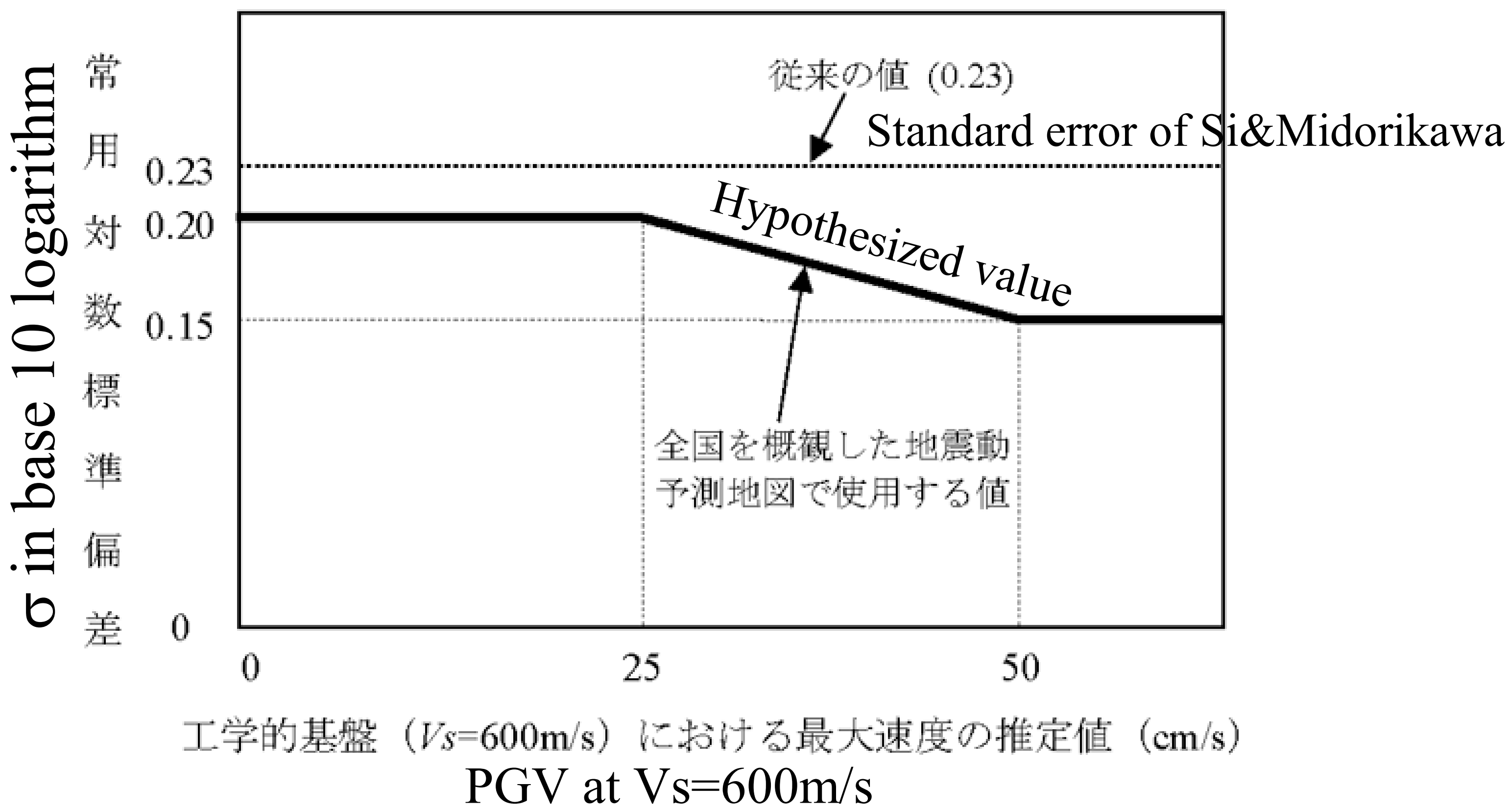

図 2.7-1　使用する距離減衰式のばらつきの値

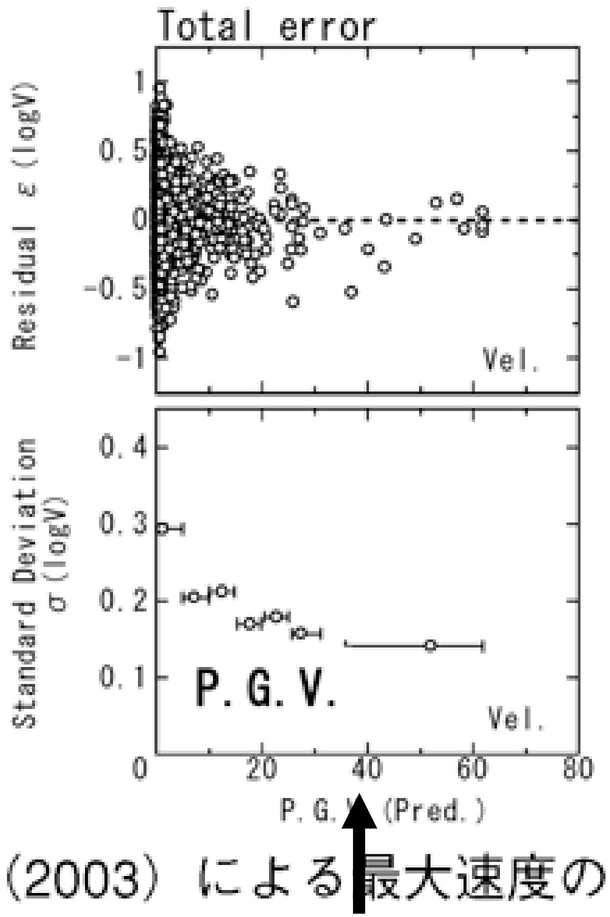

図 5.1-9 翠川・大竹（2003）による最大速度のばらつきの振幅依存性

A priori weighting scheme

Horizontal axis should be logarithmic scale.

X≦25km 6times
25<X ≦ 50 3times
50<X ≦ 75 1.5times

These weights are indicated in another paper,
And the residuals discussed in this separate paper.

With this weight, data in short distance constrains large amplitude of the relation.

I shall indiate residual plots.

Aleatoric uncertainty of strong motion record of high density observation network in Japan

N events were occurred in a limited area.

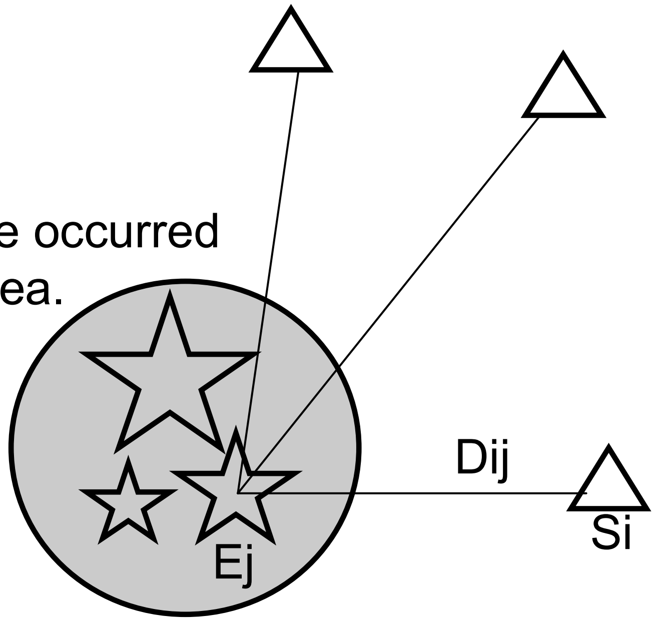

Strong motion records from these events were observed at several sites.

Site coefficient is expressed: $$S_i = \sum_{j=1}^{N} \left\{ \log\left[O_{ij} \right] - \log\left[P\left(M_j, D_{ij} \right) \right] \right\} \Big/ N$$

Where, Mj is moment magnitude of j-th event Ej, Dij is closest distance from Ej to i-th site Si, P(Mj, Dij) is predicted amplitude for Mj and Dij, and Oij is strong motion record from Ej at Si. Dij $\simeq$constant for all events at i-th site.

$$\log\left[P\left(M_j, D_{ij} \right) \right] + S_i - \log\left[O_{ij} \right] \cong \text{Aleatoric uncertainty}$$

Epistemic uncertainties of
source effect was reduced by using only events from a limited area,
path effect was reduced by using only records from the limited area at specific sites, and
site effect was reduced by using averaged error at the specific site.

Removing epistemic uncertainty

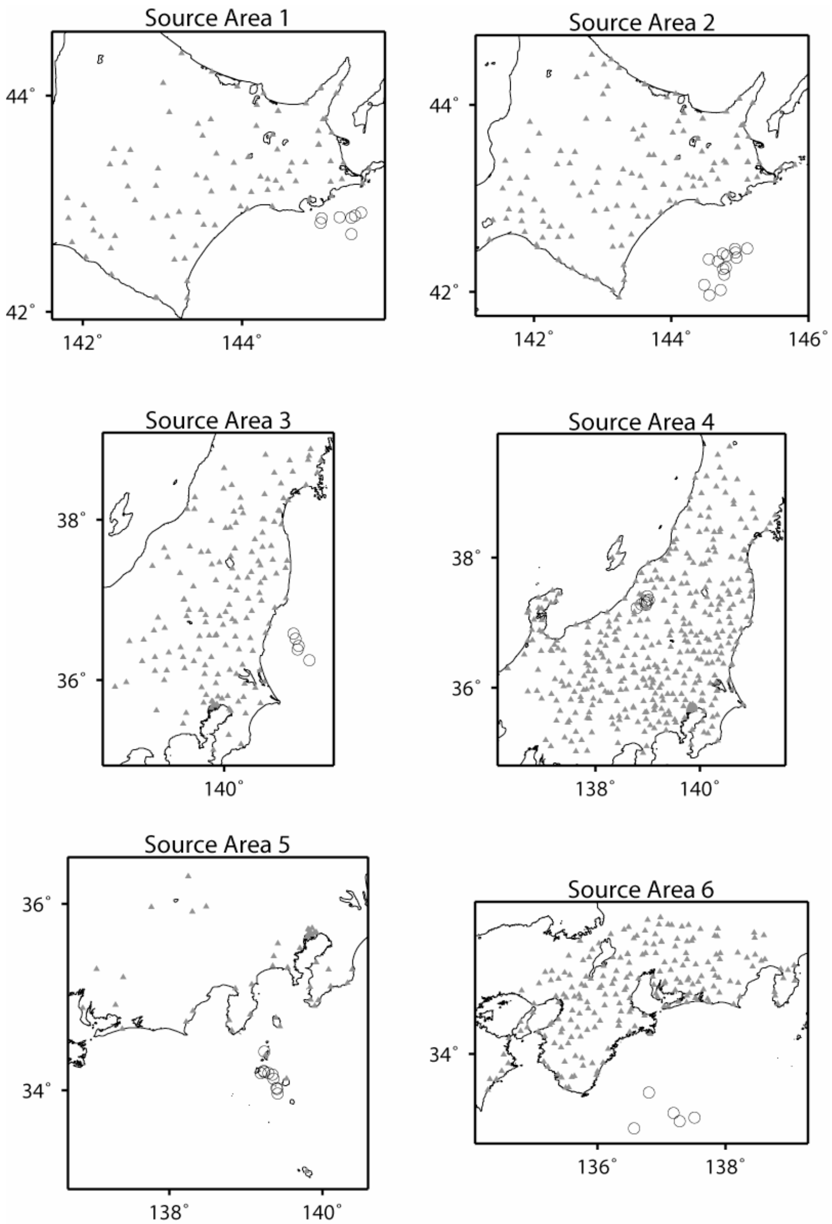

Data selection

Several events in narrow region At least 5 records at a station

Station correction

Averaging residual between observed and predicted at the station

Reduce the station correction
then estimate the residual again

Circles are epicenters and triangles are stations

Intra event errors are less than 0.2.
However, amplitude dependence
is opposite to Midorikawa&Otake.

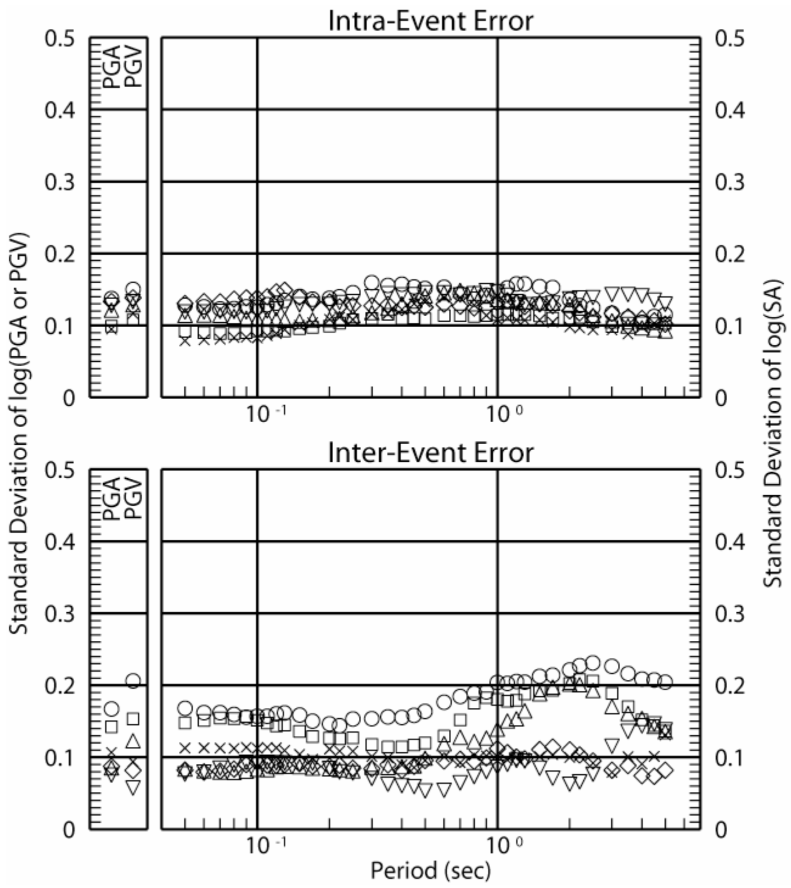

Residuals for individual periods and peak values in each areas

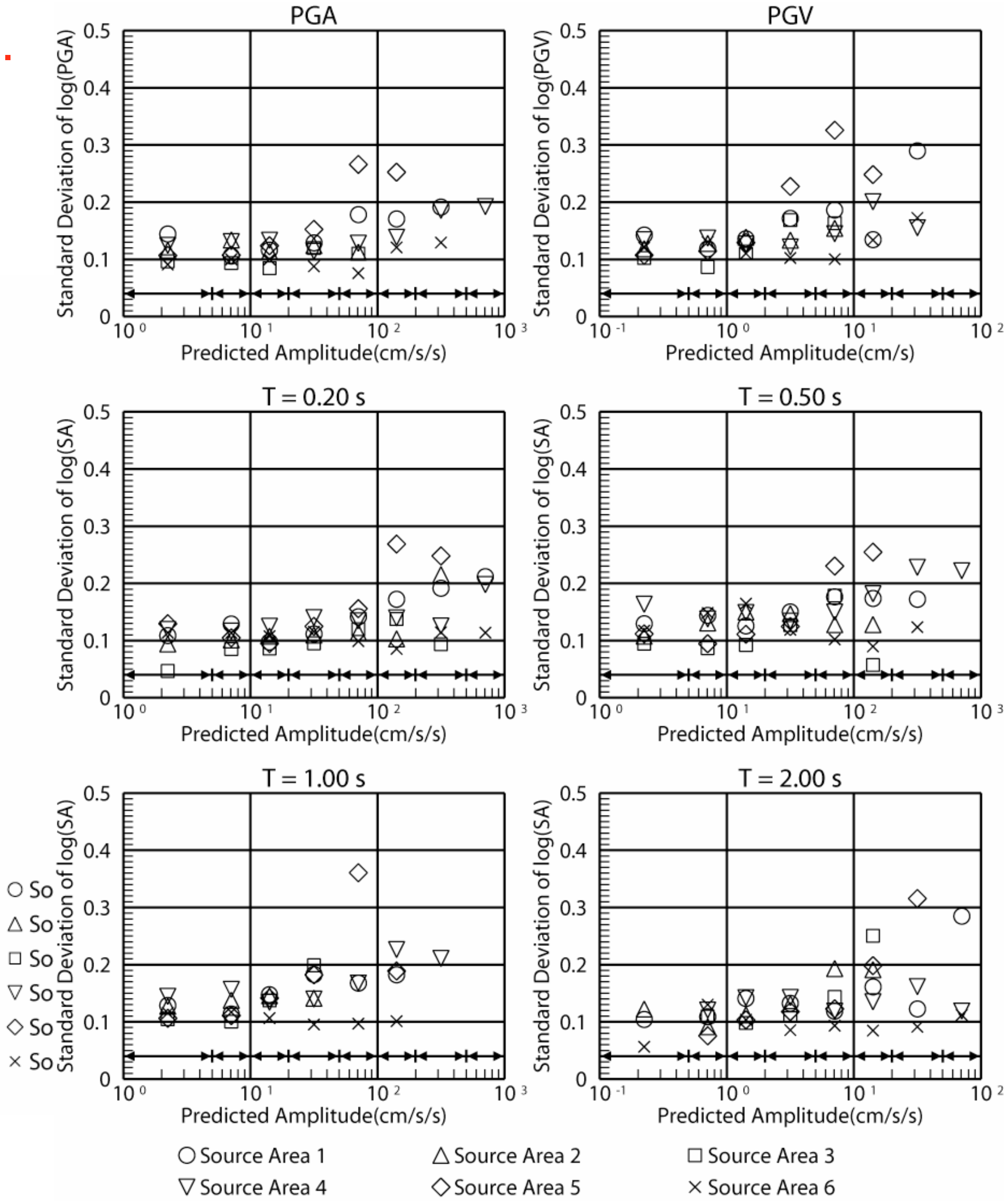

Relation between residuals and predicted amplitudes

Source and site effects

Attenuation Relations of Strong Ground Motion in Japan Using Site Classification Based on Predominant Period

Zhao, J. X., J. Zhang, A. Asano, Y. Ohno, T. Oouchi, T. Takahashi, H. Ogawa, K. Irikura, H. K. Thio, P. G. Somerville, Y. Fukushima and Y. Fukushima

Bull. Seism. Soc. Am. (in press)

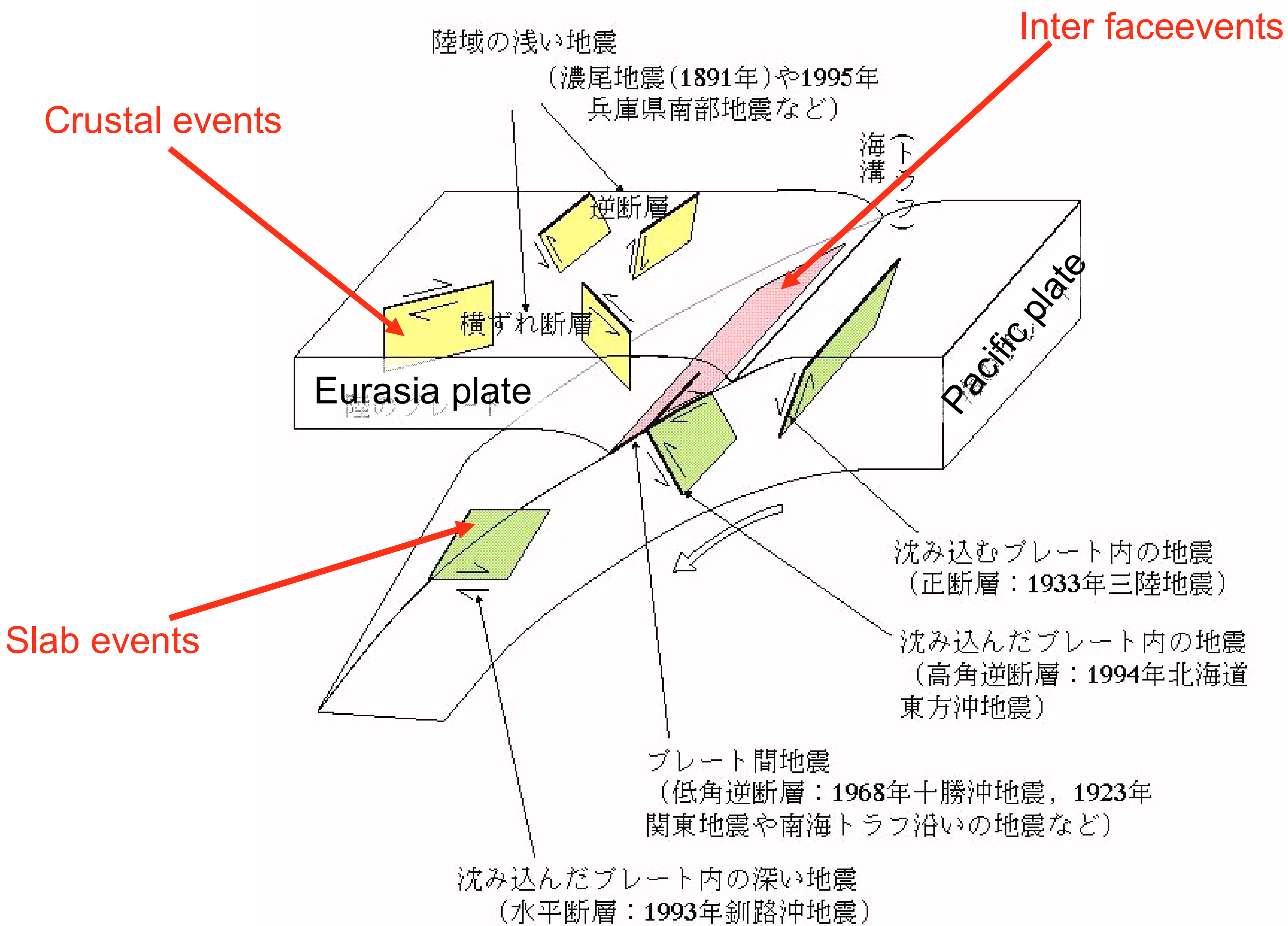
Crustal events
陸域の浅い地震
（濃尾地震（1891年）や1995年
兵庫県南部地震など）
Inter faceevents
海溝（トラフ）
逆断層
横ずれ断層
Eurasia plate
Pacific plate
Slab events
沈み込むプレート内の地震
（正断層：1933年三陸地震）
沈み込んだプレート内の地震
（高角逆断層：1994年北海道
東方沖地震）
プレート間地震
（低角逆断層：1968年十勝沖地震，1923年
関東地震や南海トラフ沿いの地震など）
沈み込んだプレート内の深い地震
（水平断層：1993年釧路沖地震）

Table 1 Numbers of records by source type, faulting mechanism, and region

Japan				
Focal mechanism	Crustal	Interface	Slab	Total for each focal mech.
Reverse	250	1492	408	2150
Strike-slip	1011	13	574	1598
Normal	24	3	735	762
Unknown			8	8
Total for each source type	1285	1508	1725	4518
Iran and Western USA				
Reverse	123	12		135
Strike-slip	73			73
Total for each source type	196	12		208
Total for each source type from all regions				Grand total
	1481	1520	1725	4726

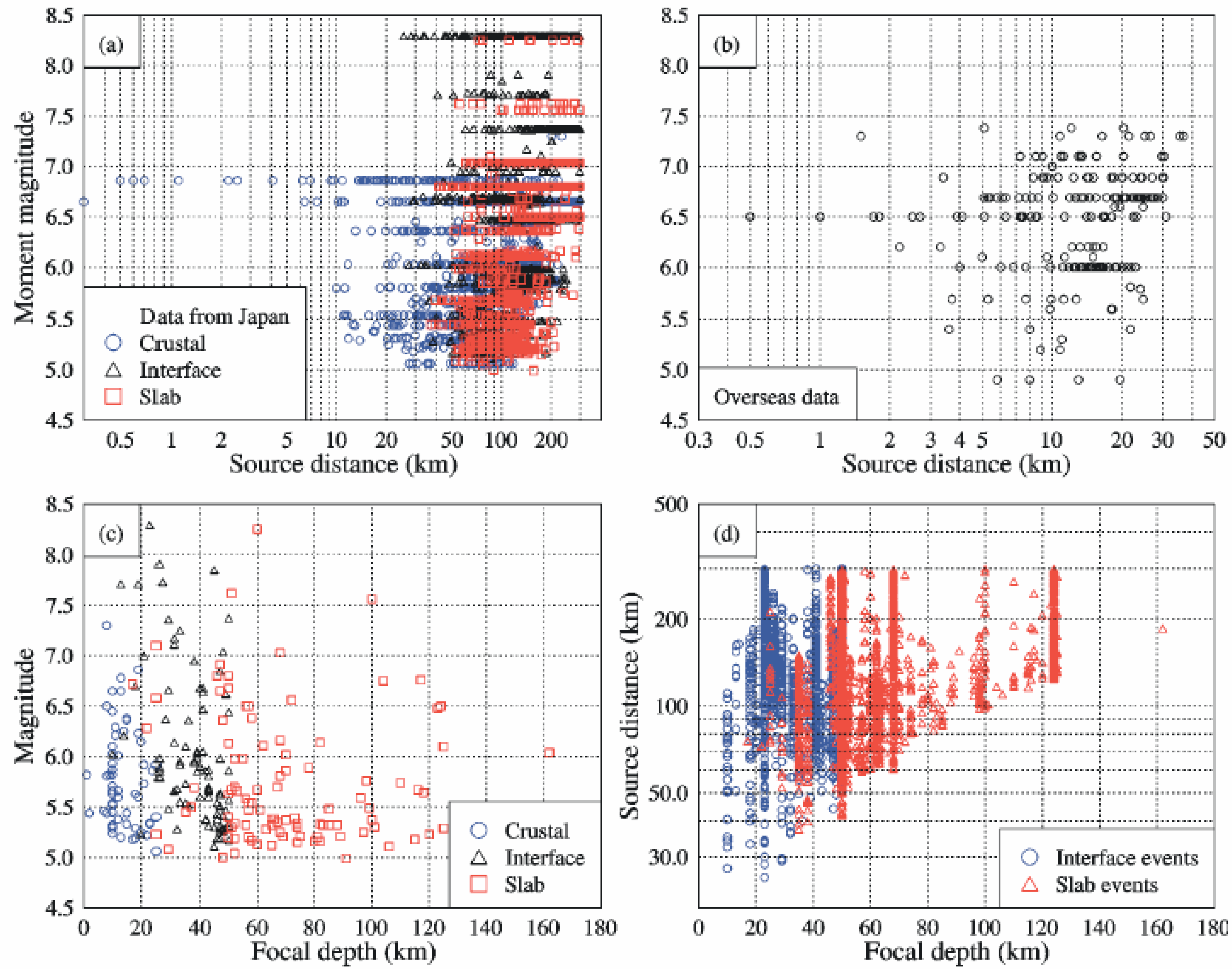

Figure 1 Magnitude-distance distribution for (a) data from Japan; (b) overseas data; (c) magnitude-focal depth distribution; and (d) source distance-focal depth distribution of Japanese data.

Functional form of the attenuation models used in the present study

The functional form of attenuation models for PGA and Sa of 5% damping

$$\ln[y_{i,j}(T)]=aM+bx_{i,j}-\ln(r_{i,j})+e(h-h_c)\,\delta_h+S_R+S_I+S_S+S_{SL}\ln(x_{i,j})+S_k+\xi_{i,j}+\eta_i$$

$$r_{i,j}=x_{i,j}+c\exp(dM_j)$$

- i – earthquake number
- j – station number
- M – moment magnitude
- x – closest distance to source
- h – focal depth
- h_c – depth constant (15km)
- δ_h – dummy variable
- S_R – reverse fault term for crustal events
- S_I – interface event term
- S_S – Slab event term
- S_{SL} – path dependent term for Slab event
- ξ – intra-event error
- η – inter-event error
- S_k – site term

Comparison of normalized peak ground accelerations

Crustal and interface records

Subduction slab records

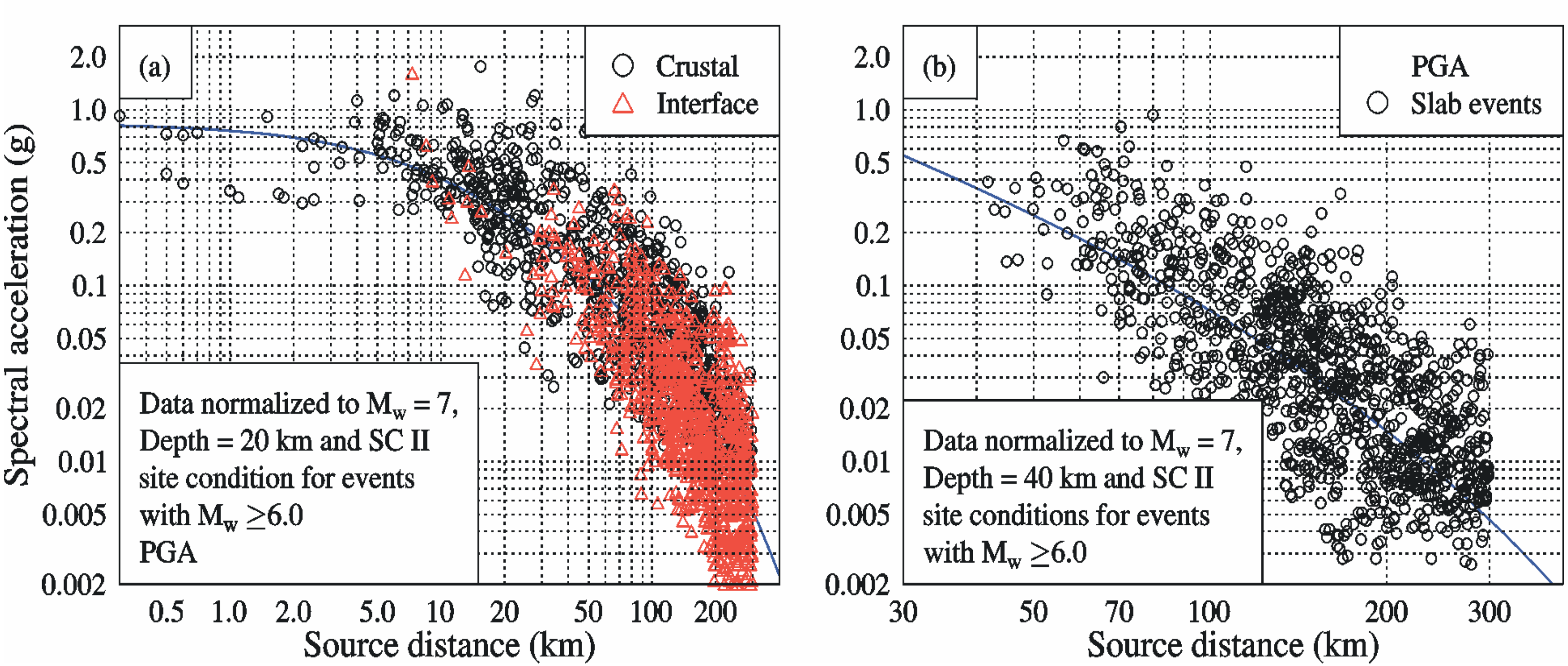

Inter-event residuals for crustal earthquakes at (a) 0.05 and (b) 4.0s spectral period

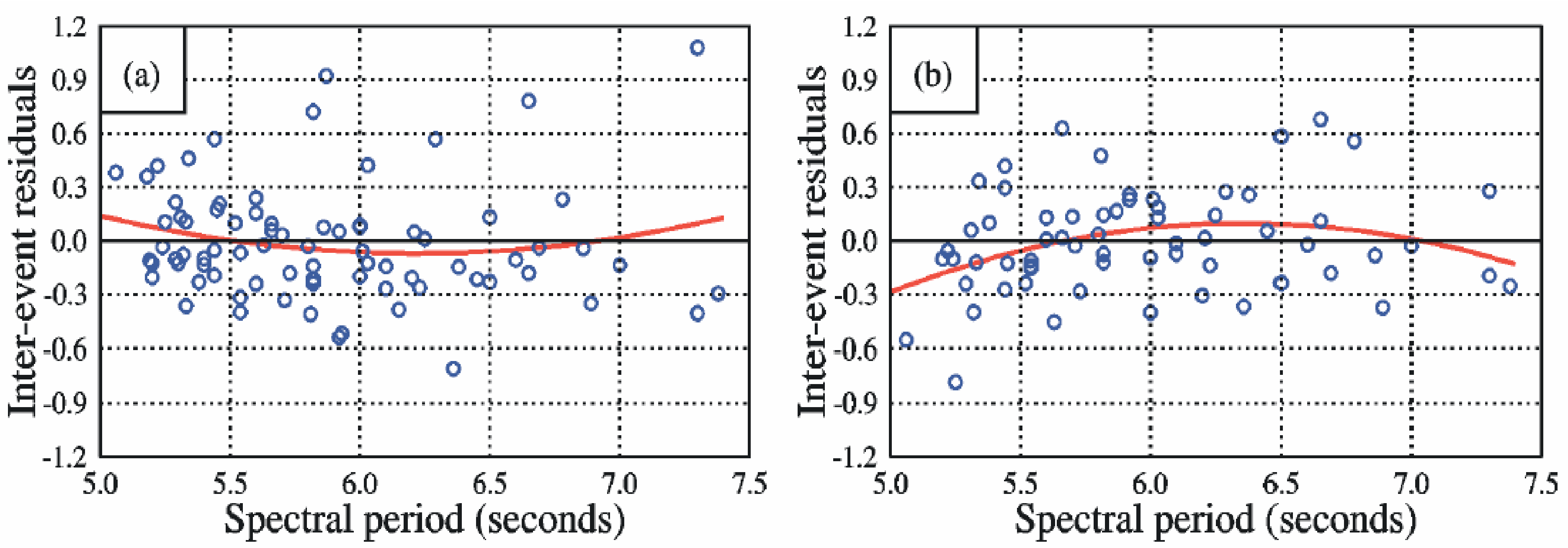

Inter-event residuals

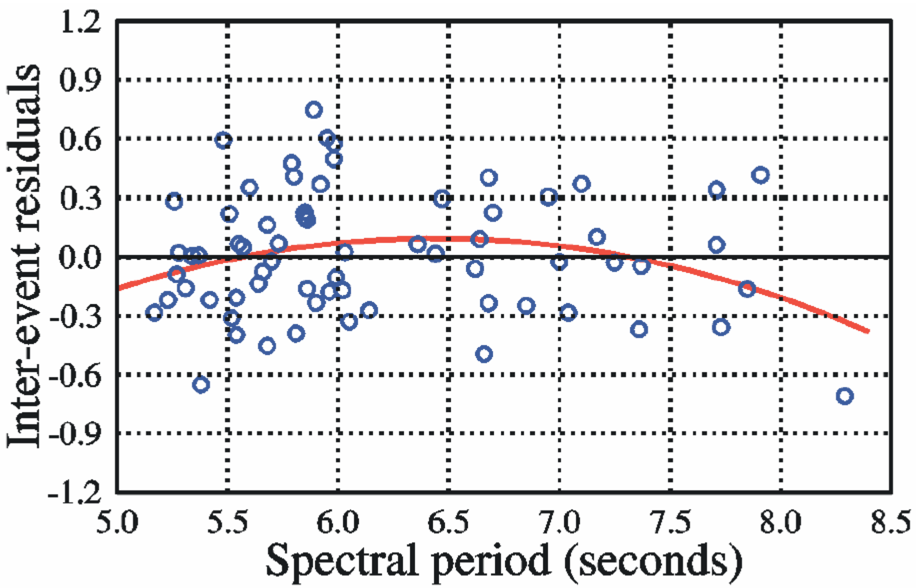

for interface earthquakes at 4.0s spectral period

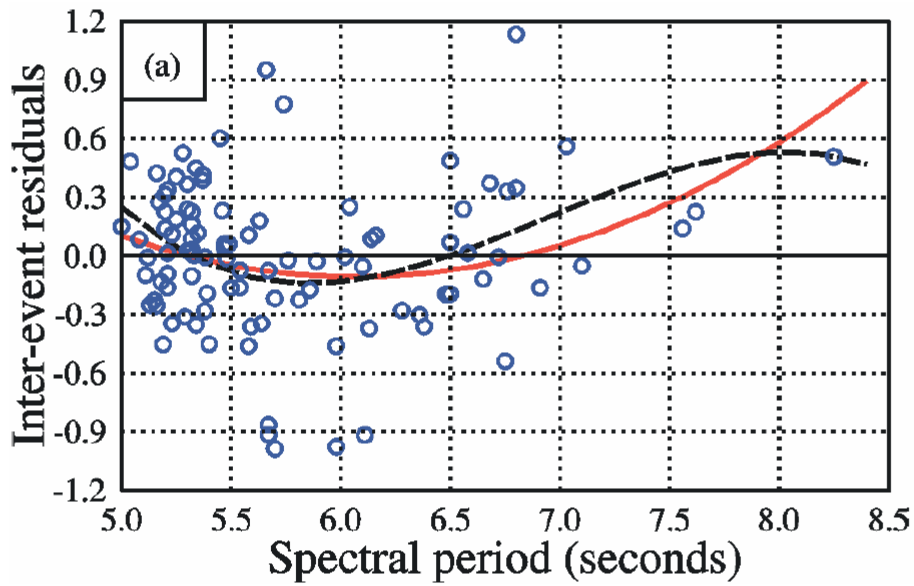

for slab earthquakes at 0.05s spectral period correction term due to the effect of magnitude-squared term

$$\log_e(S_{MSst}(T,M_W)) = P_{st}(T)(M_W - M_C) + Q_{st}(T)(M_W - M_C)^2 + W_{st}(T)$$

where subscript *st* equals c for crustal, *i* for interface and *s* for slab events.

Table 4 Coefficients for magnitude terms

Period	Q_C	W_C	τ_C	Q_I	W_I	τ_I	P_S	Q_S	W_S	τ_S
PGA	0.0	0.0	0.303	0.0	0.0	0.308	0.1392	0.1584	-0.0529	0.321
0.05	0.0	0.0	0.326	0.0	0.0	0.343	0.1636	0.1932	-0.0841	0.378
0.10	0.0	0.0	0.342	0.0	0.0	0.403	0.1690	0.2057	-0.0877	0.420
0.15	0.0	0.0	0.331	-0.0138	0.0286	0.367	0.1669	0.1984	-0.0773	0.372
0.20	0.0	0.0	0.312	-0.0256	0.0352	0.328	0.1631	0.1856	-0.0644	0.324
0.25	0.0	0.0	0.298	-0.0348	0.0403	0.289	0.1588	0.1714	-0.0515	0.294
0.30	0.0	0.0	0.300	-0.0423	0.0445	0.028	0.1544	0.1573	-0.0395	0.284
0.40	0.0	0.0	0.346	-0.0541	0.0511	0.271	0.1460	0.1309	-0.0183	0.278
0.50	-0.0126	0.0116	0.338	-0.0632	0.0562	0.277	0.1381	0.1078	-0.0008	0.272
0.60	-0.0329	0.0202	0.349	-0.0707	0.0604	0.296	0.1307	0.0878	0.0136	0.285
0.70	-0.0501	0.0274	0.351	-0.0771	0.0639	0.313	0.1239	0.0705	0.0254	0.290
0.80	-0.0650	0.0336	0.356	-0.0825	0.0670	0.329	0.1176	0.0556	0.0352	0.299
0.90	-0.0781	0.0391	0.348	-0.0874	0.0697	0.324	0.1116	0.0426	0.0432	0.289
1.00	-0.0899	0.0440	0.338	-0.0917	0.0721	0.328	0.1060	0.0314	0.0498	0.286
1.25	-0.1148	0.0545	0.313	-0.1009	0.0772	0.339	0.0933	0.0093	0.0612	0.277
1.50	-0.1351	0.0630	0.306	-0.1083	0.0814	0.352	0.0821	-0.0062	0.0674	0.282
2.00	-0.1672	0.0764	0.283	-0.1202	0.0880	0.360	0.0628	-0.0235	0.0692	0.300
2.50	-0.1921	0.0869	0.287	-0.1293	0.0931	0.356	0.0465	-0.0287	0.0622	0.292
3.00	-0.2124	0.0954	0.278	-0.1368	0.0972	0.338	0.0322	-0.0261	0.0496	0.274
4.00	-0.2445	0.1088	0.273	-0.1486	0.1038	0.307	0.0083	-0.0065	0.0150	0.281
5.00	-0.2694	0.1193	0.275	-0.1578	0.1090	0.272	-0.0117	0.0246	-0.0268	0.296

Note that M_C=6.3 and P_C=0.0 for crustal and interface events, and M_C=6.5 for slab events.

Site class definitions used in the present study and the approximately corresponding NEHRP site classes

Site class	Site natural period (s)	Average shear-wave velocity	NEHRP class
SC I: (Rock/stiff soil)	$T_G < 0.2$s	$V_{30} > 600$ m/s	A+B
SC II: (Hard soil)	$0.2\text{s} \leq T_G < 0.4$s	300 m/s < $V_{30} \leq$600 m/s	C
SC III: (Medium soil)	$0.4\text{s} \leq T_G < 0.6$s	200 m/s < $V_{30} \leq$ 300 m/s	D
SC IV: (Soft soil)	T_G ³ 0.6s	$V_{30} \leq$ 200 m/s	E

Site natural period - four times the S wave travel time (1-D)

Table 2 Number of K-net Stations

SC I	SC II	SC III	SC IV	Unknown	Total
359	182	24	38	271	874

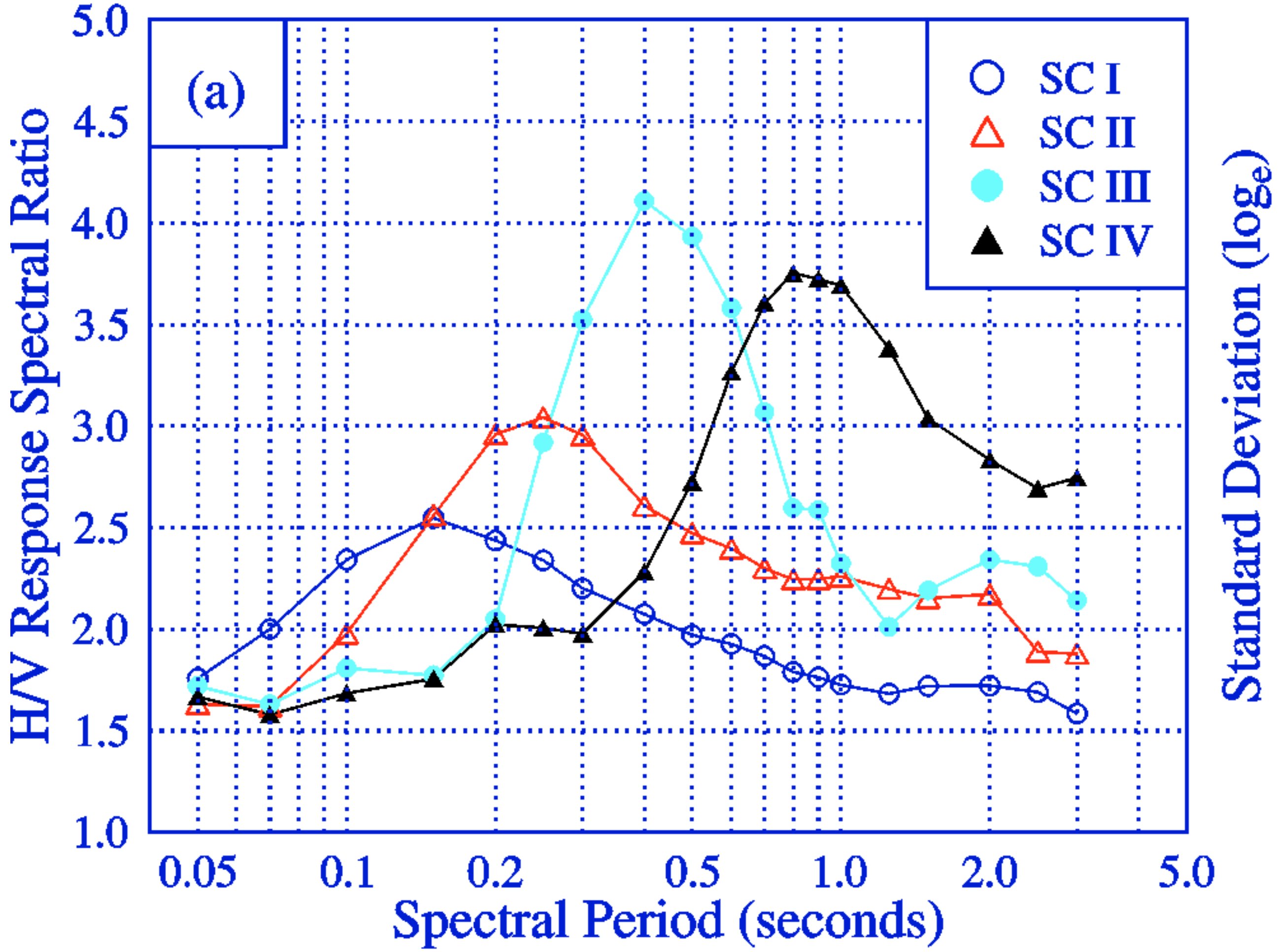

site classification index $SI_k = \frac{2}{n} \sum_{i=1}^{n} \Phi\left(-\mathrm{abs}[\ln(\mu_i) - \ln(\bar{\mu}_{ki})]\right)$

Where, k - site class number, n - the total number of periods, Φ( ) – normal cumulative distribution function, μ_i - the mean H/V ratio for the site of interest for the ith period, μ_{ki} - mean H/V ratio for the kth site class averaged over all sites of the data base for the ith period.

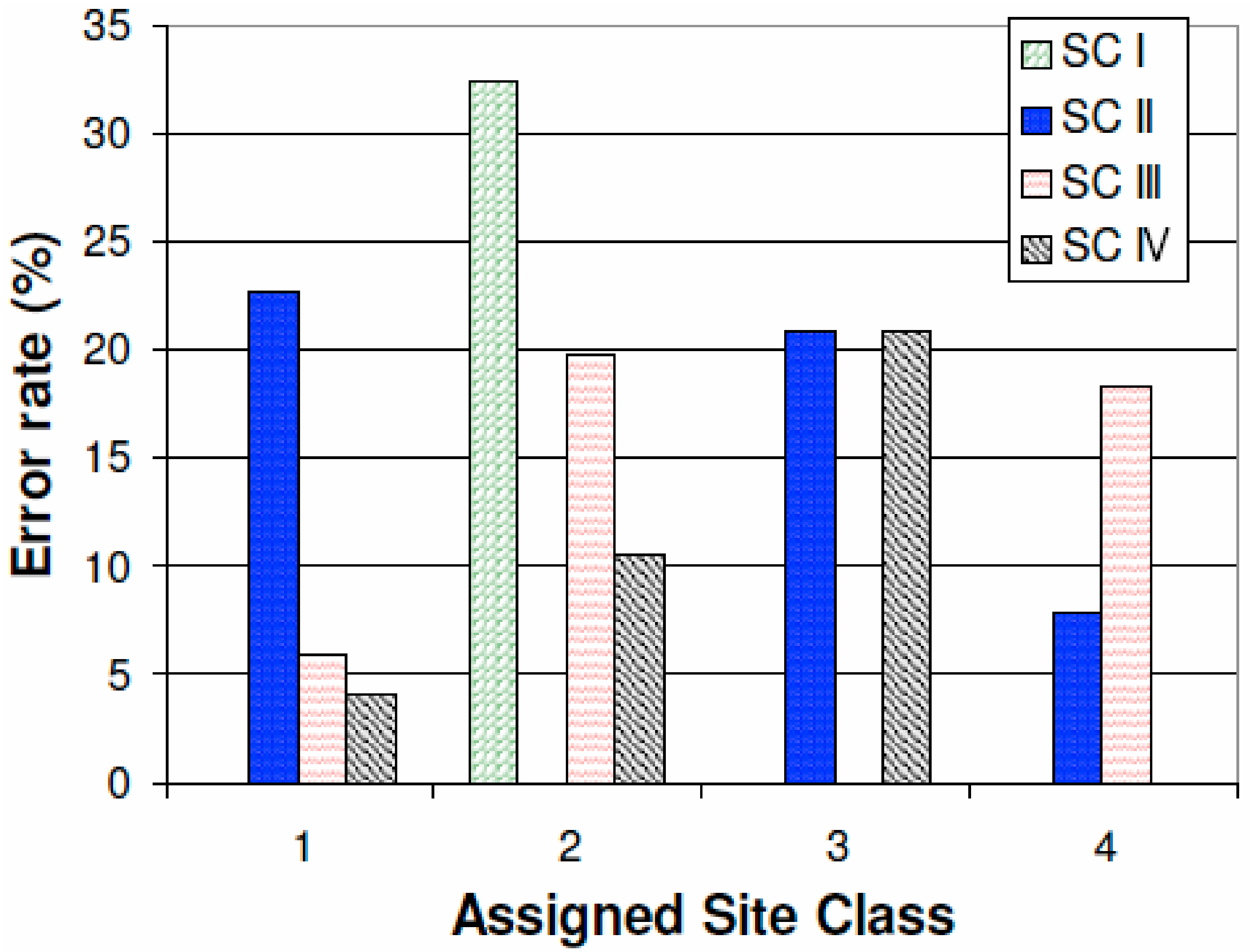

Error rates of classification scheme using the shape of H/V spectral ratios
(inspected for K-net site)

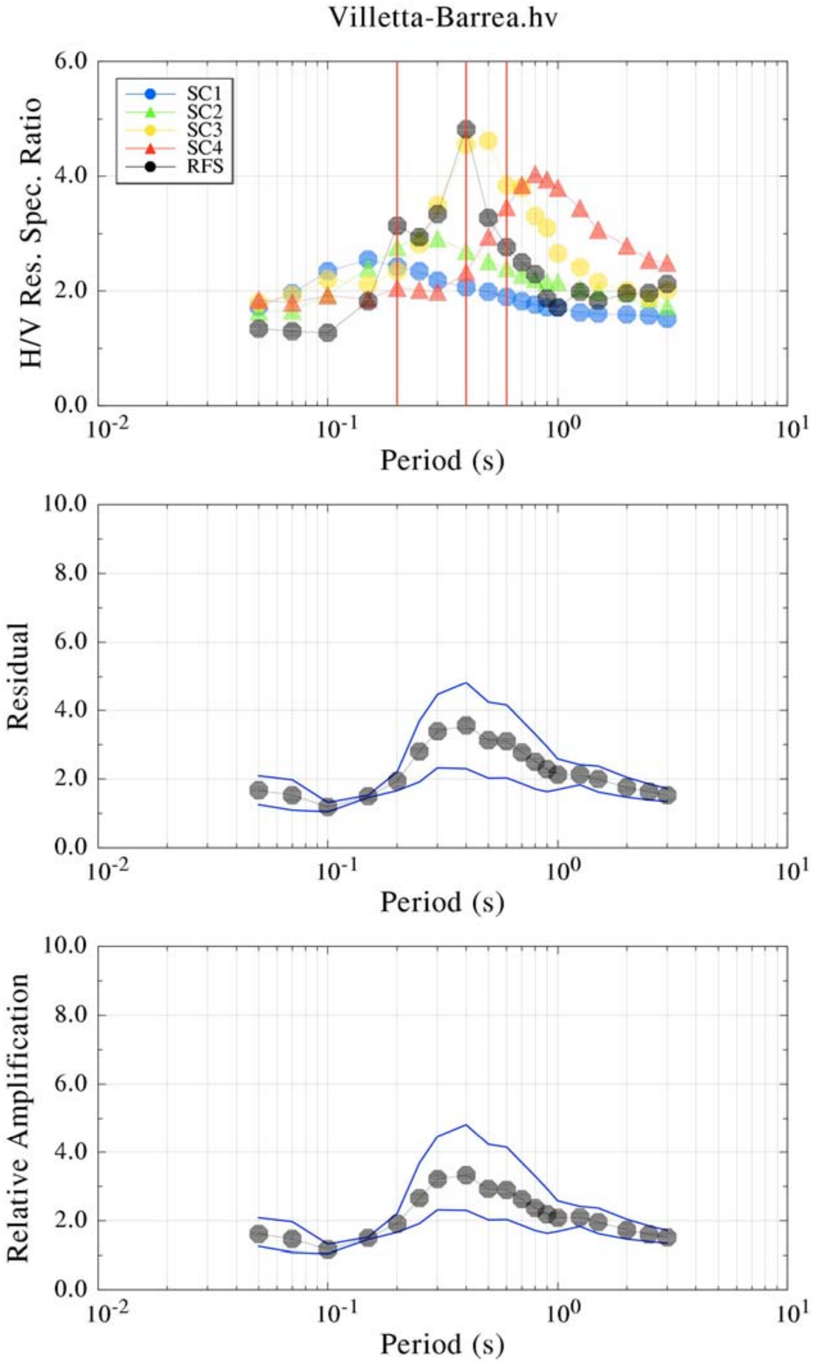

H/V scheme applied for Italian data

I_{JMA}

(Intensity of Japan Meteorological Agency)

Attenuation relation of JMA Seismic Intensity Applicable to Near Source Region

MATSUSAKI, S., Y. HISADA and Y. FUKUSHIMA

Japanese local Journal of AIJ in Press

Data base

2002, CD-ROM was published by JMA
Added representative events after 2003

After 1996 April, all Ijma is calculated from instrumental records.

-First screaming: 273,217 records of 51962 events from 93,154 events

-Second screaming: 27,531 records of 554 events
($Mj \geq 5$, depth≤200km, events with more than 10 records, truncated far distance)

Result

$$Ijma = 1.36Mj - 4.03 \cdot \log(X + 0.00675 \cdot 10^{0.5Mj}) + 0.0155 \cdot h + 2.05$$

Where Ijma is JMA intensity, Mj is JMA magnitude, X is distance from fault plane to site if available otherwise hypocentral distance and h is focal depth in km.

Total standard error is 0.7, Inter and intra event errors are 0.36 and 0.60 respectively.

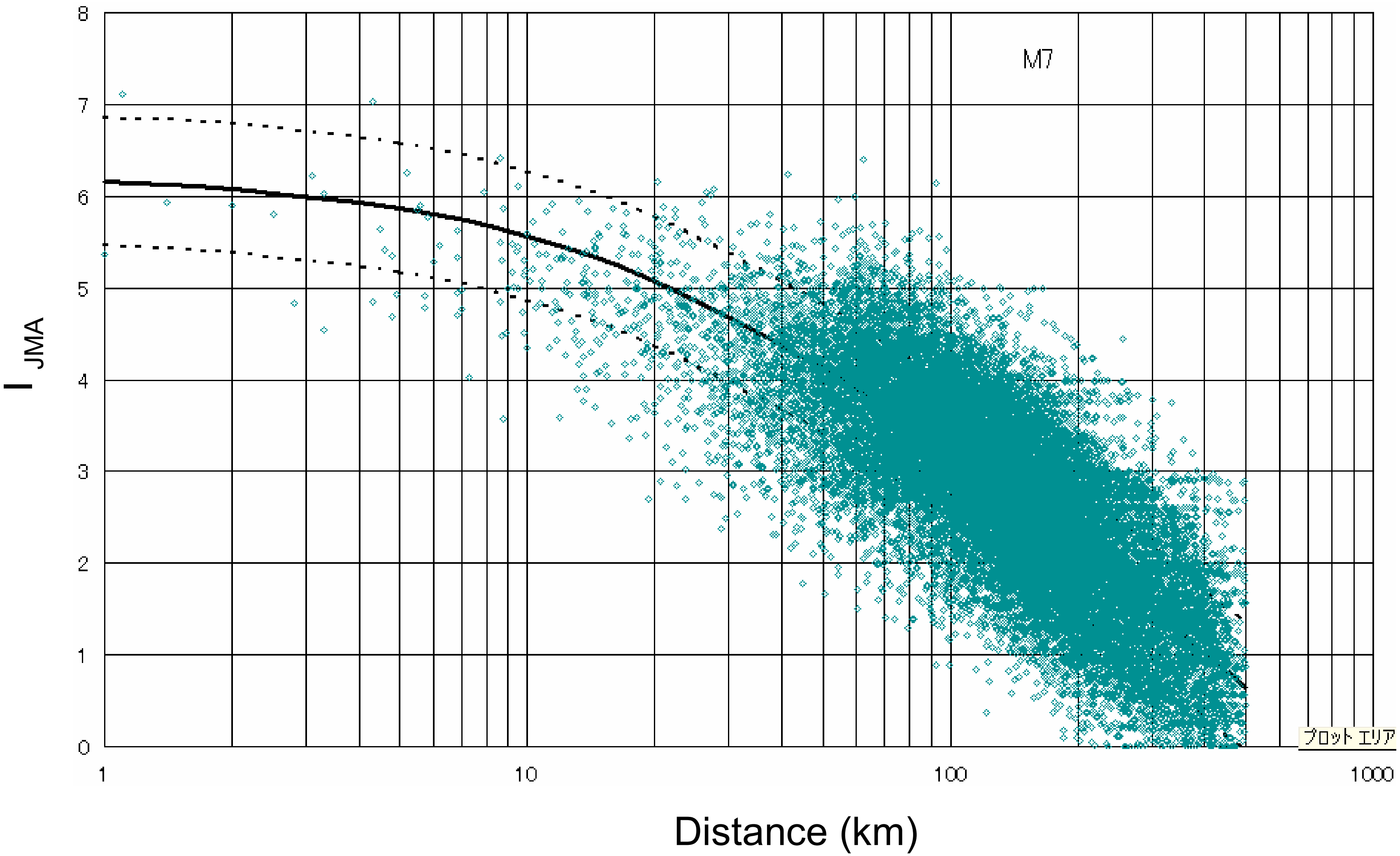

M7
I JMA
8
7
6
5
4
3
2
1
0
1
10
100
1000
Distance (km)
プロット エリア

Recent extreme data

2004 Chuetsu, Niigata, Japan

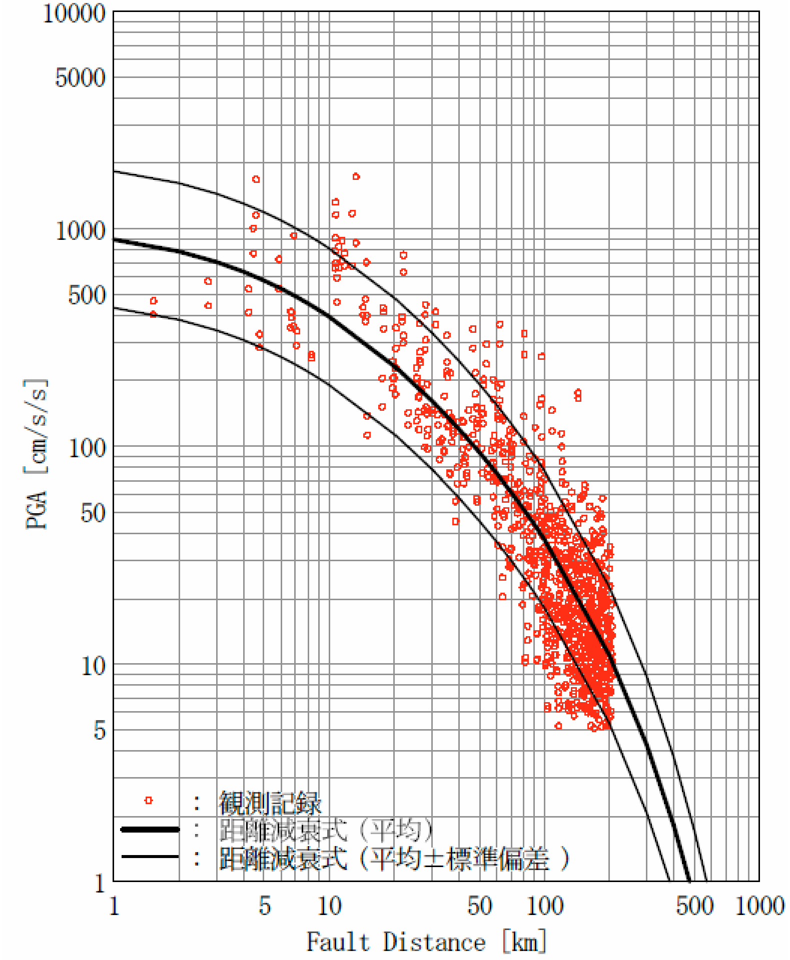

10000
5000
1000
500
100
50
10
5
1
PGA [cm/s/s]
1
5
10
50
100
500
1000
Fault Distance [km]
: 観測記録
: 距離減衰式 (平均)
: 距離減衰式 (平均±標準偏差)

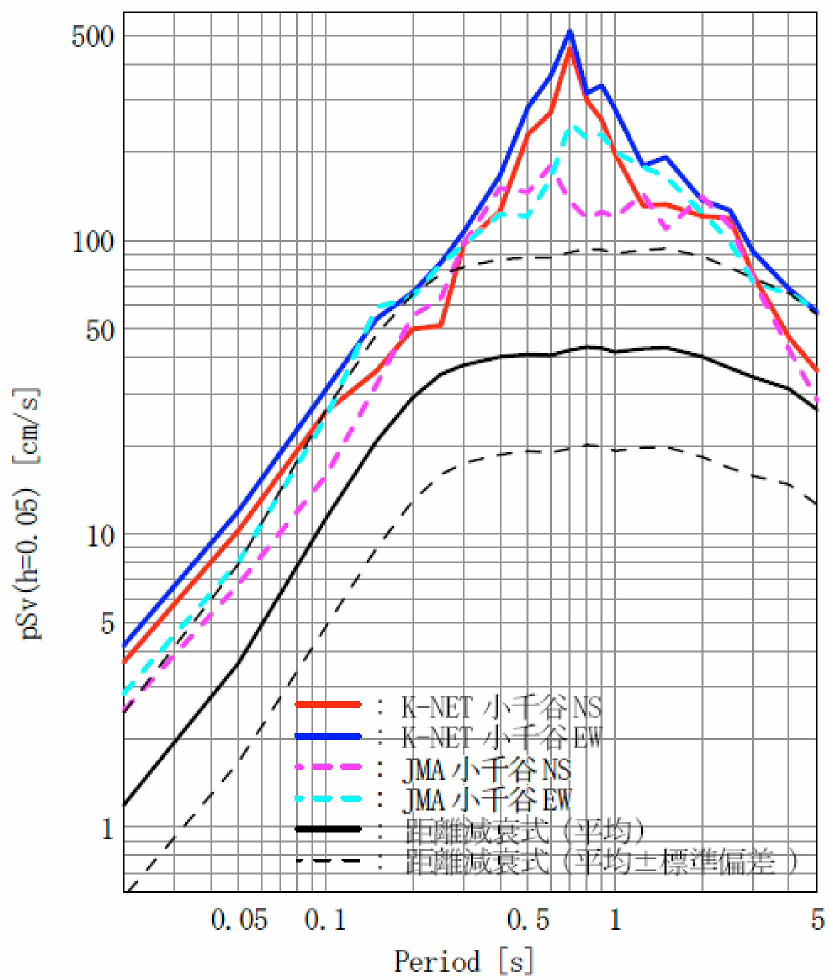

500
100
50
10
5
1
pSv(h=0.05) [cm/s]
0.05
0.1
0.5
1
5
Period [s]
: K-NET 小千谷NS
: K-NET 小千谷EW
: JMA 小千谷NS
: JMA 小千谷EW
: 距離減衰式 (平均)
: 距離減衰式 (平均±標準偏差)

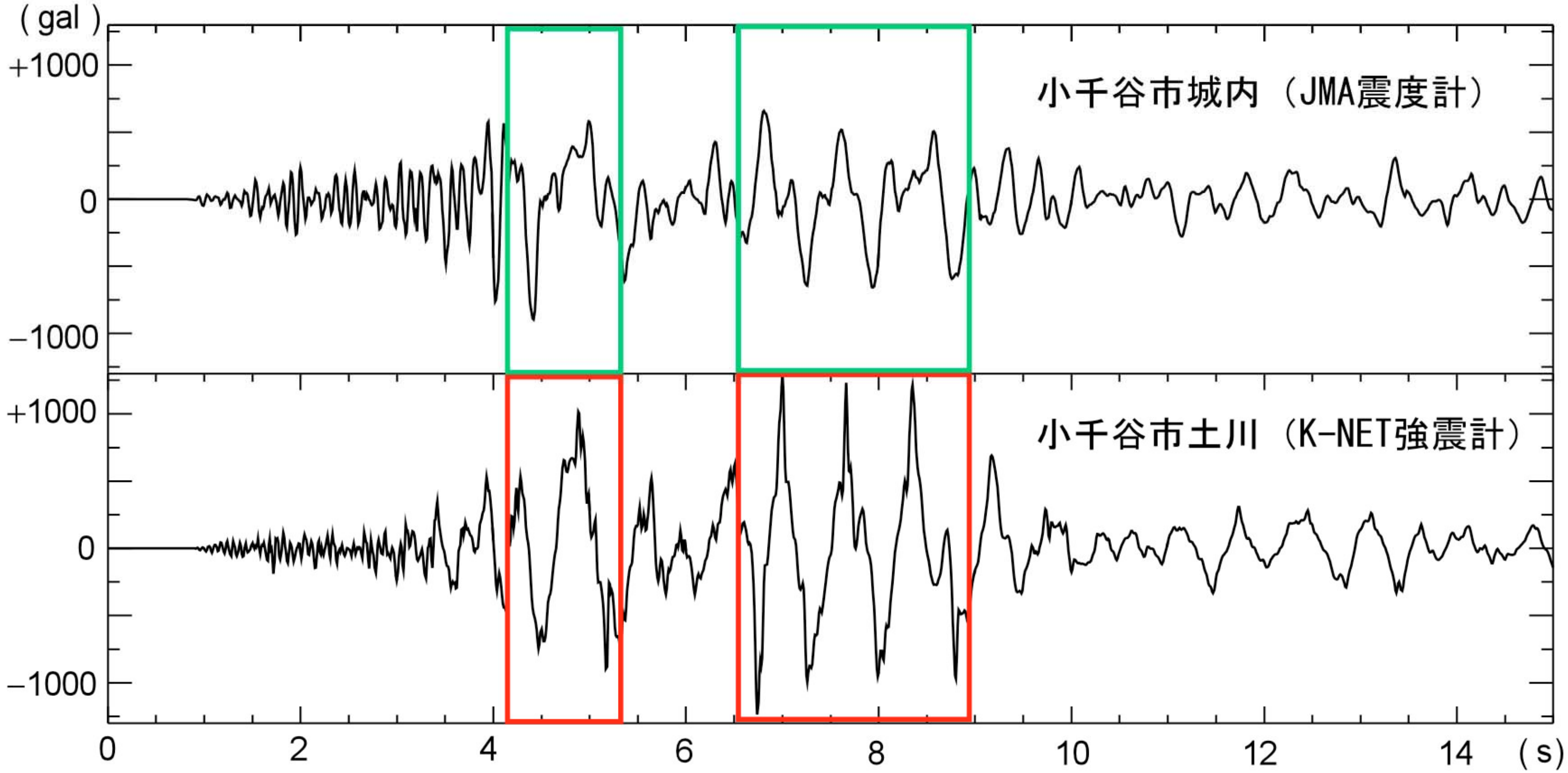

From Prof. Koketsu, ERI, Tokyo Univ.

Mark of exploded mud water were found on bridge columns, where Sinkan-sen super express was derailed. Right: zoom

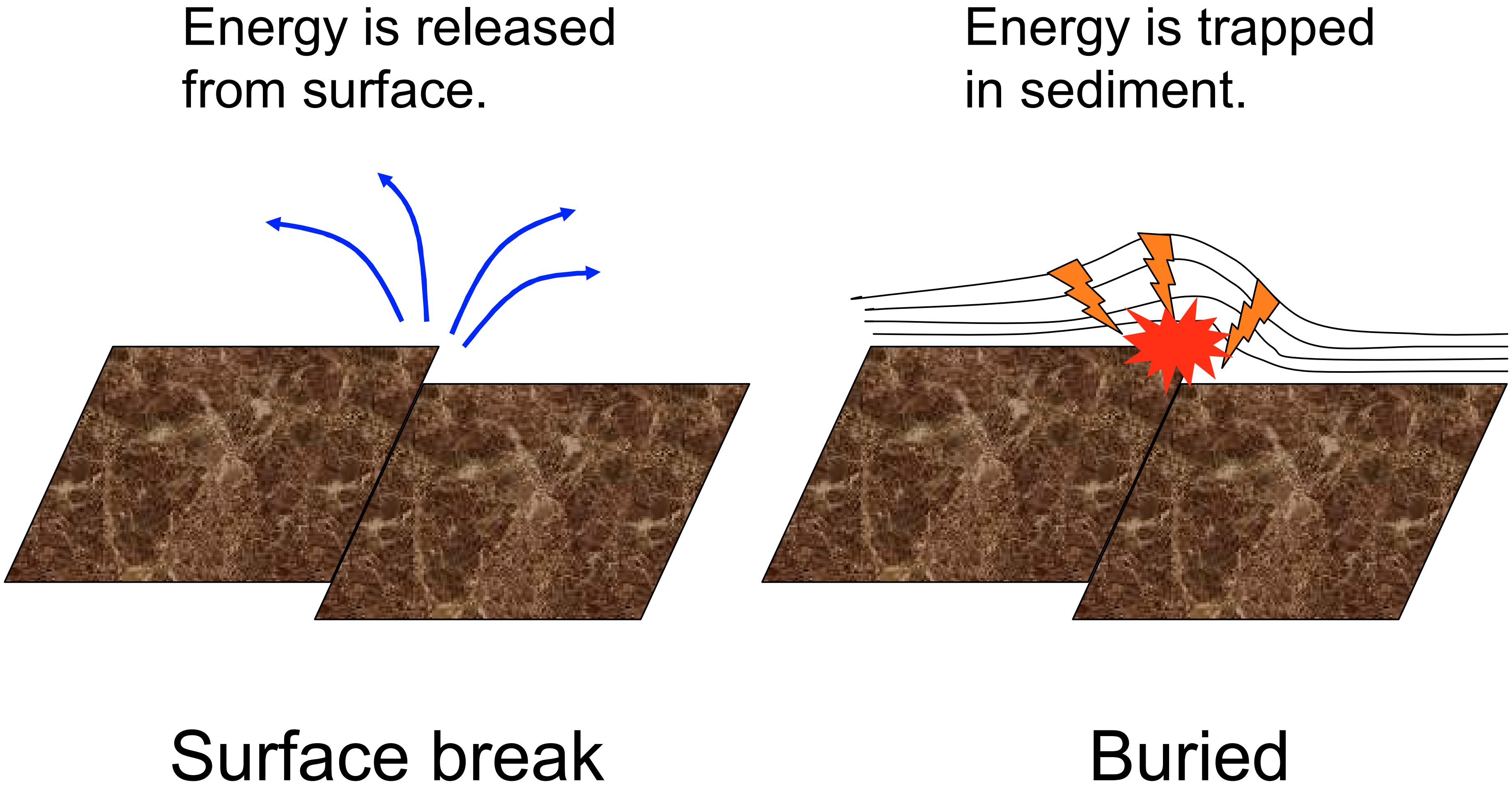
Energy is released from surface.
Energy is trapped in sediment.
Surface break
Buried

http://unit.aist.go.jp/actfault/niigata/report/04.11.30/photo1_5.html

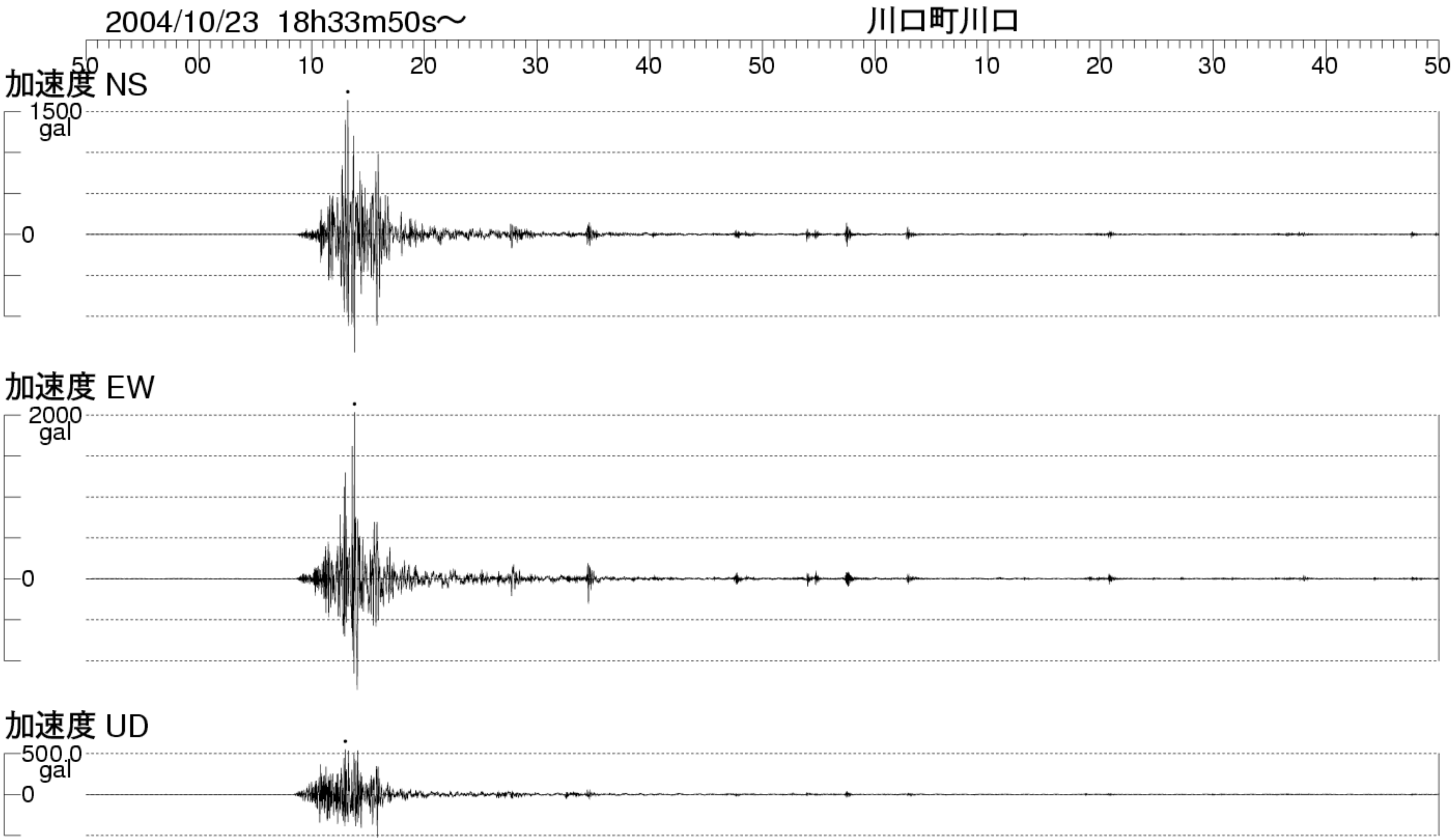

Extreme strong motion from aftershock event.

http://www.seisvol.kishou.go.jp/eq/2004_10_23_niigata/event.html

2004 Sumatra

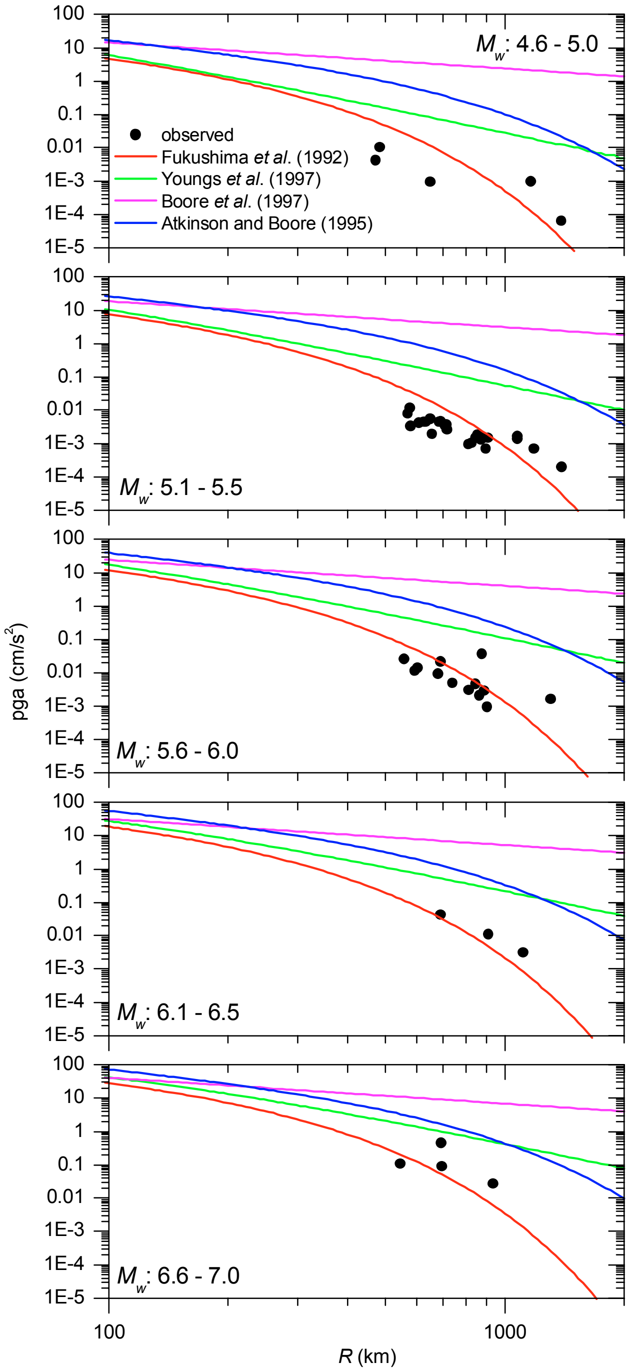

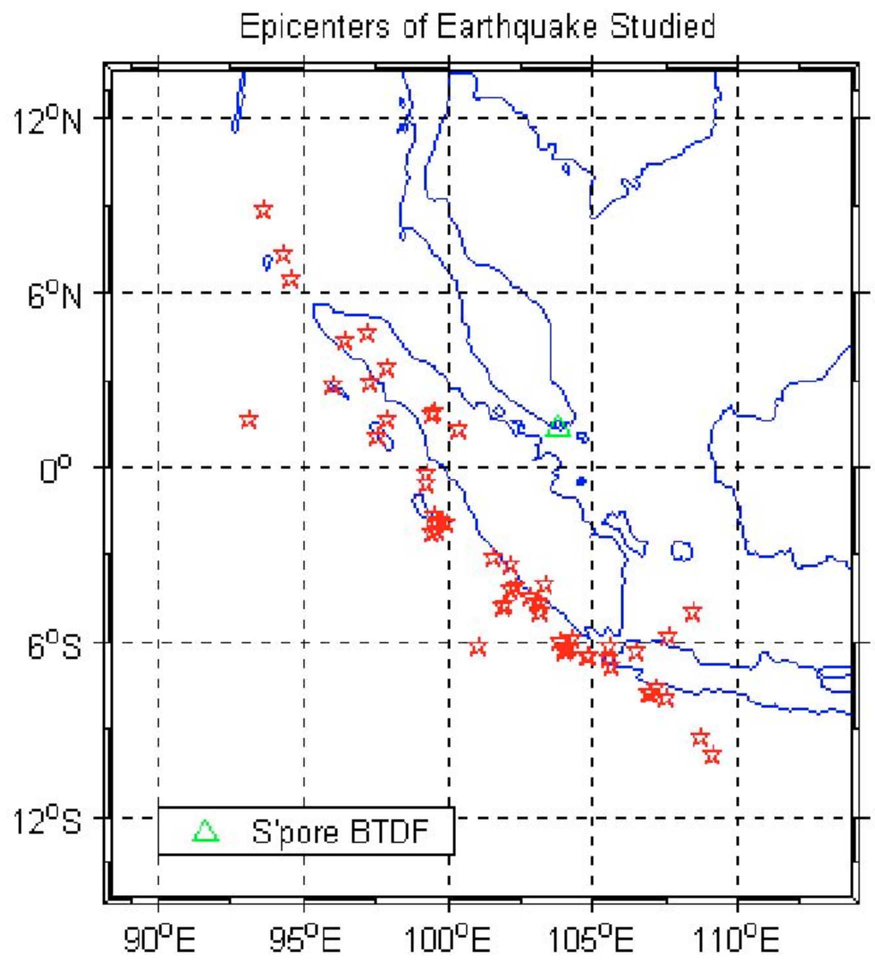

Attenuation relation (Fukushima and Tanaka) correlates well with the recorded data.
By Nanyang Technological University, Singapore

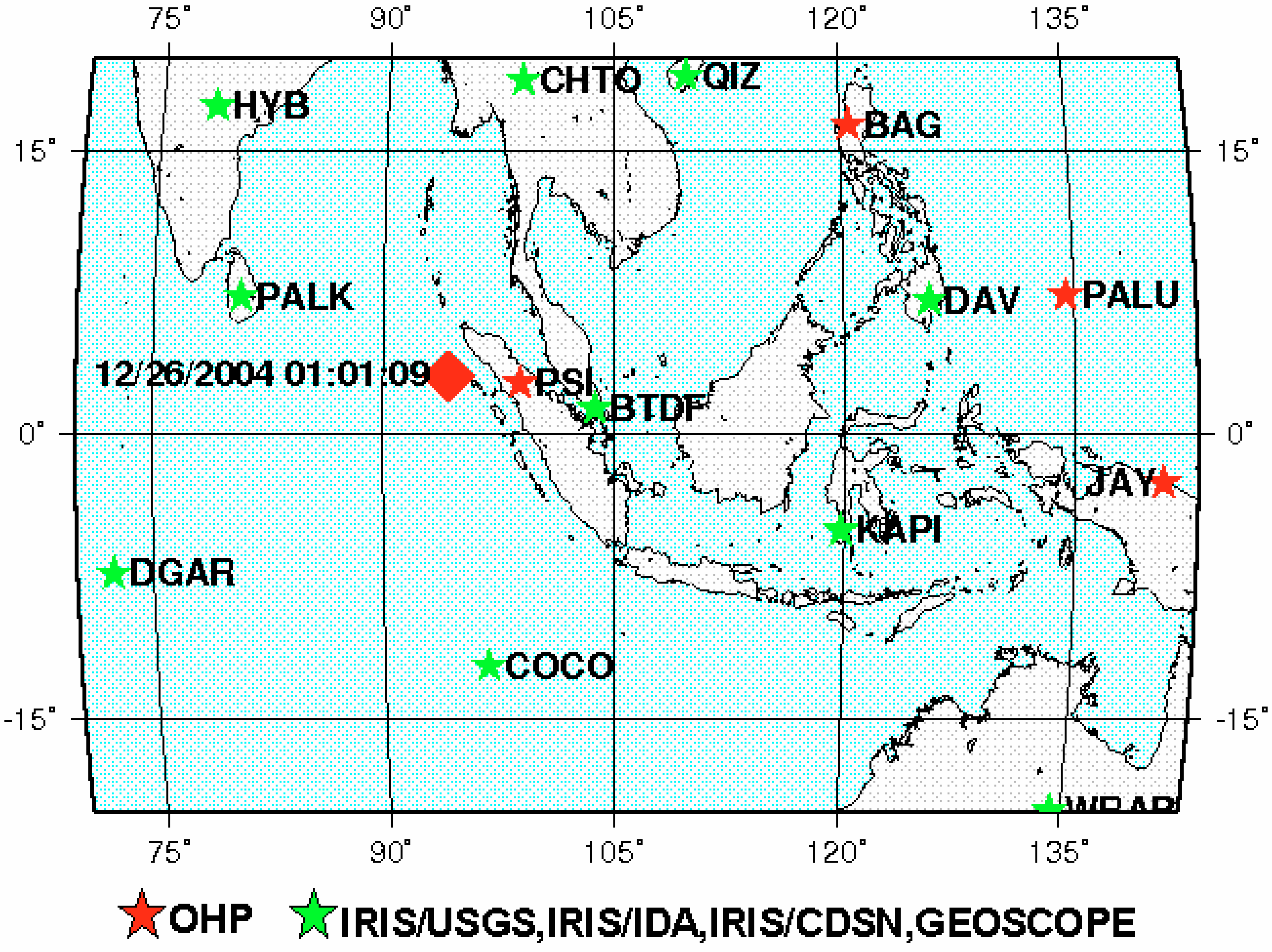

75°
90°
105°
120°
135°
15°
0°
-15°
HYB
CHTO
QIZ
BAG
PALK
DAV
PALU
12/26/2004 01:01:09
PSI
BTDF
JAY
KAPI
DGAR
COCO
OHP
IRIS/USGS,IRIS/IDA,IRIS/CDSN,GEOSCOPE

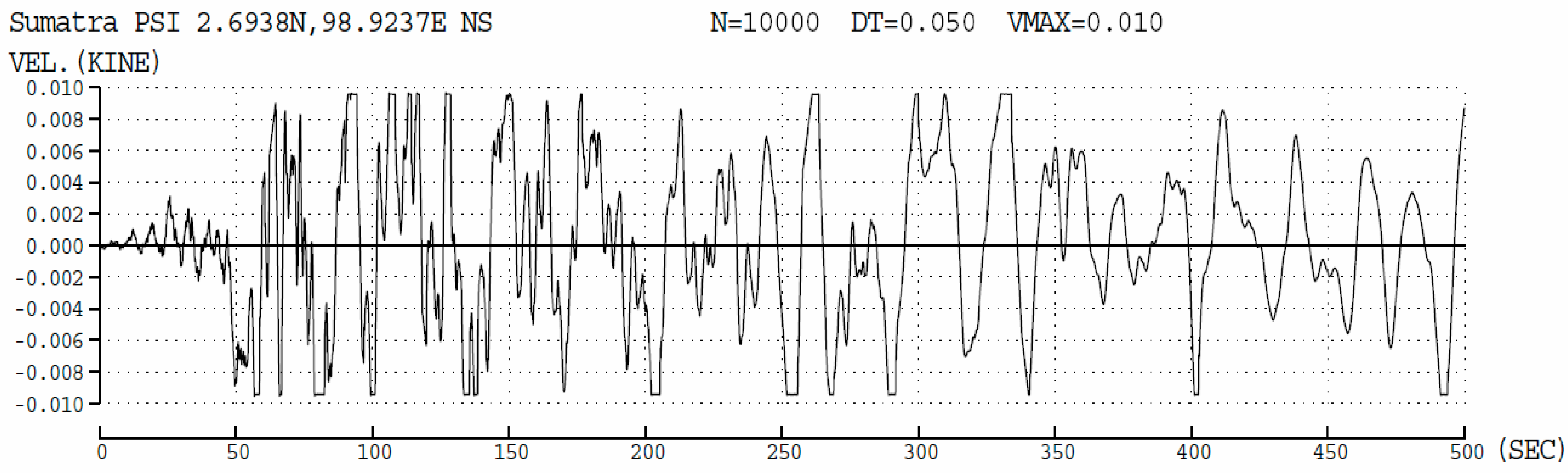
Sumatra PSI 2.6938N,98.9237E NS
N=10000 DT=0.050 VMAX=0.010
VEL.(KINE)
0.010
0.008
0.006
0.004
0.002
0.000
-0.002
-0.004
-0.006
-0.008
-0.010
0
50
100
150
200
250
300
350
400
450
500
(SEC)

Every thing was carried away by TSUNAMI.

(Courtesy of Darren Whiteside-Reuters)

Conclusion

- Quality and quantity of database of strong motion
- Regression model based on seismological background
- Appropriate statistical analysis

After a large earthquake, particularly one that has been especially destructive, the derived attenuation relation should be confirmed by comparing it with the observed strong motion data.